Equivalent Circuits of Linear Active Four-Terminal Networks*

By

LISS C. PETERSON

INTRODUCTION

THE art of equivalent network representation has grown very considerably since its inception by Dr. G. A. Campbell. In his paper "Cissoidal Oscillations" which was published in 1911 he proved that any passive network made up of a finite number of invariable elements and having one pair of input terminals and one pair of output terminals is externally equivalent to an unsymmetrical T or Π network. From this modest beginning the field of applications of the equivalent circuit concept has steadily expanded so that by now the whole field of linear passive circuit theory has been subjected to equivalent circuit interpretation.

With the advent of the thermionic vacuum tube amplifier, linear active network theory had to be considered and almost immediately the attempt was made to obtain an equivalent circuit whose performance would depict the linear characteristic of the tube. The equivalent circuit art has also, in recent years, been used to describe the performance of certain classes of non-linear devices, such as mixers, and further applications in this field will no doubt be made.

Equivalent circuit concepts have played an important part in electrical

---

* This paper appears substantially as it was originally prepared some years ago as a technical memorandum for internal distribution within Bell Telephone Laboratories. Its publication is rendered timely by the applicability to the recently announced transistor devices. Present experience indicates, in fact, that the configuration of Fig. 13 furnishes the most useful equivalent four-pole network for the transistor.

Mr. J. A. Morton has called my attention to an early paper in this field by Strecker and Feldtkeller (E.N.T. Vol. 6, page 93, 1929) in which the general theory of active networks has been well developed. However, the early state of the then prevailing art prevented the full demonstration of the power of the method and of course precluded the possibility of application to modern devices. This paper enlarges the general theory and makes logical applications of the method to modern devices. Since the appearance of the Strecker-Feldtkeller paper several other papers touching upon this subject have appeared. However, no attempt at giving a complete bibliography will be made, except to call attention to the contributions of Prof. M. J. O. Strutt, who also has adopted the four-pole point of view.

The I.R.E. Electron Tube Committee has adopted the four-pole viewpoint and has proposed methods of tests for experimentally determining the four-pole parameters of electron tubes. This material will be published in the new I.R.E. standards on electron tubes.

engineering, particularly in communication engineering. One might almost say that a problem is not solved unless an equivalent circuit has been found whose performance will exhibit some of the characteristics of the actual problem. This need for circuit concepts reflects a desire to make the phenomena more alive and subject to physical interpretation, for it is true that equivalent circuit concepts have greatly contributed towards physical interpretation of analytical expressions. A problem may very well be studied without recourse to the equivalent circuit concept and a correct answer obtained, yet the development of an equivalent circuit adds greatly to the complete interpretation of the physical phenomena.

In this paper we shall be concerned only with linear a-c amplifier operation where the term *linear* indicates that the analytical expressions connecting currents and voltages are linear, that is, involve only the first power of any instantaneous current or its derivative. We shall further restrict our attention to the usual mode of four-terminal amplifier operation in which one pair of terminals is associated with the signal to be amplified and the other pair with the amplified signal. The equivalent a-c circuit of such a transducer will require the development and interpretation of the linear relations connecting the a-c currents and voltages at the input terminals with corresponding quantities at the output terminals. At this point we can logically postulate that the important formal difference between an active and a passive four-pole lies in that the law of reciprocity no longer can be assumed to hold for the active network. Since passive four-poles require three independent parameters for their complete specification the active four-pole will require at least one additional parameter.

In the practical applications we shall be principally concerned with the various triode four-pole connections. A short review of the various stages involved in deriving the newer forms of equivalent triode circuits will therefore be considered prior to the introduction of generalized concepts. Such a review is in the main concerned with the effect of frequency upon the early forms of the equivalent triode circuit.

In the review we shall confine ourselves to the usual grounded cathode mode of operation since it is only in recent times that grounded grid and grounded plate operation have come into use. This distinction is, however, not necessary and is introduced solely for simplicity.

The conventional notation as well as the positive current directions are indicated on Fig. 1 for a general four-pole N. It is assumed here that terminals 1 are the available input and terminals 2 the available output terminals. This choice of current direction appears to the writer to be the most convenient to use when the four-pole is energized at the input terminals 1 only.

Consider, now, a grounded triode operated at such a low frequency that

all displacement or capacity currents can be disregarded, and let it first be supposed that the grid is negatively polarized with respect to the cathode so that grid current is absent. This represents the most primitive form of operation, governed by a law which has been termed "The equivalent-plate-circuit Theorem."[1] With reference to the assumed current direction this theorem may be expressed by saying that the application of the voltage $\bar{V}_1$ to the grid is equivalent, so far as phenomena in the plate circuit are concerned, to the application of the voltage $-\mu V_1$ in series with a resistance r_p, where μ is the amplification factor and r_p the internal plate resistance. The
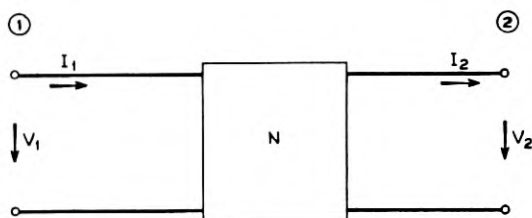

Fig. 1—Current-voltage relations for a general four-pole.
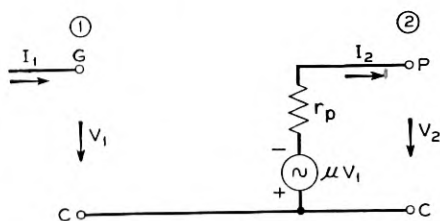

Fig. 2—Equivalent circuit of a negative grid triode at low frequencies.

equivalent circuit for this mode of operation is thus as shown in Fig. 2, where the input terminals 1 are represented by the grid G and the cathode C and the output terminals by the anode P and the cathode C. In terms of analysis the circuit is described by the two equations

$$
\left.
\begin{aligned}
I_1 &= 0 \\
-\mu V_1 &= I_2 r_p + V_2
\end{aligned}
\right\}
\tag{1}
$$

Equations (1) and their associated circuit Fig. 2 are expressions of the fact that in any closed loop the voltages must be in equilibrium.

By a slight rearrangement of (1) a network representation based on current

[1] Chaffee, "Theory of Thermionic Vacuum Tubes," page 192.

equilibrium may be obtained. For this purpose (1) is written as

$$I_1 = 0$$

$$I_2 = -\frac{\mu}{r_p} V_1 - \frac{1}{r_p} V_2$$

$$\left. \right\} \qquad (2)$$

The corresponding network representation is as shown in Fig. 3, where the energizing source in the plate circuit consists of a constant current generator of strength $-\dfrac{\mu}{r_p} V_1$ impressed across the output terminals 2.
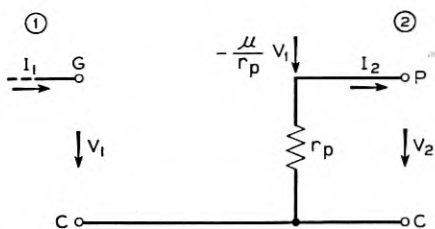

Fig. 3—Equivalent circuit of a negative grid triode at low frequencies.
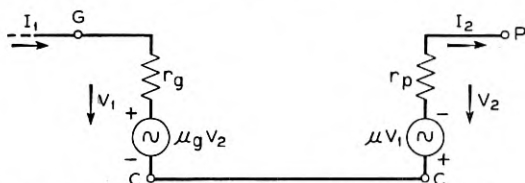

Fig. 4—Equivalent circuit of a positive grid triode at low frequencies.

Let us now consider a further step and assume that the grid is positive so that grid current is also flowing. In regard to the grid circuit there is a theorem called the "Equivalent-grid-circuit Theorem" which is exactly similar to the corresponding plate circuit theorem. The theorem says that the a-c grid current can be calculated by assuming that an e.m.f. $\mu_g V_2$ acts in series with a resistance r_g where μ_g is the reflex factor and r_g the internal grid resistance. In symbols and by using the notation of Fig. 1 this is expressed by:

$$V_1 = \mu_g V_2 + I_1 r_g \qquad (3)$$

By combining the two theorems the equivalent circuit of Fig. 4 results. Again by writing (3) as

$$I_1 = \frac{1}{r_g} V_1 - \frac{\mu_g}{r_g} V_2 \qquad (4)$$

a corresponding network based upon current equilibrium may be found.

It is well to note that this general low-frequency case is governed by the two simultaneous equations

$$\left.\begin{aligned}
I_1 &= \frac{1}{r_g} V_1 - \frac{\mu_g}{r_g} V_2 \\[2mm]
I_2 &= -\frac{\mu}{r_p} V_1 - \frac{1}{r_p} V_2
\end{aligned}\right\} \tag{5}$$

which are of the general form

$$\left.\begin{aligned}
I_1 &= \beta_{11} V_1 + \beta_{12} V_2 \\
I_2 &= \beta_{21} V_1 + \beta_{22} V_2
\end{aligned}\right\} \tag{6}$$

where

$$\left.\begin{aligned}
\beta_{11} &= \frac{1}{r_g} \quad \beta_{12} = -\frac{\mu_g}{r_g} \\[2mm]
\beta_{21} &= -\frac{\mu}{r_p} \quad \beta_{22} = -\frac{1}{r_p}
\end{aligned}\right\} \tag{7}$$

The network of Fig. 4 is thus a possible form of circuit interpretation of (5) or (6). It may also be observed that (6) represents at least formally the most general formulation of the linear active four-pole so that even at very low frequencies the general four-pole point of view might be useful.

Several observations may now be made. In the first place it should be noted that these networks are not based on any study of the internal action of the tube, but rather on the purely formal mathematical process of differentiating the two functional relations which express the broad fact that plate and grid currents are some unspecified linear continuous functions of the grid and plate potentials in the neighborhood of the operating point.

In the second place it may be observed that the network of Fig. 4 represents in a sense two separate networks interacting with each other by means of voltage or current generators. This method of equivalent circuit representation is the result of separate interpretation of the equivalent plate and grid circuit theorems. As a corollary it follows that such a four-pole equivalence involves at least two generators within the network in order to take the effect of interaction into account.

We may say that the networks discussed were satisfactory so long as the frequency was low enough to allow displacement currents to be disregarded. With the operation of circuits at higher frequencies (up to the order of 10^6 cps, say) it became necessary to take the internal tube capacitances into account. This was done by the superposition of a capacity network as shown in Fig. 5. It is interesting as well as instructive to formulate this network transi-

tion in analytical terms.   The transition rests upon the physical fact that the total current entering or leaving an electrode is the sum of conduction and
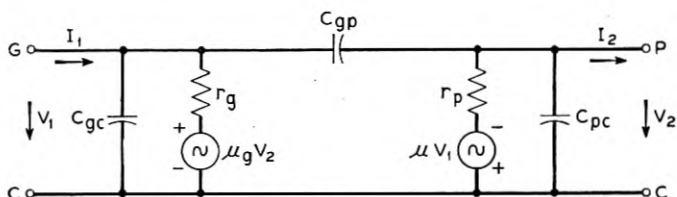

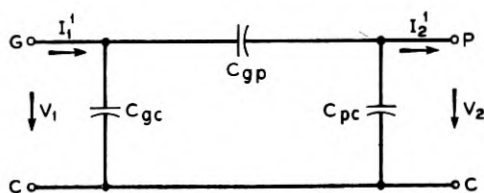Fig. 5—Equivalent circuit of a positive grid triode at moderately low frequencies.

Fig. 6—Parasitic triode network.

displacement current.   The network for the displacement currents is passive and is shown on Fig. 6.   For this network:

$$I_1' = \beta_{11}'V_1 + \beta_{12}'V_2 \atop I_2' = -\beta_{12}'V_1 + \beta_{22}'V_2 \Bigg\} \tag{8}$$

where I_1' is input and I_2' the output displacement current.   The coefficients appearing have the values

$$\begin{aligned} \beta_{11}' &= i\omega(C_{gc} + C_{gp}) \\ \beta_{12}' &= -i\omega C_{gp} \\ \beta_{22}' &= -i\omega(C_{pc} + C_{gp}) \end{aligned} \Bigg\} \tag{9}$$

The potentials appearing in (8) are the same as those which occur in the conduction current equations (5), this being the physical condition which also must be satisfied.   By adding (5) and (8) and by letting I_1 and I_2 mean total currents we get:

$$\begin{aligned} I_1 &= \left[\frac{1}{r_g} + i\omega(C_{gc} + C_{gp})\right] V_1 - \left[\frac{\mu_g}{r_g} + i\omega\, C_{gp}\right] V_2 \\ I_2 &= \left[-\frac{\mu}{r_p} + i\omega C_{gp}\right] V_2 - \left[\frac{1}{r_p} + i\omega(C_{pc} + C_{gp})\right] V_2 \end{aligned} \Bigg\} \tag{10}$$

These equations are again of the form

$$
\left.
\begin{aligned}
I_1 &= \beta_{11} V_1 + \beta_{12} V_2 \\
I_2 &= \beta_{21} V_1 + \beta_{22} V_2
\end{aligned}
\right\}
\tag{11}
$$

where now

$$
\left.
\begin{aligned}
\beta_{11} &= \frac{1}{r_g} + i\omega(C_{gc} + C_{gp}) \\
\beta_{12} &= -\left[\frac{\mu_g}{r_g} + i\omega C_{gp}\right] \\
\beta_{21} &= -\frac{\mu}{r_p} + i\omega C_{gp} \\
\beta_{22} &= -\left[\frac{i}{r_p} + i\omega(C_{pc} + C_{gp})\right]
\end{aligned}
\right\}
\tag{12}
$$

The network interpretation of Fig. 5 is consistent with (10) and so does, in fact, constitute a possible network representation.

From (12) the relation

$$
\beta_{21} + \beta_{12} = -\left[\frac{\mu}{r_g} + \frac{\mu_g}{r_g}\right]
\tag{13}
$$

is obtained. The thing to emphasize is that this sum is independent of the passive feedback admittance and that it is a constant independent of frequency within the range considered. It is, moreover, a quantity which only is correlated with the conduction currents in the tube. For lack of a better name the sum (13) will be referred to as "the effective transconductance." It will play an important role in the later discussion.

As still higher frequencies (above 10^7 cps) were employed it necame necessary to take into account lead effects, usually in the form of self and mutual inductances, and by incorporating them in the network of Fig. 5 a slightly more involved circuit was obtained. This more general network is still determined by equations of the form (11), for adding the new network elements merely means that linear transformations are applied to the potentials V_1 and V_2 with the result that a new set of β-coefficients is obtained, the new set being merely of somewhat more complicated form than the first.

With the utilization of frequencies so high that the electron transit times became comparable with the period of the applied signal, further complications arose and the equivalent network idea was put to a severe test. In

this development we may distinguish between two methods of approach. In one the attempt was made to modify the low-frequency network of Fig. 5 to include transit time effects to a first order of approximation.[2] The second approach differed in that attention was directed only toward the electron stream itself, while the circuit elements connecting the stream with the physically available terminals were grouped together with the external circuit elements.[3] The latter approach represented a particularly useful one from a physical point of view and it also extended the use of basic circuit elements to include the general diode impedance as a new circuit element complete in itself. However, even in this latest approach the four-pole point of view was not adopted, with consequent loss of generality and unity in viewpoint. Moreover, the fact that only the electron stream itself was considered caused some confusion.

With this brief review of the development of equivalent circuit representation of vacuum tube amplifiers in mind we turn now to the main body of the paper in which a more general treatment of the problem is considered. It will be shown, in the coming sections, how it is possible to lump all the factors involved in vacuum tube amplifiers, i.e., physical circuit parameter and internal electronic effects involving the electron transit time, into a single coordinated picture with an equivalent circuit representation of the overall effect.

Equivalent Circuit Representation of Active Linear Four-Pole Pole Equations

Whenever the response of a general transducer is related in a linear manner to the stimulus, the transducer behavior is described by two linear relations. Although we are primarily concerned with electromagnetic transducers the concepts to be used are of broader utility and may, for example, also be applied to mechanical and electromechanical transducers.

There are various ways in which the behavior of the four-pole may be expressed analytically. The form expressing current equilibrium has already been given and it may well serve as a starting point for the following discussion:

Thus we have:

$$\left.\begin{aligned} I_1 &= \beta_{11}V_1 + \beta_{12}V_2 \\ I_2 &= \beta_{21}V_1 + \beta_{22}V_2 \end{aligned}\right\} \tag{14}$$

[2] F. B. Llewellyn, "Electron-Inertia Effects," Cambridge University Press, 1941.
[3] F. B. Llewellyn and L. C. Peterson, Interpretation of Ultra-High Frequency Tube Performance in Terms of Equivalent Networks, Proceedings of the National Electronics Conference, 1944.

as expressions for current equilibrium at any frequency. The four parameters β which appear have simple physical meanings, and it is seen that

β_{11} is the input admittance with output shorted

$-\beta_{22}$ is the output admittance with input shorted

$-\beta_{12}$ is the feedback admittance with input shorted

β_{21} is the transfer admittance with output shorted.

Before proceeding to the network representations of (14) it seems well to state briefly some of the reasons which almost force one to adopt the four-pole point of view when dealing with vacuum tubes in the higher frequency range.

There are the pedagogical reasons that classical methods long employed for passive networks are merely extended into the realm of active networks, thus providing unity in viewpoints.

The basic analysis involving the four-pole parameters for a particular transducer needs to be performed only once and, once obtained, all problems involving terminal impedances may, in any particular case, be solved in a routine manner.

There are also further practical reasons. We saw above that with increase in frequency the classical equivalent network had to be modified to a considerable extent in order to include the parasitic elements. This poses a serious problem for the tube designer, whose task it is to estimate the tube performance between known terminations. Such a task based upon the modified classical circuit becomes very difficult and cumbersome. Moreover, it is also difficult to segregate and measure the parasitic elements. Hence it appears that one could gain much if design parameters could be developed capable of reflecting parasitic and transit time effects. Finally, it is desirable to develop equivalent circuits with a minimum number of parameters bearing simple relationships to quantities which can be measured directly.

These general desires arising from the practical needs of the tube designer can be satisfied if tube behavior is specified by means of four-pole parameters.

All in all the four-pole point of view can be made to satisfy the logical needs of integrated concepts as well as the practical needs of simplicity in the specification of tube performance.

After this brief presentation of the argument for the four-pole point of view, the network representation of (14) will now be considered.

Stated in broadest terms: we are seeking a network representation by considering the two equations as a single unit and not by the trivial considera tion of each equation by itself.

We need, to begin with, the well-known network representation of a passive four-pole. Equation (14) has, then, the form

$$I_1 = \beta_{11}V_1 + \beta_{12}V_2$$
$$I_2 = -\beta_{12}V_1 + \beta_{22}V_2$$
$$(15)$$

and one equivalent circuit representation is that given by the Π network having the element values shown in Fig. 7. If so desired the Π network can of course also be transferred into an equivalent T network.
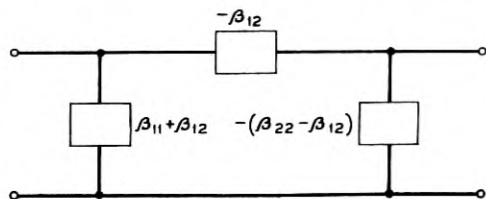

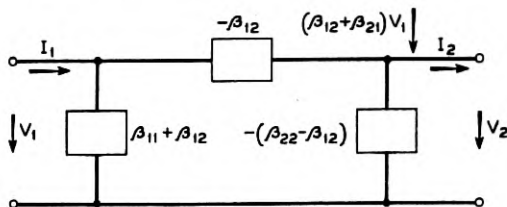Fig. 7—Equivalent circuit of a passive four-pole.

Fig. 8—Equivalent circuit of an active four-pole; current impressed at the output.

Now write (14) as

$$I_1 = \beta_{11}V_1 + \beta_{12}V_2$$
$$I_2 = -\beta_{12}V_1 + \beta_{22}V_2 + (\beta_{12} + \beta_{21})V_1$$
$$(16)$$

Whence it is seen by a comparison with (15) that the network representation of the active four-pole differs from the passive one merely by the presence of the impressed current $(\beta_{12} + \beta_{21})V_1$. A possible network representation of the general active four-pole is thus as shown on Fig. 8.

An immediate application may be illuminating. Consider, for example, the triode operated with positive grid, with interelectrode capacitances taken into account. The four-pole equations are given by (11) and (12) and the classical network is that of Fig. 5. From (12) and Fig. 8 we get the network of Fig. 9. It may be observed that, while in Fig. 5 the source and source-free constituents are intermingled, this is not the case in Fig. 9 where, on the contrary, a clear demarcation is present between such constituents.

In regard to the general network of Fig. 8 it may be noted that the network is composed of two parts. One part obeys the reciprocal law and is represented by a Π (or T) network and is consequently specified by three parameters. The other part is merely an impressed current controlled by the input potential V_1. From the fact that the Π (or T) network obeys the
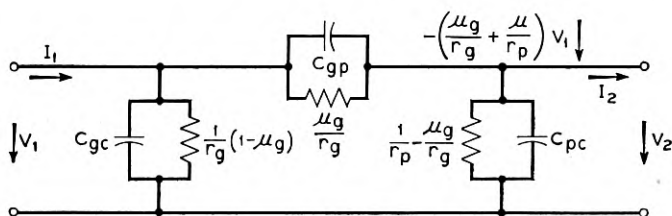

Fig. 9—Equivalent circuit of a positive grid triode at moderately low frequencies; current impressed at the output.
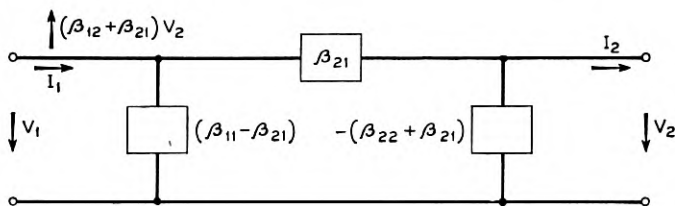
Fig. 10—Equivalent circuit of an active four-pole; current impressed at the input.
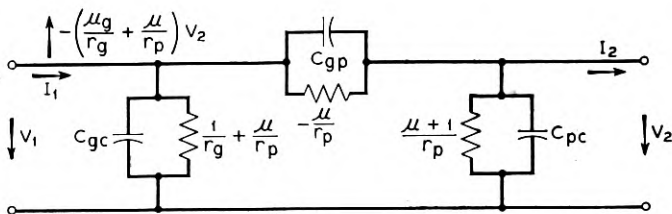
Fig. 11—Equivalent circuit of a positive grid triode at moderately low frequencies; current impressed at the input.

reciprocal law, the conclusion does not follow that it in general behaves as a passive network. The element values may, for example, be negative, and Bode's integral relations may not necessarily be true for this network.

It should further be noted that the network representation holds for all frequencies. The effect of frequency will be that the admittances in the network change and in changing they will, for example, reflect effects due to parasitics and electron transit time.

We next observe that the network of Fig. 8 is not unique; in other words it is not the only possible network. To see this it need merely be observed that from the group of four independent β parameters in (15) there are several ways in which a subgroup may be selected containing only three of them. For example the "passive part" of the network in Fig. 8 was constructed from the three parameters β_{11}, β_{12} and β_{22}. But this is evidently not the only choice. Moreover, the impressed force was taken to be voltage-controlled but this again does not represent the only possibility.

In general it follows that the "passive part" of the network will reflect at least three properties of the complete network. In Fig. 8, for example, the "passive part" reproduces faithfully the two short-circuit driving-point admittances and the feedback admittance of the complete network.

Finally it is well to observe that only one driving force is needed in the general network formulation.

With this background of the general ideas involved let us now further explore some of the possibilities suggested as to other "passive network" constituents. Let us, for example, use β_{11}, β_{22} and β_{21} for the "passive part". We then write (14) as

$$\left.\begin{aligned}
I_1 &= \beta_{11}V_1 - \beta_{21}V_2 + (\beta_{12} + \beta_{21})V_2 \\
I_2 &= \beta_{21}V_1 + \beta_{22}V_2
\end{aligned}\right\} \tag{17}$$

and from (17) the network representation of Fig. 10 follows. In addition this network differs from that of Fig. 8, in that the impressed current appears on the input side and that it is controlled by the output rather than by the input voltage. As an illustration consider again the triode operated with positive grid. The equivalent network is now as shown in Fig. 11.

Now let it be supposed that the impressed force be current rather than voltage-controlled. We then first transform (14) into

$$\left.\begin{aligned}
V_1 &= \frac{I_1}{\beta_{11}} - \frac{\beta_{12}}{\beta_{11}}V_2 \\
I_2 &= \frac{\beta_{21}}{\beta_{11}}I_1 + V_2\left(\beta_{22} - \frac{\beta_{21}\beta_{12}}{\beta_{11}}\right)
\end{aligned}\right\} \tag{18}$$

and then rewrite (18) as

$$\left.\begin{aligned}
V_1 &= \frac{I_1}{\beta_{11}} - \frac{\beta_{12}}{\beta_{11}}V_2 \\
I_2 &= -\frac{\beta_{12}}{\beta_{11}}I_1 + V_2\left(\beta_{22} - \frac{\beta_{21}\beta_{12}}{\beta_{11}}\right) + \frac{\beta_{12} + \beta_{21}}{\beta_{11}}I_1
\end{aligned}\right\} \tag{19}$$

It can be shown that the network representation of Fig. 12 is consistent with (19). This network representation suffers from two obvious disadvantages. One is that the "passive network" is determined by only one short-circuit driving-point admittance of the complete network. The other short-circuit driving-point admittance of the "passive part" appears to be unrelated to any simple admittance which may be found from measurements at the output terminals of the complete network. The second disadvantage is that the coefficient of the current in the impressed force is of a complicated nature, since a driving-point admittance enters. Moreover, a closer investigation shows that in this network representation the "passive part" besides preserving the driving-point admittance β_{11} and the feedback admittance β_{12}, also preserves the quantity $\Delta_\beta = \beta_{11}\beta_{22} - \beta_{12}\beta_{21}$ of the complete network.
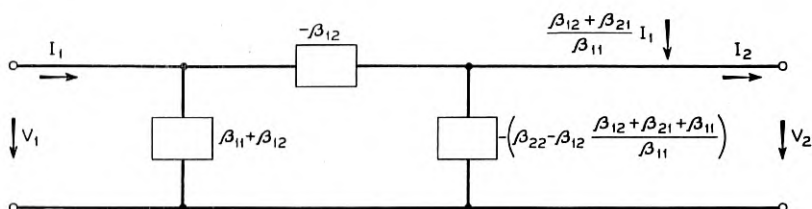

Fig. 12—Equivalent circuit of an active four-pole; current impressed at the output.

By proceeding from (19) in a way similar to that used in (17) the network in Fig. 12 transforms into another in which the impressed force appears on the input side. Many other networks can also be found.

The networks discussed were based on (14), which expressed the fact of current equilibrium and leads rather naturally to Π networks together with an impressed current source. On the other hand, starting with the four-pole equations which express voltage equilibrium, one encounters T networks together with impressed electromotive forces. These networks must now also be considered. In regard to the details involved in their derivation we may be very brief since the methods are similar to those already employed.

The four-pole equations expressing voltage equilibrium may be written as

$$\left.\begin{aligned} V_1 &= Z_{11}I_1 + Z_{12}I_2 \\ V_2 &= Z_{21}I_1 + Z_{22}I_2 \end{aligned}\right\} \tag{20}$$

where current and voltage directions are assumed to be taken in accordance with the conventions of Fig. 1.

The four parameters Z are of simple physical significance and it follows that:

Z_{11} is the input impedance with output open

$-Z_{22}$ is the output impedance with input open

$-Z_{12}$ is the feedback impedance with input open

Z_{21} is the transfer impedance with output open.

The relations between the β's and the Z's are given by the expressions:

$$\left.\begin{aligned}
\beta_{11} &= \frac{Z_{22}}{\Delta_Z} \\[2mm]
\beta_{12} &= -\frac{Z_{12}}{\Delta_Z} \\[2mm]
\beta_{21} &= -\frac{Z_{21}}{\Delta_Z} \\[2mm]
\beta_{22} &= \frac{Z_{11}}{\Delta_Z}
\end{aligned}\right\} \tag{21}$$

where

$$\Delta_Z = \begin{vmatrix} Z_{11} & Z_{12} \\ Z_{21} & Z_{22} \end{vmatrix} \tag{22}$$

We have also

$$\Delta_Z = \frac{1}{\Delta_\beta} \tag{23}$$

where

$$\Delta_\beta = \begin{vmatrix} \beta_{11} & \beta_{12} \\ \beta_{21} & \beta_{22} \end{vmatrix} \tag{24}$$

Applying now to (20) the transformations which led to the networks of Figs. 9, 10 and 12, we get the networks of Figs. 13, 14 and 15.

The "passive part" of the network in Fig. 13 reproduces the two open circuit impedances Z_{11} and Z_{22} as well as the feedback impedance Z_{12} of the complete network.

The network in Fig. 14 differs from that of Fig. 13 because of the use of the transfer impedance Z_{21} in the "passive part" with the result that the impressed current appears on the input side.

The "passive part" in Fig. 15, finally, preserves the open-circuit imped-ance Z_{11}, the feedback impedance Z_{12} and the determinant Δ_z of the com-plete network. This network shows incidentally a close resemblance to one already published.[3]
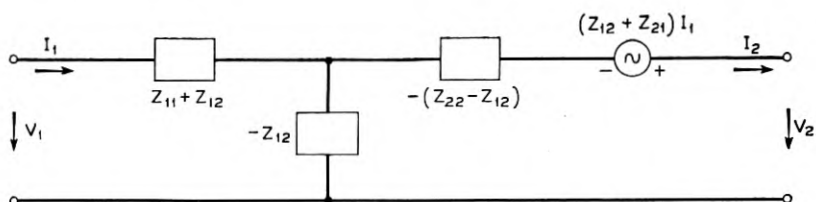
Fig. 13—Equivalent circuit of an active four-pole; voltage impressed in series with the output.
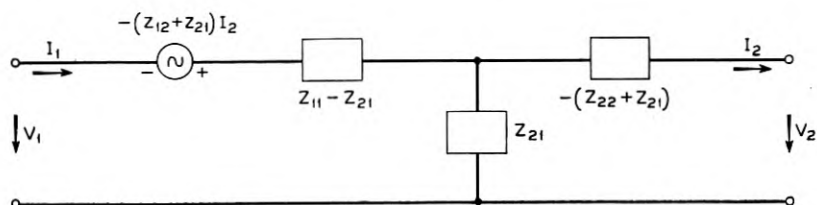
Fig. 14—Equivalent circuit of an active four-pole; voltage impressed in series with the input.
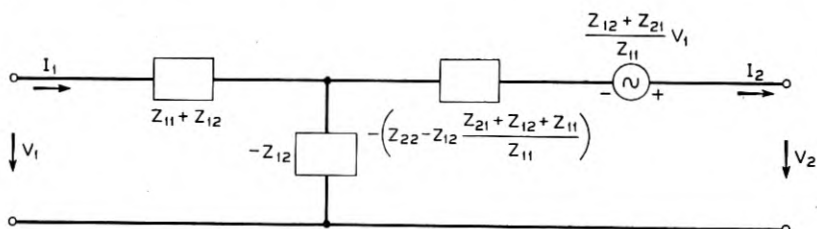
Fig. 15—Equivalent circuit of an active four-pole; voltage impressed in series with the output.

It is well to emphasize that, while all the complete networks are equiva-lent, this is not true for the "passive parts." In fact from their derivation it follows that none are equivalent. Specific circumstances may make it desirable to perform transformations on the passive parts. For example, it might be more convenient to work with a II than with a T network. Such transformations are of course perfectly legitimate and raise the question of choice of equivalent networks. A few remarks on this subject may be

[3] Loc. cit.

appropriate, since the choice is not quite a matter of indifference. Broadly speaking, the choice will depend upon the relative advantages of nodal and mesh analysis and in most practical situations the former has proved to be the more convenient of the two. One cannot, however, be too dogmatic in this regard. Consider the networks of Figs. 8 and 13. Suppose, for example, that parasitic elements appearing as a passive II network had to be superimposed. It is then more convenient to use Fig. 8, not only on account of the ease with which this may be done, but also on account of the fact that the effective transadmittance $\beta_{12} + \beta_{21}$ is invariant with respect to such a superposition. If, on the other hand, parasitic elements appear as series elements (lead inductances for example) the network of Fig. 13 might be more convenient since the effective transimpedance $Z_{12} + Z_{21}$ now remains invariant.

It is also desirable to choose an equivalent network whose elements are capable of being determined by simple measurements; from this consideration the network on Fig. 8 is of distinct advantage.

APPLICATION TO TRIODES

The preceding section was primarily directed towards the development of possible forms of network representations of the general four-pole equations. In this section one of these forms, namely that given in Fig. 8, will be used to represent the three modes of triode operation. Depending upon which electrode is at a-c ground potential, we may distinguish between the following methods of operation:

1. Grounded cathode operation.

2. Grounded grid operation.

3. Grounded plate operation.

The schematic diagrams, together with assumed voltage and current directions for these modes, are shown on Figs. 16, 17 and 18 respectively.

With a given set of available terminals the first step in obtaining the networks consists in calculating the four-pole parameters with respect to these terminals. It will be assumed that the coupling circuits have been designed with such efficiency that lead effects can be disregarded, so that the available terminals actually coincide with anode, grid and cathode. This set of available terminals brings us as close to the electron stream as it is physically possible to attain and it represents the ideal towards which design tends.

It is beyond the scope of this paper to consider the details involved in the calculations of the four-pole parameters. The basic tools needed are the result of a study of the dynamics of the electron stream, which started from

fundamentals,[4] and some familiarity with this work is assumed on the part of the reader. Concerning these tools two reservations need be made. In the first place the tools apply to planar rather than to cylindrical structures. Since, however, there is a decided tendency toward planar structures, especially in the high-frequency field, because of a desire for uniform electron streams, this limitation does not seem serious. In the second place the tools are also subject to the limitation of a single-valued velocity electron stream.
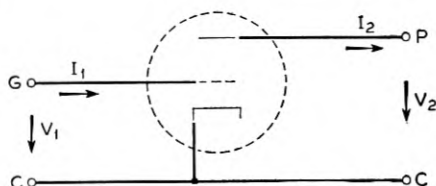
Fig. 16—Vurrent-voltage relations for the grounded cathode triode.
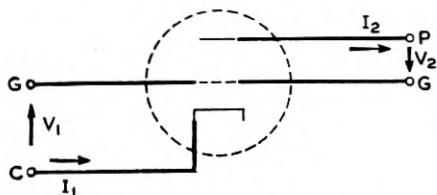
Fig. 17—Current-voltage relations for the grounded grid triode.
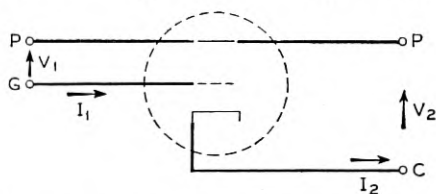
Fig. 18—Current-voltage relations for the grounded plate triode.

This, again, is not too serious, since one of the aims in present high-frequency tube design is to produce as uniform a stream as possible. Nevertheless, the effects produced by multiple velocities are important to know. Studies along such lines have been made by Mr. Frank Gray of these Laboratories.

The operating conditions of the triode are assumed to be quite general. There are, for example, no restrictions placed upon frequency and space charge and the grid may, moreover, have either positive or negative d-c potential with respect to the cathode.

[4] F. B. Llewellyn and L. C. Peterson, "Vacuum Tube Networks," Proceedings of the I.R.E., March, 1944.

With current and voltage directions as in Figs. 16, 17 and 18, the following Tables I, II and III list the four-pole parameters for the three modes of triode operation in both β and Z forms.

<div align="center">

TABLE I

FOUR-POLE PARAMETERS FOR GROUNDED CATHODE TRIODE

</div>

$$\beta_{11} = \frac{y_{11} + y_{21} + y_{22}}{D} \qquad \beta_{12} = -\frac{y_{22}}{D}$$

$$\beta_{21} = \frac{y_{21} + y_{22}}{D} \qquad \beta_{22} = -\frac{y_{22} + \dfrac{y_{11}}{\mu}}{D}$$

$$\Delta_\beta = \begin{vmatrix} \beta_{11} & \beta_{12} \\ \beta_{21} & \beta_{22} \end{vmatrix} = -\frac{y_{11}\, y_{22}}{D}$$

$$D = 1 + \frac{y_{11} + y_{21} + y_{22}}{\mu y_{22}}$$

$$Z_{11} = \frac{1}{y_{11}} + \frac{1}{\mu y_{22}} \qquad Z_{12} = -\frac{1}{y_{11}}$$

$$Z_{21} = \frac{1}{y_{11}} + \frac{y_{21}}{y_{11}\, y_{22}} \qquad Z_{22} = -\left[\frac{1}{y_{11}} + \frac{1}{y_{22}} + \frac{y_{21}}{y_{11}\, y_{22}}\right]$$

$$\Delta_Z = \begin{vmatrix} Z_{11} & Z_{12} \\ Z_{21} & Z_{22} \end{vmatrix} = \frac{1}{\Delta_\beta} = -\frac{D}{y_{11}\, y_{22}}$$

μ = amplication factor.

The y admittance coefficients appearing in the above tables were fully explained and discussed in the paper on Vacuum Tube Networks, to which reference has already been made. Suffice it here to say that y_{11} is the admittance of the diode coinciding with cathode and equivalent grid plane and y_{22} the admittance of the diode coinciding with the equivalent grid plane and the anode and finally y_{21} the transadmittance between these fictitious diodes. The admittance y_{11} depends upon the d-c conditions between cathode and grid and upon the transit angle for this region alone. The diode admittance y_{22} depends in a similar manner upon the d-c space charge conditions in the grid-anode region as well as upon the transit angle for this region alone. For the small degree of space charge which usually exists between grid and plate of most triodes, y_{22} can be represented by a simple capacitance. The transadmittance y_{21} can be resolved into two factors, the first of which depends only upon the transit angle between cathode and grid, and the second only upon the transit angle between grid and anode. In the paper on vacuum tube networks all these admittances were plotted

TABLE II

FOUR-POLE PARAMETERS FOR GROUNDED GRID TRIODE

$$\beta_{11} = \frac{y_{11}\left(1 + \dfrac{1}{\mu}\right)}{D} \qquad \beta_{12} = -\frac{y_{11}}{\mu D}$$

$$\beta_{21} = -\frac{y_{21} - \dfrac{y_{11}}{\mu}}{D} \qquad \beta_{22} = -\frac{y_{22} + \dfrac{y_{11}}{\mu}}{D}$$

$$\Delta_\beta = \begin{vmatrix} \beta_{11} & \beta_{12} \\ \beta_{21} & \beta_{22} \end{vmatrix} = -\frac{y_{11}\,y_{22}}{D}$$

$$D = 1 + \frac{y_{11} + y_{21} + y_{22}}{\mu y_{22}}$$

$$Z_{11} = \frac{1}{y_{11}} + \frac{1}{\mu y_{22}} \qquad Z_{12} = -\frac{1}{\mu y_{22}}$$

$$Z_{21} = \frac{1}{\mu y_{22}} - \frac{y_{22}}{y_{11}\,y_{22}} \qquad Z_{22} = -\left[\frac{1}{y_{22}} + \frac{1}{\mu y_{22}}\right]$$

$$\Delta_Z = \begin{vmatrix} Z_{11} & Z_{12} \\ Z_{21} & Z_{22} \end{vmatrix} = \frac{1}{\Delta_\beta} = -\frac{D}{y_{11}\,y_{22}}$$

μ = amplification factor.

TABLE III

FOUR-POLE PARAMETERS FOR GROUNDED PLATE TRIODE

$$\beta_{11} = \frac{y_{11} + y_{21} + y_{22}}{D} \qquad \beta_{12} = -\frac{y_{11} + y_{21}}{D}$$

$$\beta_{21} = \frac{y_{11}}{D} \qquad \beta_{22} = -\frac{y_{11}\left(1 + \dfrac{1}{\mu}\right)}{D}$$

$$\Delta_\beta = \begin{vmatrix} \beta_{11} & \beta_{12} \\ \beta_{21} & \beta_{22} \end{vmatrix} = -\frac{y_{11}\,y_{22}}{D}$$

$$D = 1 + \frac{y_{11} + y_{21} + y_{22}}{\mu y_{22}}$$

$$Z_{11} = \frac{1}{y_{22}} + \frac{1}{\mu y_{22}} \qquad Z_{12} = -\left[\frac{1}{y_{22}} + \frac{y_{21}}{y_{11}\,y_{22}}\right]$$

$$Z_{21} = \frac{1}{y_{22}} \qquad Z_{22} = -\left[\frac{1}{y_{11}} + \frac{1}{y_{22}} + \frac{y_{12}}{y_{11}\,y_{22}}\right]$$

$$\Delta_Z = \begin{vmatrix} Z_{11} & Z_{12} \\ Z_{21} & Z_{22} \end{vmatrix} = \frac{1}{\Delta_\beta} = -\frac{D}{y_{11}\,y_{22}}$$

μ = amplication factor.

graphically, showing both phase and magnitude, and this paper is referred
to for details.[4]

Tables I, II and III, in conjunction with Figs. 8, 13 and 15, allow us to
derive the equivalent networks of Figs. 19, 20 and 21.

We must now undertake a discussion of the results given in the tables as
well as of the networks which were derived from them.
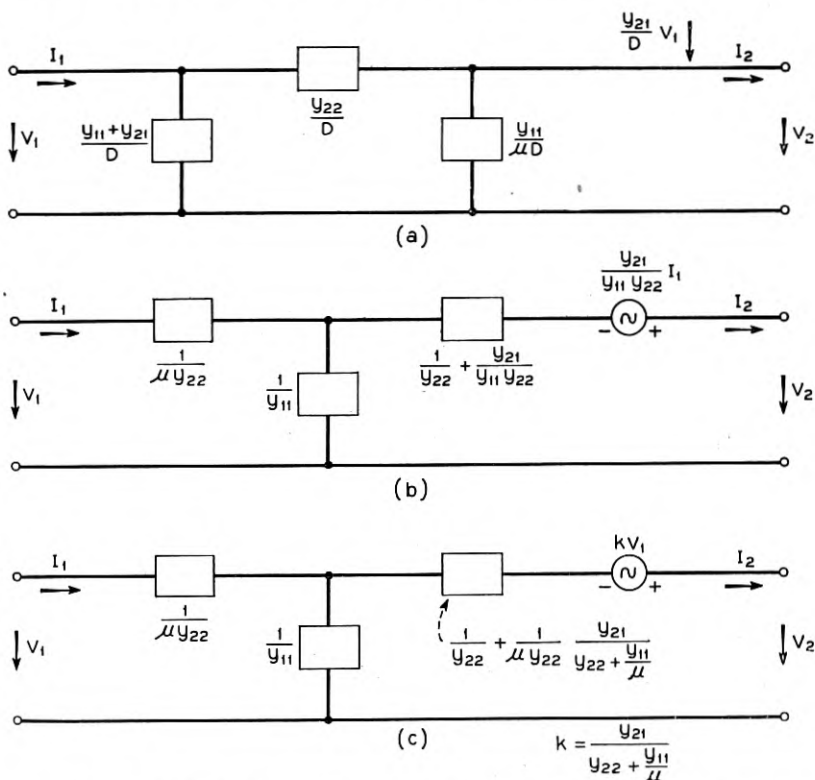
Fig. 19 (a, b, c)—Three forms of equivalent circuits of the grounded cathode triode
valid at all frequencies.

Initially, it is well to emphasize again that the four-pole parameters and
the corresponding networks are different but equivalent ways through which
the triode signal behavior becomes completely specified for all conditions of
space charge and for all frequencies.

Secondly, there are certain general relations which should be noted. We
observe, first, that the determinants Δ_β and Δ_z are invariants for the dif-
ferent modes of triode operation, and with exception of phase reversals this

[4] Loc. cit.

is also the case for the effective transadmittance $\beta_{12} + \beta_{21}$ as well as for the effective transimpedance $Z_{12} + Z_{21}$. On the other hand, the quantity $\dfrac{Z_{12} + Z_{21}}{Z_{11}}$, which appears in the network of Fig. 15 and which represents the driving force per unit input voltage, is invariant (except for reversal in phase) only for grounded grid and grounded cathode operation. Several
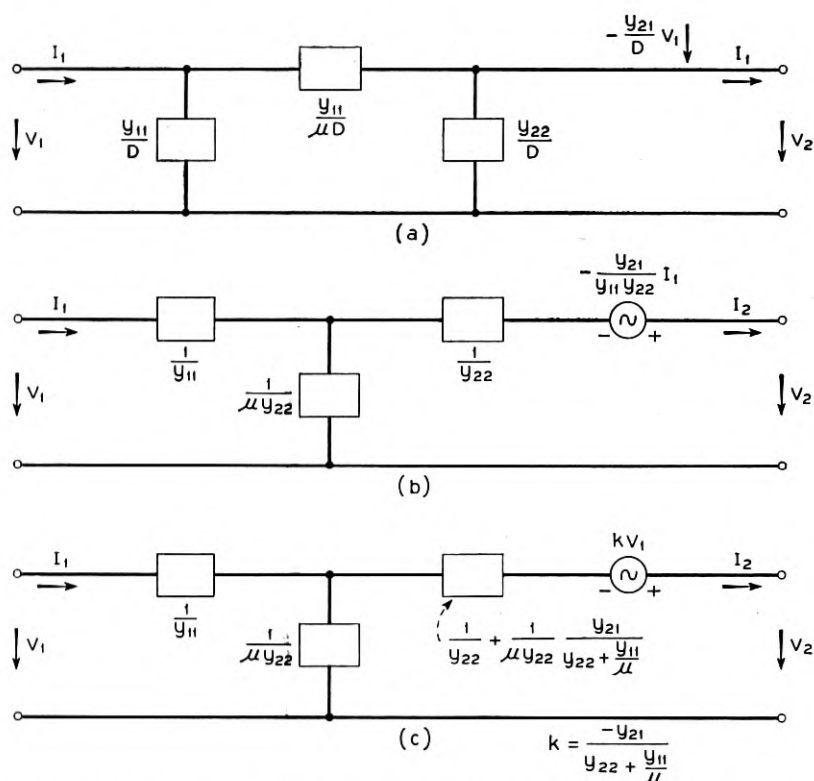
Fig. 20 (a, b, c)—Three forms of equivalent circuits of the grounded grid triode valid at all frequencies.

admittance and impedance relations may also be pointed out. For example, the input short-circuit driving-point admittance β_{11} is equal for grounded cathode and grounded plate operation and the same is true for the output short-circuit driving-point admittances β_{22} for grounded cathode and grounded grid operation. Moreover, it is also seen that the input short-circuit driving-point admittance β_{11} for grounded grid operation is equal to the output driving-point admittance β_{22} for grounded plate operation. A

similar set of reciprocal relations between the open-circuit driving-point impedances is also present.

In regard to the networks it may first be observed that, since they were derived from parameters upon which no restrictions had been placed on either frequency or space charge, they are also generally valid. In passive circuit theory one is accustomed to the use of only the three basic elements
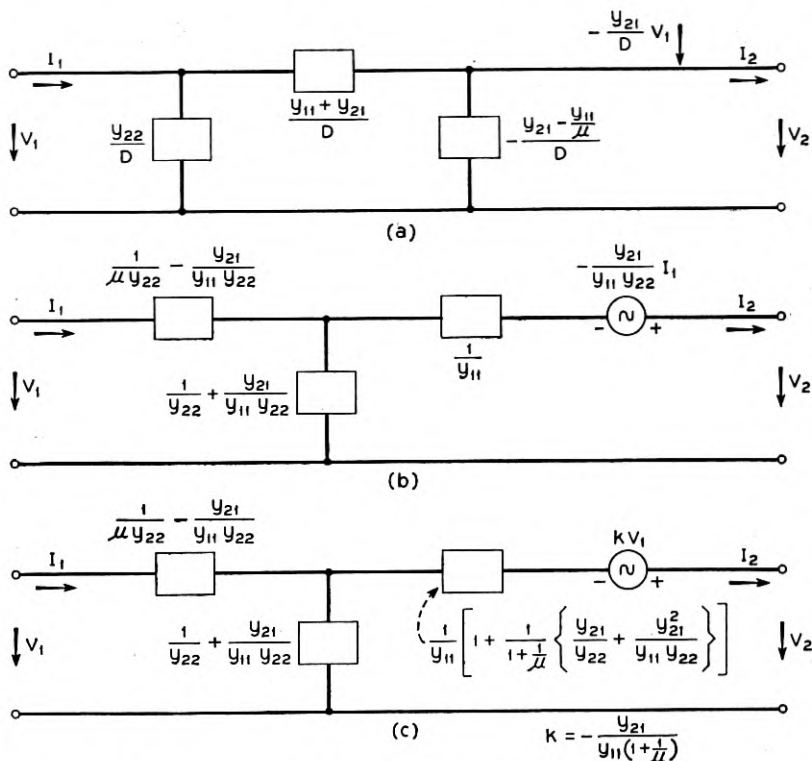
Fig. 21 (a, b, c)—Three forms of equivalent circuits of the grounded plate triode valid at all frequencies.

of resistance, inductance and capacitance. For the networks now under consideration other quantities also need to be included. However, as normally operated there is usually complete space-charge in the cathode-grid region and a very small amount of space charge in the grid-plate region. Under such circumstances the admittance y_{22} is a simple capacitance and the amplification factor μ is a real number. The admittances y_{11} and y_{21}, on the other hand, do not allow accepted circuit interpretation to be made, except in the range of moderately low frequencies when electron transit

time is taken into account only to a first order of approximation. It is believed that, in general, these admittances should be considered complete by themselves as new admittance elements, and, as already remarked, their values in magnitude and phase may be found in the paper on vacuum tube networks to which repeated reference has been made.

As a further property of the networks, consider the expressions for the β's in Tables I, II and III. It is observed that each β_{ij} of a set of β's contains a common term, suggesting that the networks might be broken up into at least two elementary constituents. The same observation applies to each of the three sets of Z's. In Table I, for example, it is seen that this constant term is represented by y_{22}/D. The network of Fig. 19a can thus be thought of as arising from the superposition of two networks, one of which is determined by the parameters

$$\left.\begin{array}{ll} \beta'_{11} = \dfrac{y_{11} + y_{21}}{D} & \beta'_{12} = 0 \\[3mm] \beta'_{21} = \dfrac{y_{21}}{D} & \beta'_{22} = -\dfrac{y_{11}}{\mu D} \end{array}\right\} \tag{25}$$

and the other by the parameters

$$\left.\begin{array}{ll} \beta''_{11} = \dfrac{y_{22}}{D} & \beta''_{12} = -\dfrac{y_{22}}{D} \\[3mm] \beta''_{21} = \dfrac{y_{22}}{D} & \beta''_{22} = -\dfrac{y_{22}}{D} \end{array}\right\} \tag{26}$$

The admittance coefficients given by (25) correspond to the perfectly unilateral active network shown in Fig. 22a, while the admittance coefficients in (26) correspond to the "passive" network in Fig. 22b. The two elementary constituents thus take the general forms of these networks. It should be noticed that these two network constituents are unrelated to the fact that the total current entering the complete network is the sum of conduction and displacement current.

Corresponding to the Z's other elementary constituents are obtained, with general forms as shown on Figs. 23a and 23b.

These elementary constituents are merely reflections of certain mathematical identities. For example, the networks in Fig. 22 depend upon the matrix identity

$$\left\| \begin{array}{l} \beta_{11}\beta_{12} \\ \beta_{21}\beta_{22} \end{array} \right\| \equiv \left\| \begin{array}{cc} \beta_{11} + \beta_{12} & 0 \\ \beta_{21} + \beta_{12} & \beta_{22} - \beta_{12} \end{array} \right\| + \left\| \begin{array}{c} -\beta_{12}\beta_{12} \\ -\beta_{12}\beta_{12} \end{array} \right\| \tag{27}$$

while those in Fig. 23 depend upon a corresponding identity.   The identity (27) expresses the fact that the general "β-network" can be considered as arising from the parallel connections of the two networks in Fig. 24.
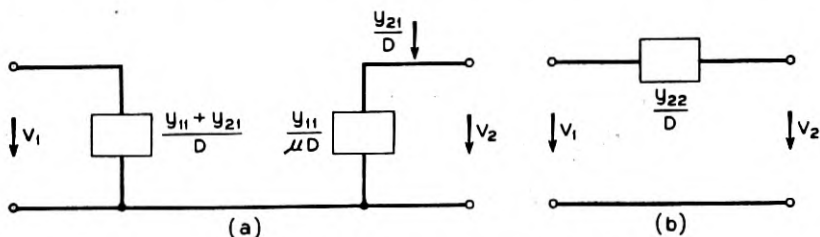
Fig. 22 (a, b)—Elementary constituents of Fig. 19a.
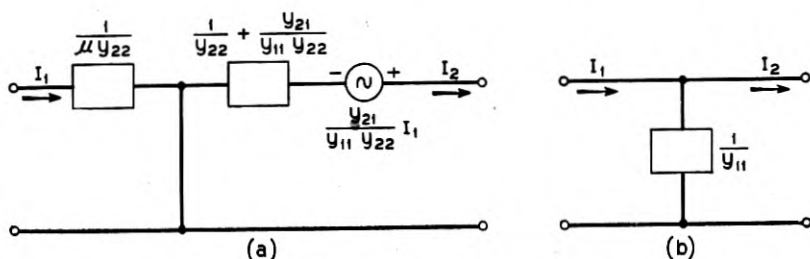
Fig. 23 (a, b)—Elementary constituents of Fig. 19b.
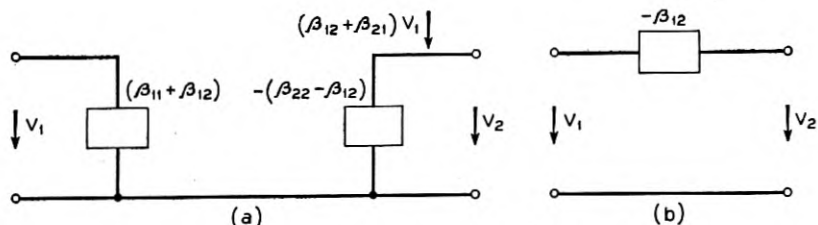
Fig. 24 (a, b)—Elementary constituents of Fig. 8.

There is at present a tendency towards grid designs of very fine mesh. Such a grid design results in a very large value of the amplification factor and, for many purposes, sufficient accuracy may be obtained by disregarding terms containing $\dfrac{1}{\mu}$ as a factor.   Under these conditions the network for grounded cathode operation reduces to an L-network, that for grounded grid operation to a unilateral network transmitting in the direction from grid to plate only, while the cathode follower network remains essentially unchanged.

TABLE IV

FOUR-POLE PARAMETERS FOR GROUNDED CATHODE TRIODE IN THE RANGE OF MODERATELY LOW FREQUENCIES

$$\beta_{11} = \frac{1}{5}\frac{(\omega C_1)^2}{g_0}\frac{F}{\left[1 + \dfrac{1}{\mu}\left(1 + \dfrac{4}{3}\dfrac{x_2}{x_1}f\right)\right]^2} + i\omega\frac{\frac{4}{3}C_1 f + C_2}{1 + \dfrac{1}{\mu}\left(1 + \dfrac{4}{3}\dfrac{x_2}{x_1}f\right)}$$

$$\beta_{12} = -\left[-\frac{(\omega C_1)^2}{g_0}\frac{1}{5\mu}\frac{F}{\left[1 + \dfrac{1}{\mu}\left(1 + \dfrac{4}{3}\dfrac{x_2}{x_1}f\right)\right]^2} + i\omega\frac{C_2}{1 + \dfrac{1}{\mu}\left(1 + \dfrac{4}{3}\dfrac{x_2}{x_1}f\right)}\right]$$

$$\beta_{22} = -\left[\frac{g_0}{\mu}\frac{1}{1 + \dfrac{1}{\mu}\left(1 + \dfrac{4}{3}\dfrac{x_2}{x_1}f\right)} + i\omega\frac{C_2 + \dfrac{6}{10\mu}C_1}{1 + \dfrac{1}{\mu}\left(1 + \dfrac{4}{3}\dfrac{x_2}{x_1}f\right)}\right]$$

$$\beta_{12} + \beta_{21} = -\frac{g_0}{1 + \dfrac{1}{\mu}\left(1 + \dfrac{4}{3}\dfrac{x_2}{x_1}f\right)}$$

$$\left[1 - i\frac{11}{30}\theta_1\left(1 - \frac{3}{11\mu}\frac{\dfrac{x_2}{x_1}F}{1 + \dfrac{1}{\mu}\left(1 + \dfrac{4}{3}\dfrac{x_2}{x_1}f\right)}\right) - i\frac{1}{3}\theta_2 k\right]$$

TABLE V

FOUR-POLE PARAMETERS FOR GROUNDED GRID TRIODE IN THE RANGE OF MODERATELY LOW FREQUENCIES

$$\beta_{11} = g_0\frac{1 + \dfrac{1}{\mu}}{1 + \dfrac{1}{\mu}\left(1 + \dfrac{4}{3}\dfrac{x_2}{x_1}f\right)} + i\omega\frac{6}{10}C_1\frac{1 + \dfrac{1}{\mu}}{1 + \dfrac{1}{\mu}\left(1 + \dfrac{4}{3}\dfrac{x_2}{x_1}f\right)}\left[1 + \frac{\dfrac{1}{\mu}\dfrac{x_2}{x_1}}{1 + \dfrac{1}{\mu}\left(1 + \dfrac{4}{3}\dfrac{x_2}{x_1}f\right)}\right]$$

$$\beta_{12} = -\frac{g_0}{\mu}\cdot\frac{1}{1 + \dfrac{1}{\mu}\left(1 + \dfrac{4}{3}\dfrac{x_2}{x_1}f\right)} - i\omega\frac{6}{10}\frac{C_1}{\mu}$$

$$\cdot\frac{1}{1 + \dfrac{1}{\mu}\left(1 + \dfrac{4}{3}\dfrac{x_2}{x_1}f\right)}\left[1 + \frac{1}{3}\frac{\dfrac{1}{\mu}\dfrac{x_2}{x_1}F}{1 + \dfrac{1}{\mu}\left(1 + \dfrac{4}{3}\dfrac{x_2}{x_1}f\right)}\right]$$

$$\beta_{22} = -\left[\frac{g_0}{\mu}\cdot\frac{1}{1 + \dfrac{1}{\mu}\left(1 + \dfrac{4}{3}\dfrac{x_2}{x_1}f\right)} + i\omega\left(\frac{C_2 + \dfrac{6}{10\mu}C_1}{1 + \dfrac{1}{\mu}\left(1 + \dfrac{4}{3}\dfrac{x_2}{x_1}f\right)}\right)\right]$$

$$\beta_{12} + \beta_{21} = \frac{g_0}{1 + \dfrac{1}{\mu}\left(1 + \dfrac{4}{3}\dfrac{x_2}{x_1}f\right)}\left[1 - i\frac{11}{30}\theta_1\left(1 - \frac{3}{11\mu}\frac{\dfrac{x_2}{x_1}F}{1 + \dfrac{1}{\mu}\left(1 + \dfrac{4}{3}\dfrac{x_2}{x_1}f\right)}\right) - i\frac{1}{3}\theta_2 k\right]$$

In the foregoing, the behavior of an active four-pole has been described either in terms of four-pole parameters or in terms of elements of an equivalent circuit. The particular four-pole parameters, which are of customary use in communication engineering, are the so-called image parameters, but they have usually been used only in connection with passive four-poles. They may, however, also be used in the more general vacuum tube four-pole now under discussion, but whether their employment would be of practical

TABLE VI

FOUR-POLE PARAMETERS FOR GROUNDED PLATE TRIODE IN THE RANGE OF MODERATELY LOW FREQUENCIES

$$\beta_{11} = \frac{1}{5}\frac{(\omega C_1)^2}{g_0}\frac{F}{\left[1 + \frac{1}{\mu}\left(1 + \frac{4}{3}\frac{x_2}{x_1}f\right)\right]^2} + i\omega\frac{\frac{4}{3}C_1 f + C_2}{1 + \frac{1}{\mu}\left(1 + \frac{4}{3}\frac{x_2}{x_1}f\right)}$$

$$\beta_{12} = -\left[\frac{1}{5}\frac{(\omega C_1)^2}{g_0}\frac{F\left(1 + \frac{1}{\mu}\right)}{\left[1 + \frac{1}{\mu}\left(1 + \frac{4}{3}\frac{x_2}{x_1}f\right)\right]^2} + i\omega\frac{\frac{4}{3}C_1 f}{1 + \frac{1}{\mu}\left(1 + \frac{4}{3}\frac{x_2}{x_1}f\right)}\right]$$

$$\beta_{22} = -\left[g_0\frac{1 + \frac{1}{\mu}}{1 + \frac{1}{\mu}\left(1 + \frac{4}{3}\frac{x_2}{x_1}f\right)} + i\omega\frac{6}{10}C_1\frac{1 + \frac{1}{\mu}}{1 + \frac{1}{\mu}\left(1 + \frac{4}{3}\frac{x_2}{x_1}f\right)}\right.$$
$$\left.\cdot\left[1 + \frac{1}{3}\frac{\frac{1}{\mu}\frac{x_2}{x_1}F}{1 + \frac{1}{\mu}\left(1 + \frac{4}{3}\frac{x_2}{x_1}f\right)}\right]\right]$$

$$\beta_{12} + \beta_{21} = \frac{g_0}{1 + \frac{1}{\mu}\left(1 + \frac{4}{3}\frac{x_2}{x_1}f\right)}\left[1 - i\frac{11}{30}\theta_1\left(1 - \frac{3}{11\mu}\frac{\frac{x_2}{x_1}F}{1 + \frac{1}{\mu}\left(1 + \frac{4}{3}\frac{x_2}{x_1}f\right)}\right) - i\frac{1}{3}\theta_2 k\right]$$

value is a matter which engineering experience will decide. In any case their use would be limited to vacuum tubes in which appreciable interaction between input and output terminals is present. From a practical standpoint this means that their usefulness would be mainly found in connection with triodes.

TRIODE NETWORKS AT MODERATELY LOW FREQUENCIES

The networks discussed in the preceding section were of general validity in respect to both operating conditions and frequency and it was mentioned

that the efforts of trying to interpret the "passive" parts of the networks in the form of lumped passive circuit elements had, in general, met with not too much success. In this section attention will be given to the range of moderately low frequencies where usual circuit interpretation is possible. The operating conditions are assumed to be the usual ones with complete
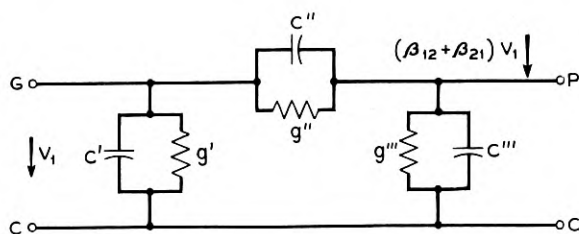
$$g' = \frac{1}{5}\frac{(\omega C_1)^2}{g_0} F \frac{1 + \frac{1}{\mu}}{\left[1 + \frac{1}{\mu}\left(1 + \frac{4}{3}\frac{x_2}{x_1}f\right)\right]^2}$$

$$C' = \frac{4}{3}C_1 \frac{f}{1 + \frac{1}{\mu}\left(1 + \frac{4}{3}\frac{x_2}{x_1}f\right)}$$

$$g'' = -\frac{(\omega C_1)^2}{5g_0}\frac{1}{\mu} \frac{F}{1 + \frac{1}{\mu}\left(1 + \frac{4}{3}\frac{x_2}{x_1}f\right)}$$

$$C'' = C_2 \frac{1}{1 + \frac{1}{\mu}\left(1 + \frac{4}{3}\frac{x_2}{x_1}f\right)}$$

$$g''' = \frac{g_0}{\mu} \frac{1}{1 + \frac{1}{\mu}\left(1 + \frac{4}{3}\frac{x_2}{x_1}f\right)}$$

Fig. 25—Equivalent circuit of grounded cathode triode at moderately high frequencies.

space charge in the cathode-grid region, and negligible space charge in the grid-plate region. Also it will be assumed that the grid is at negative d-c potential with respect to the cathode.

The first step is to expand the β coefficients in series with transit angles retained only to first or possibly to second orders. As the detailed computations are lengthy only the final result will be given. These are presented in Tables IV, V and VI.
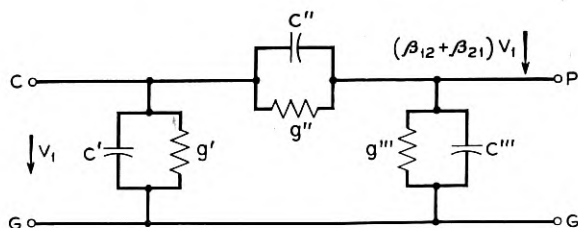
$$g' = g_0 \frac{1}{1 + \frac{1}{\mu}\left(1 + \frac{4}{3}\frac{x_2}{x_1}f\right)}$$

$$C' = \frac{6}{10}C_1 \frac{1}{1 + \frac{1}{\mu}\left(1 + \frac{4}{3}\frac{x_2}{x_1}f\right)}\left[1 + \frac{1}{3\mu}\frac{\frac{x_2}{x_1}F}{1 + \frac{1}{\mu}\left(1 + \frac{4}{3}\frac{x_2}{x_1}f\right)}\right]$$

$$g'' = \frac{1}{\mu}g'$$

$$C'' = \frac{1}{\mu}C'$$

$$g''' = -\frac{(\omega C_1)^2}{5g_0}\frac{1}{\mu}\frac{F}{\left[1 + \frac{1}{\mu}\left(1 + \frac{4}{3}\frac{x_2}{x_1}f\right)\right]^2}$$

$$C''' = C_2 \frac{1}{1 + \frac{1}{\mu}\left(1 + \frac{4}{3}\frac{x_2}{x_1}f\right)}$$

Fig. 26—Equivalent circuit of grounded grid triode at moderately high frequencies.

In these tables the symbols have the following meanings:

g_0 = static conductance of the diode formed by the cathode and equivalent grid-plane.

μ = low frequency amplification factor.

x_1 = cathode-grid distance in cm.

x_2 = grid-anode distance in cm.

C_1 = cold capacitance between cathode and equivalent grid plane

C_2 = cold capacitance between anode and equivalent grid plane.

Θ_1 = electron transit angle between cathode and equivalent grid plane. It is most simply calculated from

$$\theta_1 = 2\frac{\omega C_1}{g_0}$$

Θ_2 = electron transit angle between anode and equivalent grid plane.
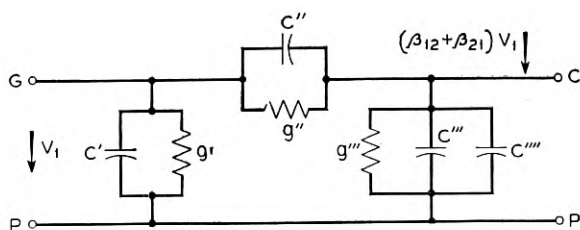
$$g' = -\frac{(\omega C_1)^2}{5g_0}\frac{1}{\mu}\frac{F}{\left[1+\frac{1}{\mu}\left(1+\frac{4}{3}\frac{x_2}{x_1}f\right)\right]^2}$$

$$C' = C_2\frac{1}{1+\frac{1}{\mu}\left(1+\frac{4}{3}\frac{x_2}{x_1}f\right)}$$

$$g'' = \frac{(\omega C_1)^2}{5g_0}F\frac{1+\frac{1}{\mu}}{\left[1+\frac{1}{\mu}\left(1+\frac{4}{3}\frac{x_2}{x_1}f\right)\right]^2}$$

$$C'' = \frac{4}{3}C_1\frac{f}{1+\frac{1}{\mu}\left(1+\frac{4}{3}\frac{x_2}{x_1}f\right)}$$

$$g''' = g_0\frac{1+\frac{1}{\mu}}{1+\frac{1}{\mu}\left(1+\frac{4}{3}\frac{x_2}{x_1}f\right)}$$

$$C''' = \frac{6}{10}\frac{C_1}{\mu}\frac{1}{1+\frac{1}{\mu}\left(1+\frac{4}{3}\frac{x_2}{x_1}f\right)}\left[1+\frac{1}{3}\frac{\frac{x_2}{x_1}F}{1+\frac{1}{\mu}\left(1+\frac{4}{3}\frac{x_2}{x_1}f\right)}\right]$$

$$C'''' = -\frac{11}{15}C_1\frac{1+\frac{10}{11}\frac{\theta_2}{\theta_1}k_1}{1+\frac{1}{\mu}\left(1+\frac{4}{3}\frac{x_2}{x_1}f\right)}$$

Fig. 27—Equivalent circuit of grounded plate triode at moderately high frequencies.

It may be calculated from

$$\theta_2 = \frac{\omega 2 x_2}{\sqrt{2\eta}\left(\sqrt{V_{D1}} + \sqrt{V_{D2}}\right)}$$

where $\eta = 10^7 \dfrac{e}{m} = 1.76 \times 10^{15}$

V_{D1} = equivalent d-c grid potential

V_{D2} = anode d-c potential

$$F = 1 + \frac{22}{9}\frac{\theta_2}{\theta_1}\frac{\sqrt{V_{D1}} + 2\sqrt{V_{D2}}}{\sqrt{V_{D1}} + \sqrt{V_{D2}}} + \frac{5}{3}\left(\frac{\theta_2}{\theta_1}\right)^2 \frac{\sqrt{V_{D1}} + 3\sqrt{V_{D2}}}{\sqrt{V_{D1}} + \sqrt{V_{D2}}}$$

$$f = 1 + \frac{1}{2}\frac{\theta_2}{\theta_1}\frac{\sqrt{V_{D1}} + 2\sqrt{V_{D2}}}{\sqrt{V_{D1}} + \sqrt{V_{D2}}}$$

$$k = \frac{\sqrt{V_{D1}} + 2\sqrt{V_{D2}}}{\sqrt{V_{D1}} + \sqrt{V_{D2}}}$$

With the aid of these tables and Fig. 8 the equivalent circuits on Figs. 25, 26 and 27 are obtained. The networks are all of the resistance-capacity type. It may be noted that, in some of the branches, negative conductance or negative capacitance appears. However, as seen from the external tube terminals they are swamped by corresponding positive elements.

The viewpoints presented in this paper have been used by the writer over a number of years. They have been given experimental application by Mr. J. A. Morton, who is principally responsible for their introduction and use in the studies in these Laboratories of electron tubes in the microwave regions.

With this, our investigation comes to a close. Much has been omitted, particularly in the field of applications, but it is nevertheless hoped the fundamental approach, as well as the networks given, may prove to be useful in practical applications. The questions of noise and of optimum noise figure design have also been left out of consideration. Mr. J. A. Morton and the writer plan to discuss these problems in a forthcoming paper.

The writer is pleased to acknowledge his indebtedness to Messrs. R. K. Potter, J. A. Morton, and R. M. Ryder, who have encouraged this work and urged its publication; and to Mr. W. E. Kirkpatrick for constructively critical scrutiny of the original technical memorandum.

A Mathematical Theory of Communication

By C. E. SHANNON

PART III: MATHEMATICAL PRELIMINARIES

In this final installment of the paper we consider the case where the signals or the messages or both are continuously variable, in contrast with the discrete nature assumed until now. To a considerable extent the continuous case can be obtained through a limiting process from the discrete case by dividing the continuum of messages and signals into a large but finite number of small regions and calculating the various parameters involved on a discrete basis. As the size of the regions is decreased these parameters in general approach as limits the proper values for the continuous case. There are, however, a few new effects that appear and also a general change of emphasis in the direction of specialization of the general results to particular cases.

We will not attempt, in the continuous case, to obtain our results with the greatest generality, or with the extreme rigor of pure mathematics, since this would involve a great deal of abstract measure theory and would obscure the main thread of the analysis. A preliminary study, however, indicates that the theory can be formulated in a completely axiomatic and rigorous manner which includes both the continuous and discrete cases and many others. The occasional liberties taken with limiting processes in the present analysis can be justified in all cases of practical interest.

18. Sets and Ensembles of Functions

We shall have to deal in the continuous case with sets of functions and ensembles of functions. A set of functions, as the name implies, is merely a class or collection of functions, generally of one variable, time. It can be specified by giving an explicit representation of the various functions in the set, or implicitly by giving a property which functions in the set possess and others do not. Some examples are:

1. The set of functions:

$$f_\theta(t) = \sin (t + \theta).$$

Each particular value of θ determines a particular function in the set.

623

2. The set of all functions of time containing no frequencies over W cycles per second.

3. The set of all functions limited in band to W and in amplitude to A.

4. The set of all English speech signals as functions of time.

An *ensemble* of functions is a set of functions together with a probability measure whereby we may determine the probability of a function in the set having certain properties.[1]   For example with the set,

$$f_\theta(t) = \sin (t + \theta),$$

we may give a probability distribution for θ, $P(\theta)$.   The set then becomes an ensemble.

Some further examples of ensembles of functions are:

1. A finite set of functions $f_k(t)$ $(k = 1, 2, \cdots, n)$ with the probability of f_k being p_k.

2. A finite dimensional family of functions

$$f(\alpha_1, \alpha_2, \cdots, \alpha_n ; t)$$

with a probability distribution for the parameters α_i :

$$p(\alpha_1, \cdots, \alpha_n)$$

For example we could consider the ensemble defined by

$$f(a_1, \cdots, a_n, \theta_1, \cdots, \theta_n ; t) = \sum_{n=1}^{n} a_n \sin n(\omega t + \theta_n)$$

with the amplitudes a_i distributed normally and independently, and the phrases θ_i distributed uniformly (from 0 to 2π) and independently.

3. The ensemble

$$f(a_i, t) = \sum_{n=-\infty}^{+\infty} a_n \frac{\sin \pi(2Wt - n)}{\pi(2Wt - n)}$$

with the a_i normal and independent all with the same standard deviation $\sqrt{N}$.   This is a representation of "white" noise, band-limited to the band from 0 to W cycles per second and with average power N.[2]

---

[1] In mathematical terminology the functions belong to a measure space whose total measure is unity.

[2] This representation can be used as a definition of band limited white noise. It has certain advantages in that it involves fewer limiting operations than do definitions that have been used in the past. The name "white noise," already firmly intrenched in the literature, is perhaps somewhat unfortunate. In optics white light means either any continuous spectrum as contrasted with a point spectrum, or a spectrum which is flat with *wavelength* (which is not the same as a spectrum flat with frequency).

4. Let points be distributed on the t axis according to a Poisson distribution. At each selected point the function $f(t)$ is placed and the different functions added, giving the ensemble

$$\sum_{k=-\infty}^{\infty} f(t + t_k)$$

where the t_k are the points of the Poisson distribution. This ensemble can be considered as a type of impulse or shot noise where all the impulses are identical.

5. The set of English speech functions with the probability measure given by the frequency of occurrence in ordinary use.

An ensemble of functions $f_\alpha(t)$ is *stationary* if the same ensemble results when all functions are shifted any fixed amount in time. The ensemble

$$f_\theta(t) = \sin (t + \theta)$$

is stationary if θ distributed uniformly from 0 to 2π. If we shift each function by t_1 we obtain

$$f_\theta(t + t_1) = \sin (t + t_1 + \theta)$$
$$= \sin (t + \varphi)$$

with φ distributed uniformly from 0 to 2π. Each function has changed but the ensemble as a whole is invariant under the translation. The other examples given above are also stationary.

An ensemble is *ergodic* if it is stationary, and there is no subset of the functions in the set with a probability different from 0 and 1 which is stationary. The ensemble

$$\sin (t + \theta)$$

is ergodic. No subset of these functions of probability $\neq$0, 1 is transformed into itself under all time translations. On the other hand the ensemble

$$a \sin (t + \theta)$$

with a distributed normally and θ uniform is stationary but not ergodic. The subset of these functions with a between 0 and 1 for example is stationary.

Of the examples given, 3 and 4 are ergodic, and 5 may perhaps be considered so. If an ensemble is ergodic we may say roughly that each function in the set is typical of the ensemble. More precisely it is known that with an ergodic ensemble an average of any statistic over the ensemble is equal (with probability 1) to an average over all the time translations of a

particular function in the set.[3] Roughly speaking, each function can be expected, as time progresses, to go through, with the proper frequency, all the convolutions of any of the functions in the set.

Just as we may perform various operations on numbers or functions to obtain new numbers or functions, we can perform operations on ensembles to obtain new ensembles. Suppose, for example, we have an ensemble of functions $f_\alpha(t)$ and an operator T which gives for each function $f_\alpha(t)$ a result $g_\alpha(t)$:

$$g_\alpha(t) = Tf_\alpha(t)$$

Probability measure is defined for the set $g_\alpha(t)$ by means of that for the set $f_\alpha(t)$. The probability of a certain subset of the $g_\alpha(t)$ functions is equal to that of the subset of the $f_\alpha(t)$ functions which produce members of the given subset of g functions under the operation T. Physically this corresponds to passing the ensemble through some device, for example, a filter, a rectifier or a modulator. The output functions of the device form the ensemble $g_\alpha(t)$.

A device or operator T will be called invariant if shifting the input merely shifts the output, i.e., if

$$g_\alpha(t) = Tf_\alpha(t)$$

implies

$$g_\alpha(t + t_1) = Tf_\alpha(t + t_1)$$

for all $f_\alpha(t)$ and all t_1. It is easily shown (see appendix 1) that if T is invariant and the input ensemble is stationary then the output ensemble is stationary. Likewise if the input is ergodic the output will also be ergodic.

A filter or a rectifier is invariant under all time translations. The operation of modulation is not since the carrier phase gives a certain time structure. However, modulation is invariant under all translations which are multiples of the period of the carrier.

Wiener has pointed out the intimate relation between the invariance of physical devices under time translations and Fourier theory.[4] He has

---

[3] This is the famous ergodic theorem or rather one aspect of this theorem which was proved is somewhat different formulations by Birkhoff, von Neumann, and Koopman, and subsequently generalized by Wiener, Hopf, Hurewicz and others. The literature on ergodic theory is quite extensive and the reader is referred to the papers of these writers for precise and general formulations; e.g., E. Hopf "Ergodentheorie" Ergebnisse der Mathematic und ihrer Grenzgebiete, Vol. 5, "On Causality Statistics and Probability" Journal of Mathematics and Physics, Vol. XIII, No. 1, 1934; N. Weiner "The Ergodic Theorem" Duke Mathematical Journal, Vol. 5, 1939.

[4] Communication theory is heavily indebted to Wiener for much of its basic philosophy and theory. His classic NDRC report "The Interpolation, Extrapolation, and Smoothing of Stationary Time Series," to appear soon in book form, contains the first clear-cut formulation of communication theory as a statistical problem, the study of operations

shown, in fact, that if a device is linear as well as invariant Fourier analysis is then the appropriate mathematical tool for dealing with the problem.

An ensemble of functions is the appropriate mathematical representation of the messages produced by a continuous source (for example speech), of the signals produced by a transmitter, and of the perturbing noise. Communication theory is properly concerned, as has been emphasized by Wiener, not with operations on particular functions, but with operations on ensembles of functions. A communication system is designed not for a particular speech function and still less for a sine wave, but for the ensemble of speech functions.

19. Band Limited Ensembles of Functions

If a function of time $f(t)$ is limited to the band from 0 to W cycles per second it is completely determined by giving its ordinates at a series of discrete points spaced $\frac{1}{2W}$ seconds apart in the manner indicated by the following result.[5]

Theorem 13: Let $f(t)$ contain no frequencies over W. Then

$$f(t) = \sum_{-\infty}^{\infty} X_n \frac{\sin \pi(2Wt - n)}{\pi(2Wt - n)}$$

where

$$X_n = f\left(\frac{n}{2W}\right).$$

In this expansion $f(t)$ is represented as a sum of orthogonal functions. The coefficients X_n of the various terms can be considered as coordinates in an infinite dimensional "function space." In this space each function corresponds to precisely one point and each point to one function.

A function can be considered to be substantially limited to a time T if all the ordinates X_n outside this interval of time are zero. In this case all but $2TW$ of the coordinates will be zero. Thus functions limited to a band W and duration T correspond to points in a space of $2TW$ dimensions.

A subset of the functions of band W and duration T corresponds to a region in this space. For example, the functions whose total energy is less

---

on time series. This work, although chiefly concerned with the linear prediction and filtering problem, is an important collateral reference in connection with the present paper. We may also refer here to Wiener's forthcoming book "Cybernetics" dealing with the general problems of communication and control.

[5] For a proof of this theorem and further discussion see the author's paper "Communication in the Presence of Noise" to be published in the *Proceedings of the Institute of Radio Engineers.*

than or equal to E correspond to points in a $2TW$ dimensional sphere with radius $r = \sqrt{2WE}$.

An *ensemble* of functions of limited duration and band will be represented by a probability distribution $p(x_1 \cdots x_n)$ in the corresponding n dimensional space.   If the ensemble is not limited in time we can consider the $2TW$ coordinates in a given interval T to represent substantially the part of the function in the interval T and the probability distribution $p(x_1, \cdots, x_n)$ to give the statistical structure of the ensemble for intervals of that duration.

20. Entropy of a Continuous Distribution

The entropy of a discrete set of probabilities $p_1, \cdots p_n$ has been defined as:

$$H = -\sum p_i \log p_i .$$

In an analogous manner we define the entropy of a continuous distribution with the density distribution function $p(x)$ by:

$$H = -\int_{-\infty}^{\infty} p(x) \log p(x) \, dx$$

With an n dimensional distribution $p(x_1, \cdots, x_n)$ we have

$$H = -\int \cdots \int p(x_1 \cdots x_n) \log p(x_1, \cdots, x_n) \, dx_1 \cdots dx_n .$$

If we have two arguments x and y (which may themselves be multi-dimensional) the joint and conditional entropies of $p(x, y)$ are given by

$$H(x, y) = -\int\int p(x, y) \log p(x, y) \, dx \, dy$$

and

$$H_x(y) = -\int\int p(x, y) \log \frac{p(x, y)}{p(x)} \, dx \, dy$$

$$H_y(x) = -\int\int p(x, y) \log \frac{p(x, y)}{p(y)} \, dx \, dy$$

where

$$p(x) = \int p(x, y) \, dy$$

$$p(y) = \int p(x, y) \, dx.$$

The entropy of continuous distributions have most (but not all) of the properties of the discrete case.   In particular we have the following:

1. If x is limited to a certain volume v in its space, then $H(x)$ is a maximum and equal to $\log v$ when $p(x)$ is constant $\left(\dfrac{1}{v}\right)$ in the volume.

2. With any two variables x, y we have

$$H(x, y) \leq H(x) + H(y)$$

with equality if (and only if) x and y are independent, i.e., $p(x, y) = p(x)$ $p(y)$ (apart possibly from a set of points of probability zero).

3. Consider a generalized averaging operation of the following type:

$$p'(y) = \int a(x, y) p(x)\, dx$$

with

$$\int a(x, y)\, dx = \int a(x, y)\, dy = 1, \qquad a(x, y) \geq 0.$$

Then the entropy of the averaged distribution $p'(y)$ is equal to or greater than that of the original distribution $p(x)$.

4. We have

$$H(x, y) = H(x) + H_x(y) = H(y) + H_y(x)$$

and

$$H_x(y) \leq H(y).$$

5. Let $p(x)$ be a one-dimensional distribution. The form of $p(x)$ giving a maximum entropy subject to the condition that the standard deviation of x be fixed at σ is gaussian. To show this we must maximize

$$H(x) = -\int p(x) \log p(x)\, dx$$

with

$$\sigma^2 = \int p(x) x^2\, dx \quad \text{and} \quad 1 = \int p(x)\, dx$$

as constraints. This requires, by the calculus of variations, maximizing

$$\int [-p(x) \log p(x) + \lambda p(x) x^2 + \mu p(x)]\, dx.$$

The condition for this is

$$-1 - \log p(x) + \lambda x^2 + \mu = 0$$

and consequently (adjusting the constants to satisfy the constraints)

$$p(x) = \frac{1}{\sqrt{2\pi}\, \sigma}\, e^{-(x^2/2\sigma^2)}.$$

Similarly in n dimensions, suppose the second order moments of $p(x_1, \cdots, x_n)$ are fixed at A_{ij} :

$$A_{ij} = \int \cdots \int x_i x_j p(x_1, \cdots, x_n)\, dx_1 \cdots dx_n \,.$$

Then the maximum entropy occurs (by a similar calculation) when $p(x_1, \cdots, x_n)$ is the n dimensional gaussian distribution with the second order moments A_{ij}.

6. The entropy of a one-dimensional gaussian distribution whose standard deviation is σ is given by

$$H(x) = \log \sqrt{2\pi e}\, \sigma.$$

This is calculated as follows:

$$p(x) = \frac{1}{\sqrt{2\pi}\, \sigma}\, e^{-(x^2/2\sigma^2)}$$

$$-\log p(x) = \log \sqrt{2\pi}\, \sigma + \frac{x^2}{2\sigma^2}$$

$$H(x) = -\int p(x) \log p(x)\, dx$$

$$= \int p(x) \log \sqrt{2\pi}\, \sigma\, dx + \int p(x)\, \frac{x^2}{2\sigma^2}\, dx$$

$$= \log \sqrt{2\pi}\, \sigma + \frac{\sigma^2}{2\sigma^2}$$

$$= \log \sqrt{2\pi}\, \sigma + \log \sqrt{e}$$

$$= \log \sqrt{2\pi e}\, \sigma.$$

Similarly the n dimensional gaussian distribution with associated quadratic form a_{ij} is given by

$$p(x_1, \cdots, x_n) = \frac{|a_{ij}|^{\frac{1}{2}}}{(2\pi)^{n/2}}\, \exp\left(-\tfrac{1}{2}\Sigma a_{ij} X_i X_j\right)$$

and the entropy can be calculated as

$$H = \log (2\pi e)^{n/2}\, |a_{ij}|^{\frac{1}{2}}$$

where $|a_{ij}|$ is the determinant whose elements are a_{ij}.

7. If x is limited to a half line ($p(x) = 0$ for $x \leq 0$) and the first moment of x is fixed at a:

$$a = \int_0^\infty p(x) x\, dx,$$

then the maximum entropy occurs when

$$p(x) = \frac{1}{a} e^{-(x/a)}$$

and is equal to log ea.

8. There is one important difference between the continuous and discrete entropies. In the discrete case the entropy measures in an *absolute* way the randomness of the chance variable. In the continuous case the measurement is *relative to the coordinate system*. If we change coordinates the entropy will in general change. In fact if we change to coordinates $y_1 \cdots y_n$ the new entropy is given by

$$H(y) = \int \cdots \int p(x_1 \cdots x_n) J \left(\frac{x}{y}\right) \log p(x_1 \cdots x_n) J \left(\frac{x}{y}\right) dy_1 \cdots dy_n$$

where $J \left(\dfrac{x}{y}\right)$ is the Jacobian of the coordinate transformation. On expanding the logarithm and changing variables to $x_1 \cdots x_n$, we obtain:

$$H(y) = H(x) - \int \cdots \int p(x_1, \cdots, x_n) \log J \left(\frac{x}{y}\right) dx_1 \cdots dx_n.$$

Thus the new entropy is the old entropy less the expected logarithm of the Jacobian. In the continuous case the entropy can be considered a measure of randomness *relative to an assumed standard*, namely the coordinate system chosen with each small volume element $dx_1 \cdots dx_n$ given equal weight. When we change the coordinate system the entropy in the new system measures the randomness when equal volume elements $dy_1 \cdots dy_n$ in the new system are given equal weight.

In spite of this dependence on the coordinate system the entropy concept is as important in the continuous case as the discrete case. This is due to the fact that the derived concepts of information rate and channel capacity depend on the *difference* of two entropies and this difference *does not* depend on the coordinate frame, each of the two terms being changed by the same amount.

The entropy of a continuous distribution can be negative. The scale of measurements sets an arbitrary zero corresponding to a uniform distribution over a unit volume. A distribution which is more confined than this has less entropy and will be negative. The rates and capacities will, however, always be non-negative.

9. A particular case of changing coordinates is the linear transformation

$$y_j = \sum_i a_{ij} x_i.$$

In this case the Jacobian is simply the determinant $|a_{ij}|^{-1}$ and

$$H(y) = H(x) + \log |a_{ij}|.$$

In the case of a rotation of coordinates (or any measure preserving transformation) $J = 1$ and $H(y) = H(x)$.

21. Entropy of an Ensemble of Functions

Consider an ergodic ensemble of functions limited to a certain band of width W cycles per second. Let

$$p(x_1 \cdots x_n)$$

be the density distribution function for amplitudes $x_1 \cdots x_n$ at n successive sample points. We define the entropy of the ensemble per degree of freedom by

$$H' = -\operatorname*{Lim}_{n \to \infty} \frac{1}{n} \int \cdots \int p(x_1 \cdots x_n) \log p(x_1, \cdots, x_n) \, dx_1 \cdots dx_n.$$

We may also define an entropy H per second by dividing, not by n, but by the time T in seconds for n samples. Since $n = 2TW$, $H' = 2WH$.

With white thermal noise p is gaussian and we have

$$H' = \log \sqrt{2\pi e N},$$

$$H = W \log 2\pi e N.$$

For a given average power N, white noise has the maximum possible entropy. This follows from the maximizing properties of the Gaussian distribution noted above.

The entropy for a continuous stochastic process has many properties analogous to that for discrete processes. In the discrete case the entropy was related to the logarithm of the *probability* of long sequences, and to the *number* of reasonably probable sequences of long length. In the continuous case it is related in a similar fashion to the logarithm of the *probability density* for a long series of samples, and the *volume* of reasonably high probability in the function space.

More precisely, if we assume $p(x_1 \cdots x_n)$ continuous in all the x_i for all n, then for sufficiently large n

$$\left| \frac{\log p}{n} - H' \right| < \epsilon$$

for all choices of $(x_1, \cdots, x_n)$ apart from a set whose total probability is less than δ, with δ and ϵ arbitrarily small. This follows from the ergodic property if we divide the space into a large number of small cells.

The relation of H to volume can be stated as follows: Under the same assumptions consider the n dimensional space corresponding to $p(x_1, \cdots, x_n)$. Let $V_n(q)$ be the smallest volume in this space which includes in its interior a total probability q. Then

$$\lim_{n \to \infty} \frac{\log V_n(q)}{n} = H'$$

provided q does not equal 0 or 1.

These results show that for large n there is a rather well-defined volume (at least in the logarithmic sense) of high probability, and that within this volume the probability density is relatively uniform (again in the logarithmic sense).

In the white noise case the distribution function is given by

$$p(x_1 \cdots x_n) = \frac{1}{(2\pi N)^{n/2}} \exp - \frac{1}{2N} \Sigma x_i^2 .$$

Since this depends only on Σx_i^2 the surfaces of equal probability density are spheres and the entire distribution has spherical symmetry. The region of high probability is a sphere of radius $\sqrt{nN}$. As $n \to \infty$ the probability of being outside a sphere of radius $\sqrt{n(N + \epsilon)}$ approaches zero and $\frac{1}{n}$ times the logarithm of the volume of the sphere approaches $\log \sqrt{2\pi eN}$.

In the continuous case it is convenient to work not with the entropy H of an ensemble but with a derived quantity which we will call the entropy power. This is defined as the power in a white noise limited to the same band as the original ensemble and having the same entropy. In other words if H' is the entropy of an ensemble its entropy power is

$$N_1 = \frac{1}{2\pi e} \exp 2H'.$$

In the geometrical picture this amounts to measuring the high probability volume by the squared radius of a sphere having the same volume. Since white noise has the maximum entropy for a given power, the entropy power of any noise is less than or equal to its actual power.
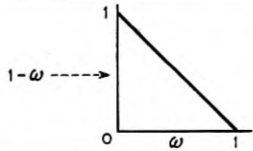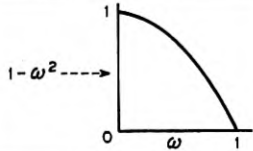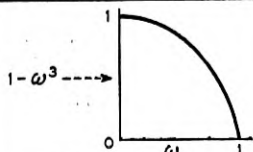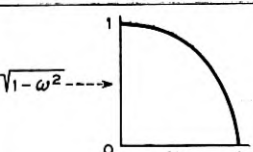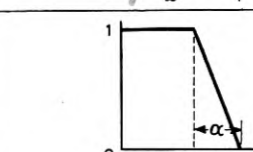
21. Entropy Loss in Linear Filters

Theorem 14: If an ensemble having an entropy H_1 per degree of freedom in band W is passed through a filter with characteristic $Y(f)$ the output ensemble has an entropy

$$H_2 = H_1 + \frac{1}{W} \int_W \log |Y(f)|^2 \, df.$$

The operation of the filter is essentially a linear transformation of coordinates. If we think of the different frequency components as the original coordinate system, the new frequency components are merely the old ones multiplied by factors. The coordinate transformation matrix is thus es-

TABLE I

GAIN	ENTROPY POWER FACTOR	ENTROPY POWER GAIN IN DECIBELS	IMPULSE RESPONSE
$1-\omega$	$\dfrac{1}{e^2}$	-8.68	$\dfrac{\sin^2 \pi t}{(\pi t)^2}$
$1-\omega^2$	$\left(\dfrac{2}{e}\right)^4$	-5.32	$2\left[\dfrac{\sin t}{t^3} - \dfrac{\cos t}{t^2}\right]$
$1-\omega^3$	0.384	-4.15	$6\left[\dfrac{\cos t - 1}{t^4} - \dfrac{\cos t}{2t^2} + \dfrac{\sin t}{t^3}\right]$
$\sqrt{1-\omega^2}$	$\left(\dfrac{2}{e}\right)^2$	-2.66	$\dfrac{\pi}{2} \dfrac{J_1(t)}{t}$
	$\dfrac{1}{e^{2\alpha}}$	$-8.68\,\alpha$	$\dfrac{1}{\alpha t^2}\left[\cos(1-\alpha)t - \cos t\right]$

sentially diagonalized in terms of these coordinates. The Jacobian of the transformation is (for n sine and n cosine components)

$$J = \prod_{i=1}^{n} |Y(f_i)|^2$$

where the f_i are equally spaced through the band W. This becomes in the limit

$$\exp \frac{1}{W} \int_W \log | Y(f) |^2 \, df.$$

Since J is constant its average value is this same quantity and applying the theorem on the change of entropy with a change of coordinates, the result follows. We may also phrase it in terms of the entropy power. Thus if the entropy power of the first ensemble is N_1 that of the second is

$$N_1 \exp \frac{1}{W} \int_W \log | Y(f) |^2 \, df.$$

The final entropy power is the initial entropy power multiplied by the geometric mean gain of the filter. If the gain is measured in db, then the output entropy power will be increased by the arithmetic mean db gain over W.

In Table I the entropy power loss has been calculated (and also expressed in db) for a number of ideal gain characteristics. The impulsive responses of these filters are also given for $W = 2\pi$, with phase assumed to be 0.

The entropy loss for many other cases can be obtained from these results. For example the entropy power factor $\frac{1}{e^2}$ for the first case also applies to any gain characteristic obtained from $1 - \omega$ by a measure preserving transformation of the ω axis. In particular a linearly increasing gain $G(\omega) = \omega$, or a "saw tooth" characteristic between 0 and 1 have the same entropy loss. The reciprocal gain has the reciprocal factor. Thus $\frac{1}{\omega}$ has the factor e^2. Raising the gain to any power raises the factor to this power.

22. Entropy of the Sum of Two Ensembles

If we have two ensembles of functions $f_\alpha(t)$ and $g_\beta(t)$ we can form a new ensemble by "addition." Suppose the first ensemble has the probability density function $p(x_1, \cdots, x_n)$ and the second $q(x_1, \cdots, x_n)$. Then the density function for the sum is given by the convolution:

$$r(x_1, \cdots, x_n) = \int \cdots \int p(y_1, \cdots, y_n)$$
$$\cdot q(x_1 - y_1, \cdots, x_n - y_n) \, dy_1, dy_2, \cdots, dy_n.$$

Physically this corresponds to adding the noises or signals represented by the original ensembles of functions.

The following result is derived in Appendix 6.

Theorem 15: Let the average power of two ensembles be N_1 and N_2 and let their entropy powers be $\bar{N}_1$ and $\bar{N}_2$. Then the entropy power of the sum, $\bar{N}_3$, is bounded by

$$\bar{N}_1 + \bar{N}_2 \leq \bar{N}_3 \leq N_1 + N_2.$$

White Gaussian noise has the peculiar property that it can absorb any other noise or signal ensemble which may be added to it with a resultant entropy power approximately equal to the sum of the white noise power and the signal power (measured from the average signal value, which is normally zero), provided the signal power is small, in a certain sense, compared to the noise.

Consider the function space associated with these ensembles having n dimensions. The white noise corresponds to a spherical Gaussian distribution in this space. The signal ensemble corresponds to another probability distribution, not necessarily Gaussian or spherical. Let the second moments of this distribution about its center of gravity be a_{ij}. That is, if $p(x_1, \cdots, x_n)$ is the density distribution function

$$a_{ij} = \int \cdots \int p(x_i - \alpha_i)(x_j - \alpha_j)\, dx_1, \cdots, dx_n$$

where the α_i are the coordinates of the center of gravity. Now a_{ij} is a positive definite quadratic form, and we can rotate our coordinate system to align it with the principal directions of this form. a_{ij} is then reduced to diagonal form b_{ii}. We require that each b_{ii} be small compared to N, the squared radius of the spherical distribution.

In this case the convolution of the noise and signal produce a Gaussian distribution whose corresponding quadratic form is

$$N + b_{ii}.$$

The entropy power of this distribution is

$$[\Pi(N + b_{ii})]^{1/n}$$

or approximately

$$= [(N)^n + \Sigma b_{ii}(N)^{n-1}]^{1/n}$$

$$\doteq N + \frac{1}{n}\Sigma b_{ii}.$$

The last term is the signal power, while the first is the noise power.

PART IV: THE CONTINUOUS CHANNEL

23. THE CAPACITY OF A CONTINUOUS CHANNEL

In a continuous channel the input or transmitted signals will be continuous functions of time $f(t)$ belonging to a certain set, and the output or received signals will be perturbed versions of these. We will consider only the case where both transmitted and received signals are limited to a certain band W. They can then be specified, for a time T, by $2TW$ numbers, and their statistical structure by finite dimensional distribution functions. Thus the statistics of the transmitted signal will be determined by

$$P(x_1, \cdots, x_n) = P(x)$$

and those of the noise by the conditional probability distribution

$$P_{x_1, \cdots, x_n}(y_1, \cdots, y_n) = P_x(y).$$

The rate of transmission of information for a continuous channel is defined in a way analogous to that for a discrete channel, namely

$$R = H(x) - H_y(x)$$

where $H(x)$ is the entropy of the input and $H_y(x)$ the equivocation. The channel capacity C is defined as the maximum of R when we vary the input over all possible ensembles. This means that in a finite dimensional approximation we must vary $P(x) = P(x_1, \cdots, x_n)$ and maximize

$$- \int P(x) \log P(x) \, dx + \int\int P(x, y) \log \frac{P(x, y)}{P(y)} \, dx \, dy.$$

This can be written

$$\int\int P(x, y) \log \frac{P(x, y)}{P(x)P(y)} \, dx \, dy$$

using the fact that $\int\int P(x, y) \log P(x) \, dx \, dy = \int P(x) \log P(x) \, dx$. The channel capacity is thus expressed

$$C = \operatorname*{Lim}_{T \to \infty} \operatorname*{Max}_{P(x)} \frac{1}{T} \int\int P(x, y) \log \frac{P(x, y)}{P(x)P(y)} \, dx \, dy.$$

It is obvious in this form that R and C are independent of the coordinate system since the numerator and denominator in $\log \dfrac{P(x, y)}{P(x)P(y)}$ will be multiplied by the same factors when x and y are transformed in any one to one way. This integral expression for C is more general than $H(x) - H_y(x)$. Properly interpreted (see Appendix 7) it will always exist while $H(x) - H_y(x)$

may assume an indeterminate form $\infty - \infty$ in some cases. This occurs, for example, if x is limited to a surface of fewer dimensions than n in its n dimensional approximation.

If the logarithmic base used in computing $H(x)$ and $H_y(x)$ is two then C is the maximum number of binary digits that can be sent per second over the channel with arbitrarily small equivocation, just as in the discrete case. This can be seen physically by dividing the space of signals into a large number of small cells, sufficiently small so that the probability density $P_x(y)$ of signal x being perturbed to point y is substantially constant over a cell (either of x or y). If the cells are considered as distinct points the situation is essentially the same as a discrete channel and the proofs used there will apply. But it is clear physically that this quantizing of the volume into individual points cannot in any practical situation alter the final answer significantly, provided the regions are sufficiently small. Thus the capacity will be the limit of the capacities for the discrete subdivisions and this is just the continuous capacity defined above.

On the mathematical side it can be shown first (see Appendix 7) that if u is the message, x is the signal, y is the received signal (perturbed by noise) and v the recovered message then

$$H(x) - H_y(x) \geq H(u) - H_v(u)$$

regardless of what operations are performed on u to obtain x or on y to obtain v. Thus no matter how we encode the binary digits to obtain the signal, or how we decode the received signal to recover the message, the discrete rate for the binary digits does not exceed the channel capacity we have defined. On the other hand, it is possible under very general conditions to find a coding system for transmitting binary digits at the rate C with as small an equivocation or frequency of errors as desired. This is true, for example, if, when we take a finite dimensional approximating space for the signal functions, $P(x, y)$ is continuous in both x and y except at a set of points of probability zero.

An important special case occurs when the noise is added to the signal and is independent of it (in the probability sense). Then $P_x(y)$ is a function only of the difference $n = (y - x)$,

$$P_x(y) = Q(y - x)$$

and we can assign a definite entropy to the noise (independent of the statistics of the signal), namely the entropy of the distribution $Q(n)$. This entropy will be denoted by $H(n)$.

Theorem 16: If the signal and noise are independent and the received signal is the sum of the transmitted signal and the noise then the rate of

transmission is

$$R = H(y) - H(n)$$

i.e., the entropy of the received signal less the entropy of the noise. The channel capacity is

$$C = \underset{P(x)}{\text{Max}}\, H(y) - H(n).$$

We have, since $y = x + n$:

$$H(x, y) = H(x, n).$$

Expanding the left side and using the fact that x and n are independent

$$H(y) + H_y(x) = H(x) + H(n).$$

Hence

$$R = H(x) - H_y(x) = H(y) - H(n).$$

Since $H(n)$ is independent of $P(x)$, maximizing R requires maximizing $H(y)$, the entropy of the received signal. If there are certain constraints on the ensemble of transmitted signals, the entropy of the received signal must be maximized subject to these constraints.

24. Channel Capacity with an Average Power Limitation

A simple application of Theorem 16 is the case where the noise is a white thermal noise and the transmitted signals are limited to a certain average power P. Then the received signals have an average power $P + N$ where N is the average noise power. The maximum entropy for the received signals occurs when they also form a white noise ensemble since this is the greatest possible entropy for a power $P + N$ and can be obtained by a suitable choice of the ensemble of transmitted signals, namely if they form a white noise ensemble of power P. The entropy (per second) of the received ensemble is then

$$H(y) = W \log 2\pi e (P + N),$$

and the noise entropy is

$$H(n) = W \log 2\pi e N.$$

The channel capacity is

$$C = H(y) - H(n) = W \log \frac{P + N}{N}.$$

Summarizing we have the following:

Theorem 17: The capacity of a channel of band W perturbed by white

thermal noise of power N when the average transmitter power is P is given by

$$C = W \log \frac{P + N}{N}.$$

This means of course that by sufficiently involved encoding systems we can transmit binary digits at the rate $W \log_2 \frac{P + N}{N}$ bits per second, with arbitrarily small frequency of errors. It is not possible to transmit at a higher rate by any encoding system without a definite positive frequency of errors.

To approximate this limiting rate of transmission the transmitted signals must approximate, in statistical properties, a white noise.[6] A system which approaches the ideal rate may be described as follows: Let $M = 2^s$ samples of white noise be constructed each of duration T. These are assigned binary numbers from 0 to $(M - 1)$. At the transmitter the message sequences are broken up into groups of s and for each group the corresponding noise sample is transmitted as the signal. At the receiver the M samples are known and the actual received signal (perturbed by noise) is compared with each of them. The sample which has the least R.M.S. discrepancy from the received signal is chosen as the transmitted signal and the corresponding binary number reconstructed. This process amounts to choosing the most probable (*a posteriori*) signal. The number M of noise samples used will depend on the tolerable frequency ϵ of errors, but for almost all selections of samples we have

$$\underset{\substack{\epsilon \to 0 \\ T \to \infty}}{\text{Lim Lim}} \frac{\log M(\epsilon, T)}{T} = W \log \frac{P + N}{N},$$

so that no matter how small ϵ is chosen, we can, by taking T sufficiently large, transmit as near as we wish to $TW \log \frac{P + N}{N}$ binary digits in the time T.

Formulas similar to $C = W \log \frac{P + N}{N}$ for the white noise case have been developed independently by several other writers, although with somewhat different interpretations. We may mention the work of N. Wiener,[7] W. G. Tuller,[8] and H. Sullivan in this connection.

In the case of an arbitrary perturbing noise (not necessarily white thermal noise) it does not appear that the maximizing problem involved in deter-

---

[6] This and other properties of the white noise case are discussed from the geometrical point of view in "Communication in the Presence of Noise," loc. cit.

[7] "Cybernetics," loc. cit.

[8] Sc. D. thesis, Department of Electrical Engineering, M.I.T., 1948.

mining the channel capacity C can be solved explicitly. However, upper and lower bounds can be set for C in terms of the average noise power N and the noise entropy power N_1. These bounds are sufficiently close together in most practical cases to furnish a satisfactory solution to the problem.

Theorem 18: The capacity of a channel of band W perturbed by an arbitrary noise is bounded by the inequalities

$$W \log \frac{P + N_1}{N_1} \le C \le W \log \frac{P + N}{N_1}$$

where

P = average transmitter power
N = average noise power
N_1 = entropy power of the noise.

Here again the average power of the perturbed signals will be $P + N$. The maximum entropy for this power would occur if the received signal were white noise and would be $W \log 2\pi e(P + N)$. It may not be possible to achieve this; i.e. there may not be any ensemble of transmitted signals which, added to the perturbing noise, produce a white thermal noise at the receiver, but at least this sets an upper bound to $H(y)$. We have, therefore

$$C = \max H(y) - H(n)$$
$$\le W \log 2\pi e(P + N) - W \log 2\pi e N_1 .$$

This is the upper limit given in the theorem. The lower limit can be obtained by considering the rate if we make the transmitted signal a white noise, of power P. In this case the entropy power of the received signal must be at least as great as that of a white noise of power $P + N_1$ since we have shown in a previous theorem that the entropy power of the sum of two ensembles is greater than or equal to the sum of the individual entropy powers. Hence

$$\max H(y) \ge W \log 2\pi e(P + N_1)$$

and

$$C \ge W \log 2\pi e(P + N_1) - W \log 2\pi e N_1$$
$$= W \log \frac{P + N_1}{N_1} .$$

As P increases, the upper and lower bounds approach each other, so we have as an asymptotic rate

$$W \log \frac{P + N}{N_1}$$

If the noise is itself white, $N = N_1$ and the result reduces to the formula proved previously:

$$C = W \log \left(1 + \frac{P}{N} \right).$$

If the noise is Gaussian but with a spectrum which is not necessarily flat, N_1 is the geometric mean of the noise power over the various frequencies in the band W. Thus

$$N_1 = \exp \frac{1}{W} \int_W \log N(f) \, df$$

where $N(f)$ is the noise power at frequency f.

Theorem 19: If we set the capacity for a given transmitter power P equal to

$$C = W \log \frac{P + N - \eta}{N_1}$$

then η is monotonic decreasing as P increases and approaches 0 as a limit.

Suppose that for a given power P_1 the channel capacity is

$$W \log \frac{P_1 + N - \eta_1}{N_1}$$

This means that the best signal distribution, say $p(x)$, when added to the noise distribution $q(x)$, gives a received distribution $r(y)$ whose entropy power is $(P_1 + N - \eta_1)$. Let us increase the power to $P_1 + \Delta P$ by adding a white noise of power ΔP to the signal. The entropy of the received signal is now at least

$$H(y) = W \log 2\pi e (P_1 + N - \eta_1 + \Delta P)$$

by application of the theorem on the minimum entropy power of a sum. Hence, since we can attain the H indicated, the entropy of the maximizing distribution must be at least as great and η must be monotonic decreasing. To show that $\eta \to 0$ as $P \to \infty$ consider a signal which is a white noise with a large P. Whatever the perturbing noise, the received signal will be approximately a white noise, if P is sufficiently large, in the sense of having an entropy power approaching $P + N$.

25. The Channel Capacity with a Peak Power Limitation

In some applications the transmitter is limited not by the average power output but by the peak instantaneous power. The problem of calculating the channel capacity is then that of maximizing (by variation of the ensemble of transmitted symbols)

$$H(y) - H(n)$$

subject to the constraint that all the functions $f(t)$ in the ensemble be less than or equal to $\sqrt{S}$, say, for all t.   A constraint of this type does not work out as well mathematically as the average power limitation.   The most we have obtained for this case is a lower bound valid for all $\frac{S}{N}$, an "asymptotic" upper band $\left(\text{valid for large } \frac{S}{N}\right)$ and an asymptotic value of C for $\frac{S}{N}$ small.

Theorem 20: The channel capacity C for a band W perturbed by white thermal noise of power N is bounded by

$$C \geq W \log \frac{2}{\pi e^3} \frac{S}{N},$$

where S is the peak allowed transmitter power.   For sufficiently large $\frac{S}{N}$

$$C \leq W \log \frac{\frac{2}{\pi e} S + N}{N} (1 + \epsilon)$$

where ϵ is arbitrarily small.   As $\frac{S}{N} \to 0$ (and provided the band W starts at 0)

$$C \to W \log \left(1 + \frac{S}{N}\right).$$

We wish to maximize the entropy of the received signal.   If $\frac{S}{N}$ is large this will occur very nearly when we maximize the entropy of the transmitted ensemble.

The asymptotic upper bound is obtained by relaxing the conditions on the ensemble.   Let us suppose that the power is limited to S not at every instant of time, but only at the sample points.   The maximum entropy of the transmitted ensemble under these weakened conditions is certainly greater than or equal to that under the original conditions.   This altered problem can be solved easily.   The maximum entropy occurs if the different samples are independent and have a distribution function which is constant from $-\sqrt{S}$ to $+\sqrt{S}$.   The entropy can be calculated as

$$W \log 4S.$$

The received signal will then have an entropy less than

$$W \log (4S + 2\pi eN)(1 + \epsilon)$$

with $\epsilon \to 0$ as $\dfrac{S}{N} \to \infty$ and the channel capacity is obtained by subtracting the entropy of the white noise, $W \log 2\pi e N$

$$W \log (4S + 2\pi e N)(1 + \epsilon) - W \log (2\pi e N) = W \log \frac{\dfrac{2}{\pi e} S + N}{N} (1 + \epsilon).$$

This is the desired upper bound to the channel capacity.

To obtain a lower bound consider the same ensemble of functions. Let these functions be passed through an ideal filter with a triangular transfer characteristic. The gain is to be unity at frequency 0 and decline linearly down to gain 0 at frequency W. We first show that the output functions of the filter have a peak power limitation S at all times (not just the sample points). First we note that a pulse $\dfrac{\sin 2\pi W t}{2\pi W t}$ going into the filter produces

$$\frac{1}{2} \frac{\sin^2 \pi W t}{(\pi W t)^2}$$

in the output. This function is never negative. The input function (in the general case) can be thought of as the sum of a series of shifted functions

$$a \frac{\sin 2\pi W t}{2\pi W t}$$

where a, the amplitude of the sample, is not greater than $\sqrt{S}$. Hence the output is the sum of shifted functions of the non-negative form above with the same coefficients. These functions being non-negative, the greatest positive value for any t is obtained when all the coefficients a have their maximum positive values, i.e. $\sqrt{S}$. In this case the input function was a constant of amplitude $\sqrt{S}$ and since the filter has unit gain for D.C., the output is the same. Hence the output ensemble has a peak power S.

The entropy of the output ensemble can be calculated from that of the input ensemble by using the theorem dealing with such a situation. The output entropy is equal to the input entropy plus the geometrical mean gain of the filter;

$$\int_0^W \log G^2 \, df = \int_0^W \log \left(\frac{W - f}{W} \right)^2 df = -2W$$

Hence the output entropy is

$$W \log 4S - 2W = W \log \frac{4S}{\epsilon^2}$$

and the channel capacity is greater than

$$W \log \frac{2}{\pi e^3} \frac{S}{N}.$$

We now wish to show that, for small $\frac{S}{N}$ (peak signal power over average white noise power), the channel capacity is approximately

$$C = W \log \left(1 + \frac{S}{N}\right).$$

More precisely $C/W \log \left(1 + \frac{S}{N}\right) \to 1$ as $\frac{S}{N} \to 0$. Since the average signal power P is less than or equal to the peak S, it follows that for all $\frac{S}{N}$

$$C \leq W \log \left(1 + \frac{P}{N}\right) \leq W \log \left(1 + \frac{S}{N}\right).$$

Therefore, if we can find an ensemble of functions such that they correspond to a rate nearly $W \log \left(1 + \frac{S}{N}\right)$ and are limited to band W and peak S the result will be proved. Consider the ensemble of functions of the following type. A series of t samples have the same value, either $+\sqrt{S}$ or $-\sqrt{S}$, then the next t samples have the same value, etc. The value for a series is chosen at random, probability $\frac{1}{2}$ for $+\sqrt{S}$ and $\frac{1}{2}$ for $-\sqrt{S}$. If this ensemble be passed through a filter with triangular gain characteristic (unit gain at D.C.), the output is peak limited to $\pm S$. Furthermore the average power is nearly S and can be made to approach this by taking t sufficiently large. The entropy of the sum of this and the thermal noise can be found by applying the theorem on the sum of a noise and a small signal. This theorem will apply if

$$\sqrt{t} \frac{S}{N}$$

is sufficiently small. This can be insured by taking $\frac{S}{N}$ small enough (after t is chosen). The entropy power will be $S + N$ to as close an approximation as desired, and hence the rate of transmission as near as we wish to

$$W \log \left(\frac{S + N}{N}\right).$$

PART V: THE RATE FOR A CONTINUOUS SOURCE

26. FIDELITY EVALUATION FUNCTIONS

In the case of a discrete source of information we were able to determine a definite rate of generating information, namely the entropy of the underlying stochastic process. With a continuous source the situation is considerably more involved. In the first place a continuously variable quantity can assume an infinite number of values and requires, therefore, an infinite number of binary digits for exact specification. This means that to transmit the output of a continuous source with *exact recovery* at the receiving point requires, in general, a channel of infinite capacity (in bits per second). Since, ordinarily, channels have a certain amount of noise, and therefore a finite capacity, exact transmission is impossible.

This, however, evades the real issue. Practically, we are not interested in exact transmission when we have a continuous source, but only in transmission to within a certain tolerance. The question is, can we assign a definite rate to a continuous source when we require only a certain fidelity of recovery, measured in a suitable way. Of course, as the fidelity requirements are increased the rate will increase. It will be shown that we can, in very general cases, define such a rate, having the property that it is possible, by properly encoding the information, to transmit it over a channel whose capacity is equal to the rate in question, and satisfy the fidelity requirements. A channel of smaller capacity is insufficient.

It is first necessary to give a general mathematical formulation of the idea of fidelity of transmission. Consider the set of messages of a long duration, say T seconds. The source is described by giving the probability density, in the associated space, that the source will select the message in question $P(x)$. A given communication system is described (from the external point of view) by giving the conditional probability $P_x(y)$ that if message x is produced by the source the recovered message at the receiving point will be y. The system as a whole (including source and transmission system) is described by the probability function $P(x, y)$ of having message x and final output y. If this function is known, the complete characteristics of the system from the point of view of fidelity are known. Any evaluation of fidelity must correspond mathematically to an operation applied to $P(x, y)$. This operation must at least have the properties of a simple ordering of systems; i.e. it must be possible to say of two systems represented by $P_1(x, y)$ and $P_2(x, y)$ that, according to our fidelity criterion, either (1) the first has higher fidelity, (2) the second has higher fidelity, or (3) they have

equal fidelity. This means that a criterion of fidelity can be represented by a numerically valued function:

$$v(P(x, y))$$

whose argument ranges over possible probability functions $P(x, y)$.

We will now show that under very general and reasonable assumptions the function $v(P(x, y))$ can be written in a seemingly much more specialized form, namely as an average of a function $\rho(x, y)$ over the set of possible values of x and y:

$$v(P(x, y)) = \int\int P(x, y)\, \rho(x, y)\, dx\, dy$$

To obtain this we need only assume (1) that the source and system are ergodic so that a very long sample will be, with probability nearly 1, typical of the ensemble, and (2) that the evaluation is "reasonable" in the sense that it is possible, by observing a typical input and output x_1 and y_1, to form a tentative evaluation on the basis of these samples; and if these samples are increased in duration the tentative evaluation will, with probability 1, approach the exact evaluation based on a full knowledge of $P(x, y)$. Let the tentative evaluation be $\rho(x, y)$. Then the function $\rho(x, y)$ approaches (as $T \to \infty$) a constant for almost all (x, y) which are in the high probability region corresponding to the system:

$$\rho(x, y) \to v(P(x, y))$$

and we may also write

$$\rho(x, y) \to \int\int P(x, y)\rho(x, y)\, dx,\, dy$$

since

$$\int\int P(x, y)\, dx\, dy = 1$$

This establishes the desired result.

The function $\rho(x, y)$ has the general nature of a "distance" between x and y.[9] It measures how bad it is (according to our fidelity criterion) to receive y when x is transmitted. The general result given above can be restated as follows: Any reasonable evaluation can be represented as an average of a distance function over the set of messages and recovered messages x and y weighted according to the probability $P(x, y)$ of getting the pair in question, provided the duration T of the messages be taken sufficiently large.

[9] It is not a "metric" in the strict sense, however, since in general it does not satisfy either $\rho(x, y) = \rho(y, x)$ or $\rho(x, y) + \rho(y, z) \geq \rho(x, z)$.

The following are simple examples of evaluation functions:

1. R.M.S. Criterion.

$$v = \overline{(x(t) - y(t))^2}$$

In this very commonly used criterion of fidelity the distance function $\rho(x, y)$ is (apart from a constant factor) the square of the ordinary euclidean distance between the points x and y in the associated function space.

$$\rho(x, y) = \frac{1}{T} \int_0^T [x(t) - y(t)]^2 \, dt$$

2. Frequency weighted R.M.S. criterion. More generally one can apply different weights to the different frequency components before using an R.M.S. measure of fidelity. This is equivalent to passing the difference $x(t) - y(t)$ through a shaping filter and then determining the average power in the output. Thus let

$$e(t) = x(t) - y(t)$$

and

$$f(t) = \int_{-\infty}^{\infty} e(\tau)k(t - \tau) \, dt$$

then

$$\rho(x, y) = \frac{1}{T} \int_0^T f(t)^2 \, dt.$$

3. Absolute error criterion.

$$\rho(x, y) = \frac{1}{T} \int_0^T |\, x(t) - y(t) \,| \, dt$$

4. The structure of the ear and brain determine implicitly an evaluation, or rather a number of evaluations, appropriate in the case of speech or music transmission. There is, for example, an "intelligibility" criterion in which $\rho(x, y)$ is equal to the relative frequency of incorrectly interpreted words when message $x(t)$ is received as $y(t)$. Although we cannot give an explicit representation of $\rho(x, y)$ in these cases it could, in principle, be determined by sufficient experimentation. Some of its properties follow from well-known experimental results in hearing, e.g., the ear is relatively insensitive to phase and the sensitivity to amplitude and frequency is roughly logarithmic.

5. The discrete case can be considered as a specialization in which we have

tacitly assumed an evaluation based on the frequency of errors. The function $\rho(x, y)$ is then defined as the number of symbols in the sequence y differing from the corresponding symbols in x divided by the total number of symbols in x.

27. The Rate for a Source Relative to a Fidelity Evaluation

We are now in a position to define a rate of generating information for a continuous source. We are given $P(x)$ for the source and an evaluation v determined by a distance function $\rho(x, y)$ which will be assumed continuous in both x and y. With a particular system $P(x, y)$ the quality is measured by

$$v = \iint \rho(x, y) \; P(x, y) \; dx \, dy$$

Furthermore the rate of flow of binary digits corresponding to $P(x, y)$ is

$$R = \iint P(x, y) \log \frac{P(x, y)}{P(x)P(y)} \, dx \, dy.$$

We define the rate R_1 of generating information for a given quality v_1 of reproduction to be the minimum of R when we keep v fixed at v_1 and vary $P_x(y)$. That is:

$$R_1 = \underset{P_x(y)}{\text{Min}} \iint P(x, y) \log \frac{P(x, y)}{P(x)P(y)} \, dx \, dy$$

subject to the constraint:

$$v_1 = \iint P(x, y)\rho(x, y) \, dx \, dy.$$

This means that we consider, in effect, all the communication systems that might be used and that transmit with the required fidelity. The rate of transmission in bits per second is calculated for each one and we choose that having the least rate. This latter rate is the rate we assign the source for the fidelity in question.

The justification of this definition lies in the following result:

Theorem 21: If a source has a rate R_1 for a valuation v_1 it is possible to encode the output of the source and transmit it over a channel of capacity C with fidelity as near v_1 as desired provided $R_1 \leq C$. This is not possible if $R_1 > C$.

The last statement in the theorem follows immediately from the definition of R_1 and previous results. If it were not true we could transmit more than C bits per second over a channel of capacity C. The first part of the theorem is proved by a method analogous to that used for Theorem 11. We may, in the first place, divide the (x, y) space into a large number of small cells and

represent the situation as a discrete case.   This will not change the evalua-
tion function by more than an arbitrarily small amount (when the cells are
very small) because of the continuity assumed for $\rho(x, y)$.   Suppose that
$P_1(x, y)$ is the particular system which minimizes the rate and gives R_1.   We
choose from the high probability y's a set at random containing

$$2^{(R_1 + \epsilon)T}$$

members where $\epsilon \to 0$ as $T \to \infty$.   With large T each chosen point will be
connected by a high probability line (as in Fig. 10) to a set of x's.   A calcu-
lation similar to that used in proving Theorem 11 shows that with large T
almost all x's are covered by the fans from the chosen y points for almost
all choices of the y's.   The communication system to be used operates as
follows: The selected points are assigned binary numbers.   When a message
x is originated it will (with probability approaching 1 as $T \to \infty$) lie within
one at least of the fans.   The corresponding binary number is transmitted
(or one of them chosen arbitrarily if there are several) over the channel by
suitable coding means to give a small probability of error.   Since $R_1 \leq C$
this is possible.   At the receiving point the corresponding y is reconstructed
and used as the recovered message.

The evaluation v_1' for this system can be made arbitrarily close to v_1 by
taking T sufficiently large.   This is due to the fact that for each long sample
of message $x(t)$ and recovered message $y(t)$ the evaluation approaches v_1
(with probability 1).

It is interesting to note that, in this system, the noise in the recovered
message is actually produced by a kind of general quantizing at the trans-
mitter and is not produced by the noise in the channel.   It is more or less
analogous to the quantizing noise in P.C.M.

28. THE CALCULATION OF RATES

The definition of the rate is similar in many respects to the definition of
channel capacity.   In the former

$$R = \underset{P_x(y)}{\text{Max}} \iint P(x, y) \log \frac{P(x, y)}{P(x)P(y)} \, dx \, dy$$

with $P(x)$ and $v_1 = \iint P(x, y)\rho(x, y) \, dx \, dy$ fixed.   In the latter

$$C = \underset{P(x)}{\text{Min}} \iint P(x, y) \log \frac{P(x, y)}{P(x)P(y)} \, dx \, dy$$

with $P_x(y)$ fixed and possibly one or more other constraints (e.g., an average
power limitation) of the form $K = \iint P(x, y) \lambda(x, y) \, dx \, dy$.

A partial solution of the general maximizing problem for determining the rate of a source can be given. Using Lagrange's method we consider

$$\iint \left[P(x, y) \log \frac{P(x, y)}{P(x)P(y)} + \mu\, P(x, y)\rho(x, y) + \nu(x)P(x, y) \right] dx\, dy$$

The variational equation (when we take the first variation on $P(x, y)$) leads to

$$P_y(x) = B(x)\, e^{-\lambda \rho(x, y)}$$

where λ is determined to give the required fidelity and $B(x)$ is chosen to satisfy

$$\int B(x)e^{-\lambda\rho(x, y)}\, dx = 1$$

This shows that, with best encoding, the conditional probability of a certain cause for various received y, $P_y(x)$ will decline exponentially with the distance function $\rho(x, y)$ between the x and y is question.

In the special case where the distance function $\rho(x, y)$ depends only on the (vector) difference between x and y,

$$\rho(x, y) = \rho(x - y)$$

we have

$$\int B(x)e^{-\lambda\rho(x-y)}\, dx = 1.$$

Hence $B(x)$ is constant, say α, and

$$P_y(x) = \alpha e^{-\lambda\rho(x-y)}$$

Unfortunately these formal solutions are difficult to evaluate in particular cases and seem to be of little value. In fact, the actual calculation of rates has been carried out in only a few very simple cases.

If the distance function $\rho(x, y)$ is the mean square discrepancy between x and y and the message ensemble is white noise, the rate can be determined. In that case we have

$$R = \text{Min}\ [H(x) - H_y(x)] = H(x) - \text{Max}\ H_y(x)$$

with $N = \overline{(x - y)^2}$. But the Max $H_y(x)$ occurs when $y - x$ is a white noise, and is equal to $W_1 \log 2\pi e\, N$ where W_1 is the bandwidth of the message ensemble. Therefore

$$R = W_1 \log 2\pi eQ - W_1 \log 2\pi eN$$

$$= W_1 \log \frac{Q}{N}$$

where Q is the average message power. This proves the following:

Theorem 22: The rate for a white noise source of power Q and band W_1 relative to an R.M.S. measure of fidelity is

$$R = W_1 \log \frac{Q}{N}$$

where N is the allowed mean square error between original and recovered messages.

More generally with any message source we can obtain inequalities bounding the rate relative to a mean square error criterion.

Theorem 23: The rate for any source of band W_1 is bounded by

$$W_1 \log \frac{Q_1}{N} \le R \le W_1 \log \frac{Q}{N}$$

where Q is the average power of the source, Q_1 its entropy power and N the allowed mean square error.

The lower bound follows from the fact that the max $H_y(x)$ for a given $(x - y)^2 = N$ occurs in the white noise case.   The upper bound results if we place the points (used in the proof of Theorem 21) not in the best way but at random in a sphere of radius $\sqrt{Q - N}$.

ACKNOWLEDGMENTS

APPENDIX 5

Let S_1 be any measurable subset of the g ensemble, and S_2 the subset of the f ensemble which gives S_1 under the operation T.   Then

$$S_1 = TS_2.$$

Let H^λ be the operator which shifts all functions in a set by the time λ. Then

$$H^\lambda S_1 = H^\lambda TS_2 = TH^\lambda S_2$$

since T is invariant and therefore commutes with H^λ.   Hence if $m[S]$ is the probability measure of the set S

$$m[H^\lambda S_1] = m[TH^\lambda S_2] = m[H^\lambda S_2]$$

$$= m[S_2] = m[S_1]$$

where the second equality is by definition of measure in the g space the third since the f ensemble is stationary, and the last by definition of g measure again.

To prove that the ergodic property is preserved under invariant operations, let S_1 be a subset of the g ensemble which is invariant under H^λ, and let S_2 be the set of all functions f which transform into S_1. Then

$$H^\lambda S_1 = H^\lambda T S_2 = T H^\lambda S_2 = S_1$$

so that $H^\lambda S_1$ is included in S_1 for all λ. Now, since

$$m[H^\lambda S_2] = m[S_1]$$

this implies

$$H^\lambda S_2 = S_2$$

for all λ with $m[S_2] \neq 0, 1$. This contradiction shows that S_1 does not exist.

APPENDIX 6

The upper bound, $\bar{N}_3 \leq N_1 + N_2$, is due to the fact that the maximum possible entropy for a power $N_1 + N_2$ occurs when we have a white noise of this power. In this case the entropy power is $N_1 + N_2$.

To obtain the lower bound, suppose we have two distributions in n dimensions $p(x_i)$ and $q(x_i)$ with entropy powers $\bar{N}_1$ and $\bar{N}_2$. What form should p and q have to minimize the entropy power $\bar{N}_3$ of their convolution $r(x_i)$:

$$r(x_i) = \int p(y_i) q(x_i - y_i) \, dy_i .$$

The entropy H_3 of r is given by

$$H_3 = - \int r(x_i) \log r(x_i) \, dx_i .$$

We wish to minimize this subject to the constraints

$$H_1 = - \int p(x_i) \log p(x_i) \, dx_i$$

$$H_2 = - \int q(x_i) \log q(x_i) \, dx_i .$$

We consider then

$$U = - \int [r(x) \log r(x) + \lambda p(x) \log p(x) + \mu q(x) \log q(x)] \, dx$$

$$\delta U = - \int [[1 + \log r(x)] \delta r(x) + \lambda [1 + \log p(x)] \delta p(x)$$
$$+ \mu [1 + \log q(x) \delta q(x)]] \, dx .$$

If $p(x)$ is varied at a particular argument $x_i = s_i$, the variation in $r(x)$ is

$$\delta r(x) = q(x_i - s_i)$$

and

$$\delta U = -\int q(x_i - s_i) \log r(x_i)\, dx_i - \lambda \log p(s_i) = 0$$

and similarly when q is varied. Hence the conditions for a minimum are

$$\int q(x_i - s_i) \log r(x_i) = -\lambda \log p(s_i)$$

$$\int p(x_i - s_i) \log r(x_i) = -\mu \log q(s_i).$$

If we multiply the first by $p(s_i)$ and the second by $q(s_i)$ and integrate with respect to s we obtain

$$H_3 = -\lambda\, H_1$$

$$H_3 = -\mu\, H_2$$

or solving for λ and μ and replacing in the equations

$$H_1 \int q(x_i - s_i) \log r(x_i)\, dx_i = -H_3 \log p(s_i)$$

$$H_2 \int p(x_i - s_i) \log r(x_i)\, dx_i = -H_3 \log p(s_i).$$

Now suppose $p(x_i)$ and $q(x_i)$ are normal

$$p(x_i) = \frac{|A_{ij}|^{n/2}}{(2\pi)^{n/2}} \exp - \tfrac{1}{2}\Sigma A_{ij} x_i x_j$$

$$q(x_i) = \frac{|B_{ij}|^{n/2}}{(2\pi)^{n/2}} \exp - \tfrac{1}{2}\Sigma B_{ij} x_i x_j.$$

Then $r(x_i)$ will also be normal with quadratic form C_{ij}. If the inverses of these forms are a_{ij}, b_{ij}, c_{ij} then

$$c_{ij} = a_{ij} + b_{ij}.$$

We wish to show that these functions satisfy the minimizing conditions if and only if $a_{ij} = K b_{ij}$ and thus give the minimum H_3 under the constraints. First we have

$$\log r(x_i) = \frac{n}{2} \log \frac{1}{2\pi} |C_{ij}| - \tfrac{1}{2}\Sigma C_{ij} x_i x_j$$

$$\int q(x_i - s_i) \log r(x_i) = \frac{n}{2} \log \frac{1}{2\pi} |C_{ij}| - \tfrac{1}{2}\Sigma C_{ij} s_i s_j - \tfrac{1}{2}\Sigma C_{ij} b_{ij}.$$

This should equal

$$\frac{H_3}{H_1}\left[\frac{n}{2}\log\frac{1}{2\pi}\,|\,A_{ij}\,| \,-\, \tfrac{1}{2}\Sigma A_{ij}s_i s_j\right]$$

which requires $A_{ij} = \dfrac{H_1}{H_3}\,C_{ij}$.

In this case $A_{ij} = \dfrac{H_1}{H_2}\,B_{ij}$ and both equations reduce to identities.

APPENDIX 7

The following will indicate a more general and more rigorous approach to the central definitions of communication theory. Consider a probability measure space whose elements are ordered pairs (x, y). The variables x, y are to be identified as the possible transmitted and received signals of some long duration T. Let us call the set of all points whose x belongs to a subset S_1 of x points the strip over S_1, and similarly the set whose y belongs to S_2 the strip over S_2. We divide x and y into a collection of non-overlapping measurable subsets X_i and Y_i approximate to the rate of transmission R by

$$R_1 = \frac{1}{T}\sum_i P(X_i, Y_i)\log\frac{P(X_i, Y_i)}{P(X_i)P(Y_i)}$$

where

$P(X_i)$ is the probability measure of the strip over X_i

$P(Y_i)$ is the probability measure of the strip over Y_i

$P(X_i, Y_i)$ is the probability measure of the intersection of the strips.

A further subdivision can never decrease R_1. For let X_1 be divided into $X_1 = X_1' + X_1''$ and let

$$P(Y_1) = a \qquad\qquad P(X_1) = b + c$$
$$P(X_1') = b \qquad\qquad P(X_1', Y_1) = d$$
$$P(X_1'') = c \qquad\qquad P(X_1'', Y_1) = e$$
$$P(X_1, Y_1) = d + e$$

Then in the sum we have replaced (for the X_1, Y_1 intersection)

$$(d + e)\log\frac{d + e}{a(b + c)} \quad\text{by}\quad d\log\frac{d}{ab} + e\log\frac{e}{ac}.$$

It is easily shown that with the limitation we have on b, c, d, e,

$$\left[\frac{d + e}{b + c}\right]^{d+e} \le \frac{d^d e^e}{b^d c^e}$$

and consequently the sum is increased. Thus the various possible subdivisions form a directed set, with R monotonic increasing with refinement of the subdivision. We may define R unambiguously as the least upper bound for the R_1 and write it

$$R = \frac{1}{T} \int\int P(x, y) \log \frac{P(x, y)}{P(x)P(y)} \, dx \, dy.$$

This integral, understood in the above sense, includes both the continuous and discrete cases and of course many others which cannot be represented in either form. It is trivial in this formulation that if x and u are in one-to-one correspondence, the rate from u to y is equal to that from x to y. If v is any function of y (not necessarily with an inverse) then the rate from x to y is greater than or equal to that from x to v since, in the calculation of the approximations, the subdivisions of y are essentially a finer subdivision of those for v. More generally if y and v are related not functionally but statistically, i.e., we have a probability measure space (y, v), then $R(x, v) \leq R(x, y)$. This means that any operation applied to the received signal, even though it involves statistical elements, does not increase R.

Another notion which should be defined precisely in an abstract formulation of the theory is that of "dimension rate," that is the average number of dimensions required per second to specify a member of an ensemble. In the band limited case 2W numbers per second are sufficient. A general definition can be framed as follows. Let $f_\alpha(t)$ be an ensemble of functions and let $\rho_T[f_\alpha(t), f_\beta(t)]$ be a metric measuring the "distance" from f_α to f_β over the time T (for example the R.M.S. discrepancy over this interval.) Let $N(\epsilon, \delta, T)$ be the least number of elements f which can be chosen such that all elements of the ensemble apart from a set of measure δ are within the distance ϵ of at least one of those chosen. Thus we are covering the space to within ϵ apart from a set of small measure δ. We define the dimension rate λ for the ensemble by the triple limit

$$\lambda = \operatorname*{Lim}_{\delta \to 0} \operatorname*{Lim}_{\epsilon \to 0} \operatorname*{Lim}_{T \to \infty} \frac{\log N(\epsilon, \delta, T)}{T \log \epsilon}.$$

This is a generalization of the measure type definitions of dimension in topology, and agrees with the intuitive dimension rate for simple ensembles where the desired result is obvious.

Transients in Mechanical Systems

By J. T. MULLER

INTRODUCTION

A study of the response of an electrical network or system to the input of transients in the form of short-duration pulses is an accepted method of analysis of the network. By comparing the input and the output, conclusions may be drawn as to the respective merit of the various components.

Until recently similar procedures were only of academic interest with mechanical systems. However, the tests for mechanical ruggedness, which are required of electronic gear in order to pass specifications for the armed forces, are an example of the application of transients to a mechanical system. These tests are known as *High Impact Shock Tests*.

A basic part of an electrical system is a damped resonant network consisting of an inductance, a capacitance and a resistance. A mass, a spring and a friction device is the equivalent mechanical network called a simple mechanical system and a combination of such networks is a general mechanical system. It is, of course, advantageous to keep the mechanical system as simple as possible without detracting from the general usefulness of the results obtained.

The problems here considered are pertinent to a system which is essentially made up of a supporting structure or table and a resilient mounting array bearing the equipment (e.g. electronic gear) which is vulnerable to shock. (See Fig. 1.)

A shock is the physical manifestation of the transfer of mechanical energy from one body to another during an extremely short interval of time. The order of magnitude of the time interval is milliseconds and quite frequently fractions of a millisecond.

The system is excited by administering large spurts of mechanical energy to the supporting table. The manner in which this energy is supplied to the base and the way it is dissipated through the system are the subjects of this paper.

The energy transfer to the supporting table is accomplished by the use of huge hammers which strike the anvil with controllable speeds. The action is assumed to be similar to that of an explosion, particularly to an underwater explosion at close range or a *near-miss*. As to the real comparison between the two, the reader is referred to the various manuscripts published by the Bureau of Ships. This particular phase of the subject is

considered outside the scope of this paper, except for the following brief statement:

Both actions fit the definition of shock stated above and the difference between the two is one of size and not of kind.

Shocks are transients and are conveniently treated by a branch of mathematics which is adapted to the solution of problems of this kind; viz, the *Laplace Transforms*, and the reader is referred to Gardner and Barnes, "Transients in Linear Systems." The nomenclature used here is identical to that of those authors.
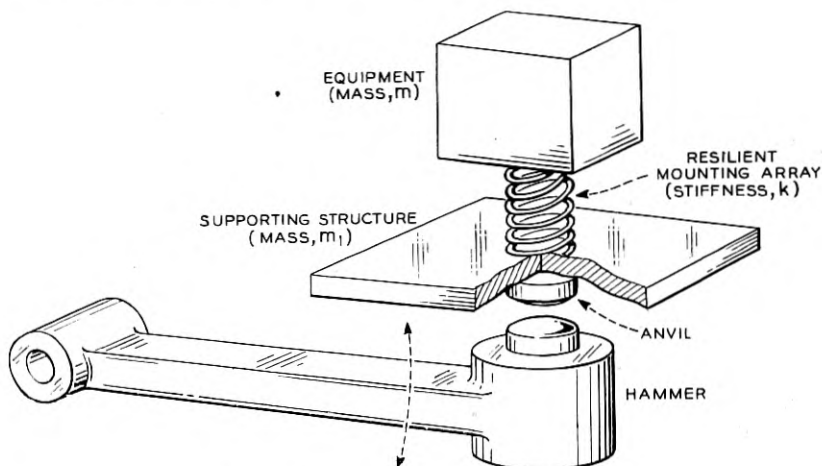

Fig. 1—Schematic layout of shock machine.

The manuscript consists of two parts: In the first, the energy transfer to the base is considered. We are dealing here with rigid bodies; consequently with very small transient displacements and very large forces. These are usually referred to as impact forces or impulses and four such functions of force and time are discussed. Displacements with associated velocities result from the action of impulses on the base.

The second part deals with the effect of these displacements on the shock-mounted equipment. Although the mathematical procedure is identical to the first part, here we deal with a function of displacement and time. There is no specific name for such a relationship but a suggestive term is "whip." However, the pulse functions represented are the same as those of the force and time function.

It is assumed that the displacement-time pulse is independent of the subsequent motion of the mass.

In considering any kind of shock problem we have the following fundamental considerations:

First, we shall want to know the magnitude of the shock present in the base or supporting structure; this will be called the "excitation."

Second, the behavior of the resilient medium interposed between the shock-producing base and the equipment. It is sometimes expressed as the coupling. We shall use the term *transmission*.

Third, the resulting disturbance of the equipment caused by the transmitted shock, which we will call the *response*.

The three functions do not exist independently, but are mathematically related. For a clearer understanding of shock phenomena it is perhaps helpful to fix in one's mind the idea that the response of a system is completely dependent upon the transmission function.

To use an electrical analogue, the voltage e_1 (t) impressed upon a system produces an output voltage e_2 (t) which is completely defined by the transmission function. For instance, if this transmission function represents a filter of some kind with given boundaries, then it is to be expected that the response of e_2 (t) is completely changed outside these limits and could even be zero. The same train of thought will hold for mechanical systems. Here the transmission function is mostly represented by the stiffness or the compliance. For a completely rigid medium the stiffness would be infinite and the input and output would be alike; in other words, a force applied to the base would appear at the equipment. This is a theoretical case because no material is perfectly rigid. Though some materials are more rigid than others they will all give if the force applied is big enough. Now the forces associated with a shock are almost always of considerable magnitude so that the stiffness of a material becomes significant.

As the stiffness diminishes the response changes and may appear to be quite different from the input. As far as the transmissibility of forces is concerned, the reader is reminded that a force is always accompanied by a reaction. The forces which put the base into motion cannot be transmitted by a soft material like rubber, unless it is compressed to extremely high values, and thus produce an equally large reactive force.

PART I

ANALYSIS OF THE EXCITATION OF THE BASE

By recording the motions of the base, we obtain time-displacement curves as shown in Fig. 2. The method of recording has been done by means of high-speed motion pictures (at the Whippany testing laboratory using a Fastex) and by using strain gages (at the Annapolis Engineering Experiment Station).

The test equipments are fundamentally mechanical impact producing machines. For technical details and description of the machines the reader

is referred to the various test specifications by the Bureau of Ships (as, for example, *Spec.* 40T9).

The characteristic of an impact is the transfer of mechanical energy from one mass to another in a relatively short time. The corresponding force as function of time is called an *impulse,* henceforth indicated as $F(t)$. A study of the pulse functions has suggested some probable theoretical shapes of $F(t)$ which could cover a wide variety of conditions. These pulse functions will be used for force-time functions as well as displacement-time-functions and it will be shown that the results are surprisingly similar.

We will let these pulses operate on the base with mass m_1 and calculate and plot the resulting time displacement curves. Since an impulse is associated with energy transfer, it must be a function of $\dfrac{m_1 v^2}{2}$. From the point of view
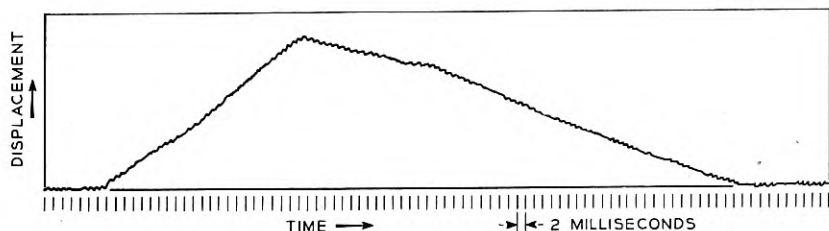

Fig. 2—Time displacement record of medium high impact machine.

of shock action, the final velocity v is extremely important, for it is this velocity which will determine the displacement and acceleration of the shock-mounted equipment.

To distinguish the various applications of the pulse functions, the following notations are adopted:

$f(t)$ represents any functions of t, without reference to its dimensional magnitude. The transform of $f(t)$ is indicated by $F(s)$.

$x(t)$ represents a function of t when it is a displacement of the mass m only. The transform is indicated by $X(s)$.

$x_1(t)$ represents a function of t when it is a displacement of the *base* (with mass m_1) only. The transform is indicated by $X_1(s)$.

$F(t)$ represents a function of t when it is a force applied to the base. The transform is indicated by $F_0(s)$.

Since $x_1(t)$ and $F(t)$ are input functions, they may be represented by the same type pulse, in which case the transforms are alike, i.e., $F(s) = X_1(s) = F_0(s)$.

Figure 3A, a rectangular pulse, is the simplest form.

Figure 3B is a triangular pulse, $f(t)$, reaching a peak and returning to zero in a linear manner.

Figure 3C consists of one-half cycle of a sine wave.

Figure 3D is a cosine pulse of one-cycle duration and is shifted along the Y axis an amount equal to the amplitude.

These are the pulses to be used in the problems under consideration.

If they represent a force as it varies with time then it is said that $F(t)$ represents a particular pulse. The Laplace transform of $F(t)$ is given as $F_0(s)$, $F_0(s)$ being some function in the complex domain. It is outside the scope of this paper to prove or show the mathematical technique in obtaining the transforms which produce $F_0(s)$. We will present them here for future reference.
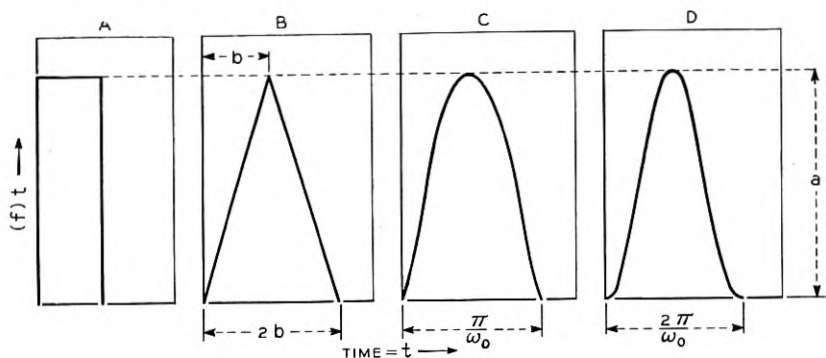

Fig. 3—Four pulses.

The Laplace transform for a very short pulse is

$$F(s) = A_r \tag{1.01}$$

and is a pulse which has a finite area but the time interval of which is approaching zero.

For a square pulse with finite time interval and magnitude a (hereafter referred to as pulse amplitude) it is

$$F(s) = a \frac{1 - \epsilon^{-bs}}{s} \tag{1.02}$$

For a triangular pulse

$$F(s) = \frac{a}{b} \left(\frac{1 - \epsilon^{-bs}}{s} \right)^2 \tag{1.03}$$

For a sine pulse

$$F(s) = \frac{a\omega_0}{s^2 + \omega_0^2} (1 + \epsilon^{-\pi s/\omega_0}) \tag{1.04}$$

For a shifted cosine pulse

$$F(s) = \frac{a\omega^2}{2s(s^2 + \omega_0^2)}(1 - \epsilon^{-2\pi s/\omega_0}) \tag{1.05}$$

Suppose we let an impulse, and to take a specific example, a triangular impulse, operate on a mass m_1. We have

$$F = m_1 a_0 \tag{1.06}$$

in which

$$F = F(t) = \text{force in lbs.}$$

$$m_1 = \text{mass in slugs}$$

$$a_0 = \ddot{x}_1 = \text{acceleration in ft/sec}^2$$

Let $\mathcal{L}[x_1(t)] = X_1(s) = X_1$
then

$$\mathcal{L}[m_1\ddot{x}_1] = m_1 s^2 X_1(s)$$

the $\mathcal{L}$ transform of a triangular pulse $F(t)$ is

$$\mathcal{L}[F(t)] = \frac{a}{b}\left(\frac{1 - \epsilon^{-bs}}{s}\right)^2 = F_0(s) \tag{1.07}$$

Substituting

$$X_1 = \frac{a}{m_1 b}\frac{1}{s^2}\left(\frac{1 - \epsilon^{-bs}}{s}\right)^2$$

The inverse transform is

$$\mathcal{L}^{-1}[X_1(s)] = x_1(t) = \mathcal{L}^{-1}\left[\frac{a}{m_1 b}\frac{1}{s^2}\left(\frac{1 - \epsilon^{-bs}}{s}\right)^2\right] \tag{1.08}$$

$$x_1(t) = \frac{a}{m_1 b}\mathcal{L}^{-1}\left[\frac{1}{s^2}\left(\frac{1 - \epsilon^{-bs}}{s}\right)^2\right] \tag{1.09}$$

The solution of 1.09

$$x_1(t) = \frac{a}{m_1}\frac{1}{b}\left[\frac{t^3}{6} - 2\frac{(t - b)^3}{6}u(t - b) + \frac{(t - 2b)^3}{6}u(t - 2b)\right] \tag{1.10}$$

After the impulse is over, i.e., for values of $t > 2b$, 1.10 becomes

$$x_1(t) = \frac{a}{m_1}b(t - b) \tag{1.11}$$

and the final velocity is

$$\frac{a}{m_1} b. \tag{1.12}$$

which represents the area of the impulse divided by the mass.

Similarly we find for the very short square impulse

$$x_1 = \frac{A_r}{m_1} t \tag{1.13}$$

For the square impulse of finite time interval b

$$x_1 = \frac{ab}{m_1}\left(t - \frac{b}{2}\right) \tag{1.14}$$

For the sine impulse

$$x_1 = \frac{2a}{m_1\omega_0}\left(t - \frac{\pi}{2\omega_0}\right) \tag{1.15}$$

For the shifted cosine impulse

$$x_1 = \frac{a\pi}{m_1\omega_0}\left(t - \frac{\pi}{\omega_0}\right) \tag{1.16}$$

The velocity is the term preceding the term in parenthesis.

In the five examples mentioned, we find that this *velocity is proportional to the area of the impulse curve and inversely proportional to the mass.* All expressions contain the factor $\frac{a}{m_1}$ and, since a is the maximum force present, this expression represents the maximum acceleration and it is this value which is so frequently mentioned when discussing the actions on the shock table.

For instance, from records we have determined approximate values for the time interval during which the energy transfer from hammer to the table takes place. The high-speed motion pictures are taken at the rate of 4,000 to 5,000 frames per second, which means an average elapsed time of .22 milliseconds or 220 microseconds. The energy transfer occurs within this time interval, because the rate of increase of the displacement from frame to frame is constant. The exposure time of one frame is $\frac{1}{12000}$ second or 83 microseconds. If the anvil moved within this time there would be evidence of blurring. Since we have been unable to detect any blurring, we may state that transfer is less than 220μs yet more than 80μs.

Let us assume it to be 100μs. That means a pulse width of $2b = 100$μs. (See Fig. 3.)

If

$$\frac{a}{m_1} = a_0 = \text{acceleration},$$

then

$$v = \frac{ab}{m_1} = a_0 b$$

For a 2000-ft. pound shock the table speed v is approximately 7 ft./sec. Substituting, we find for a_0 or the acceleration

$$7 = a_0 \times .00005$$

$$\text{or } a_0 = 140.000 \text{ ft./sec.}^2$$

$$a_0 = 4400 \text{ "g"s}$$

This is about the order of magnitude which the accelerometers have recorded.

The important conclusion we draw from this is that the acceleration and its time interval combine to produce a velocity of the base which is a complete criterion of the severity of the shock administered.

In the example just cited the weight of the table is approximately 800 lbs., and the force 4400 x 800 = 3,250,000 lbs. The result is, then, that a triangular impulse of 3,520,000 lbs. magnitude and a duration of 100μs operating on a table of 800 lbs., imparts to that table a velocity of 7 ft./sec.

PART II

ANALYSIS OF THE RESPONSE

In Part I the origin of the motion of the base has been treated. This motion of the base can now be represented by a pulse or a displacement as a function of time. To distinguish the displacement-time function from the force-time function, we have already suggested the name *Whip*. Obviously some of the pulse shapes which were used to represent impulses are not suitable as whips. For instance, the square pulse as whip could not exist, since this would suppose an infinite velocity.

The triangular whip is observed in the medium-high-impact shock machine. The sine whip may be taken to represent approximately the output of the light-high-impact machine.

The shifted cosine whip is sometimes used in the motion of cams of automatic equipment.

The problem of shock response is now reduced to the behavior of a mass and spring system when the base motion is represented by a whip.

Triangular whip (Fig. 3b).   The Laplace transform of this pulse is

$$F(s) = \frac{a}{b}\left(\frac{1 - \epsilon^{-bs}}{s}\right)^2.$$

The differential equation for a simple harmonic system is

$$m\ddot{x} + kx = 0 \tag{1}$$

or

$$\frac{\ddot{x}}{\omega^2} + x = 0. \tag{2}$$

If we let the whip operate on this system, then

$$\frac{\ddot{x}}{\omega^2} + x = f(t) = x_1(t) \tag{3}$$

in which $x_1(t)$ represents the displacement of the whip as a function of time.

Let $\mathcal{L}[x(t)] = X(s)$

and

$$\mathcal{L}[x_1(t)] = \mathcal{L}[f(t)] = F(s) = X_1(s)$$

then

$$\mathcal{L}[\ddot{x}] = s^2 X(s) - sf(0) - f^1(0)$$

By definition the initial conditions are zero, so that

$$\mathcal{L}[\ddot{x}] = s^2 X(s) \tag{4}$$

The Laplace transform of equation (3) is then

$$\frac{s^2}{\omega^2} X(s) + X(s) = \mathcal{L}[f(t)] = X_1(s)$$

or

$$\left(\frac{s^2 + \omega^2}{\omega^2}\right) X(s) = X_1(s). \tag{5}$$

Now

$$X_1(s) = \frac{a}{b}\left(\frac{1 - \epsilon^{-bs}}{s}\right)^2.$$

Substituting and rearranging,

$$X(s) = \frac{\omega^2}{s^2 + \omega^2} \frac{a}{b}\left(\frac{1 - \epsilon^{-bs}}{s}\right)^2. \tag{6}$$

This is the transform equation. To find x we use the inverse Laplace transform and the solution of (7) is

$$x = \frac{a\omega^2}{b}\left[\left(\frac{t}{\omega^2} - \frac{\sin \omega t}{\omega^3}\right) - 2\left(\frac{(t-b)}{\omega^2} - \frac{\sin \omega(t-b)}{\omega^3}\right)u(t-b)\right.$$
$$\left. + \left(\frac{t-2b}{\omega^2} - \frac{\sin \omega(t-2b)}{\omega^3}\right)u(t-2b)\right]. \tag{7}$$

The expression $u(t-b)$ simply means that the term to which it is attached is zero for all values of $t < b$.

Let us now consider what this solution consists of.

There are apparently three terms which take effect at successive intervals.

The initial whip can be considered to consist of three different displacements starting at successive times 0, b and $2b$. With the displacement of the base there is a corresponding displacement of the mass m. After the time b the second term or displacement takes hold and an associated displacement of mass m except that the initial conditions are the end conditions of the first displacement. After the time $2b$ the third displacement enters and the final result is the displacement-time pulse or whip. To make the problem somewhat simpler we introduce the following modifications:

1°. Because the motion is a simple harmonic of known frequency after the whip has passed we will only consider the maximum amplitude.

2°. Only the displacement-time function of the mass m during the pulse interval will be examined.

3°. The dimensional magnitudes of the motion of mass m will be expressed as ratios of those of the pulse.

If a is the maximum amplitude of the whip, and $T_0 = 2b$ its time interval (usually expressed in milliseconds), then we define

$\dfrac{x}{a} = \delta$ *Amplitude ratio of pulse displacement and response of mass m during pulse interval only.*

$\dfrac{T_0}{T} = \dfrac{2b}{T} = \dfrac{2b}{2\pi/\omega} \dfrac{\omega b}{\pi} = \varphi$ *Natural frequency of mass m expressed as a ratio of the pulse length.*

$\tau = \dfrac{t}{2b}$ *Elapsed time expressed as a ratio of the pulse length.*

$\Delta = \dfrac{x_{max}}{a}$ *Ratio of maximum amplitude to pulse displacement after pulse interval.*

Substituting these values in equation (7) and rearranging we obtain

$$\delta = 2\tau - \frac{\sin 2\varphi\pi\tau}{\pi\varphi} - 2\left((2\tau - 1) - \frac{\sin \pi\varphi(2\tau - 1)}{\pi\varphi}\right)u(2\tau - 1)$$
$$+ \left(2(\tau - 1) - \frac{\sin 2\pi\varphi(\tau - 1)}{\pi\varphi}\right)u(\tau - 1) \tag{8}$$

This looks somewhat complicated, but we can simplify by omitting the last term, because we are only considering values of δ during the pulse interval.

$$\therefore \ \delta = 2\tau - \frac{\sin 2\varphi\pi\tau}{\pi\varphi} - 2\left((2\tau - 1) - \frac{\sin \pi\varphi(2\tau - 1)}{\pi\varphi}\right) u(2\tau - 1) \quad (9)$$

A plot of this equation for various values of φ is shown in Fig. 4. It is seen that δ becomes a maximum when φ is approx. .9 and τ is then .75. The displacement is approximately 1.5 times the peak displacement of the whip.

After the whip has passed, or when $\tau > 1$, the transient has disappeared and a steady-state condition exists. Since the system under consideration is a simple harmonic system, the steady state is a harmonic motion of frequency ω, with an amplitude to be obtained from equation (8). Indicating the dimensionless values of the amplitude by δ_a when $\tau > 1$, equation 8 may be written

$$\begin{aligned}
\delta_a = 2\tau &- \frac{\sin 2\varphi\pi\tau}{\pi\varphi} - 2\left((2\tau - 1) - \frac{\sin \varphi(2\tau - 1)}{\pi\varphi}\right) \\
&+ \left(2(\tau - 1) - \frac{\sin 2\pi\varphi(\tau - 1)}{\pi\varphi}\right) \qquad \tau > 1
\end{aligned} \quad (10)$$

After developing (10) and rearranging we obtain

$$\delta_a = \frac{2(1 - \cos \pi\varphi)}{\pi\varphi} \sin \pi\varphi(2\tau - 1). \quad (11)$$

The maximum amplitude is

$$\Delta = \frac{2(1 - \cos \pi\varphi)}{\pi\varphi}. \quad (12)$$

A plot of equation (12) is shown in Fig. 5. Before considering the action of this whip in terms of what it does to the system, we shall take a brief look at the analysis of the two other whips; viz., the sine whip and shifted cosine whip (see Fig. 3).

Sine Whip

We have again equation (3).

$$\frac{\ddot{x}}{\omega^2} + x = f(t) = x_1(t)$$

and equation (5)

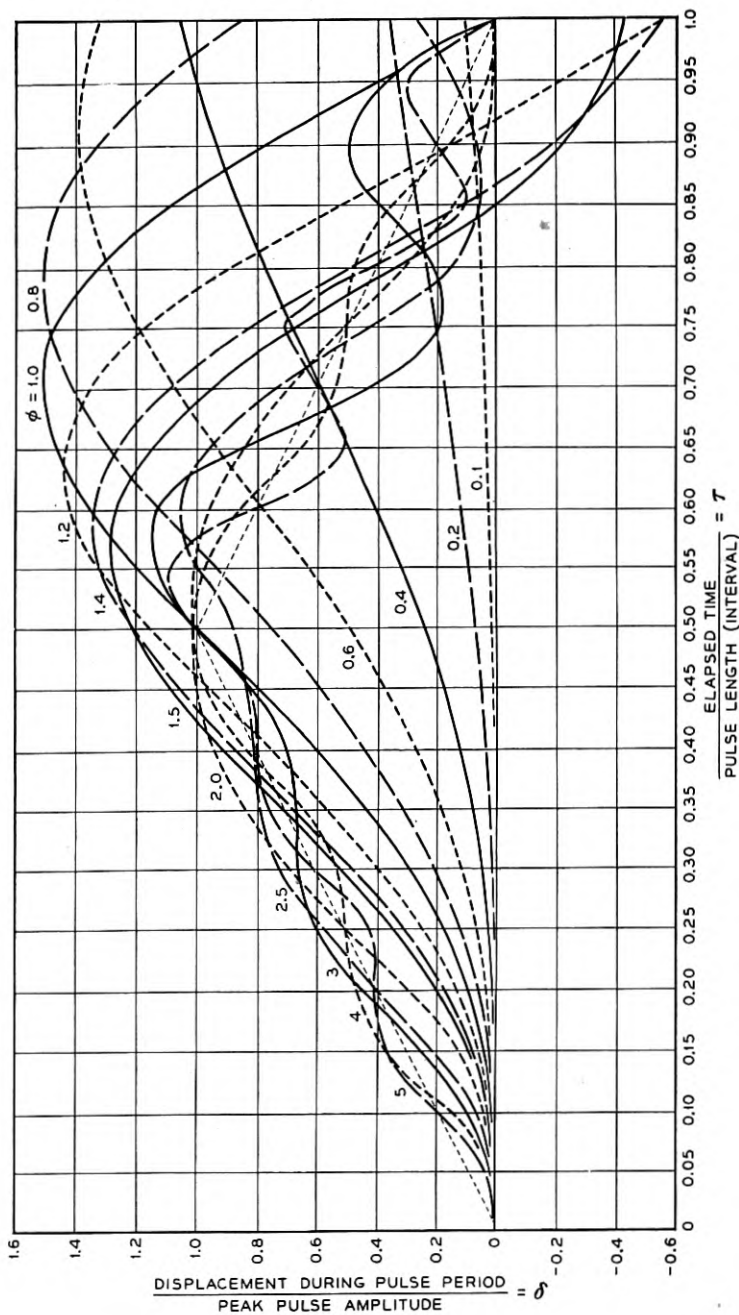$$\left(\frac{s^2 + \omega^2}{\omega^2}\right) X(s) = F(s)$$

Fig. 4—Transient time displacement curves for various values of triangular whip.

From 1.04

$$F(s) = \frac{a\omega_0}{s^2 + \omega_0^2} (1 + \epsilon^{-\pi s/\omega_0}).$$ (13)

Substituting (13) in (5) we obtain

$$X(s) = \frac{a\omega^2\omega_0}{(s^2 + \omega^2)(s^2 + \omega_0^2)} (1 + \epsilon^{-\pi s/\omega_0}).$$ (14)
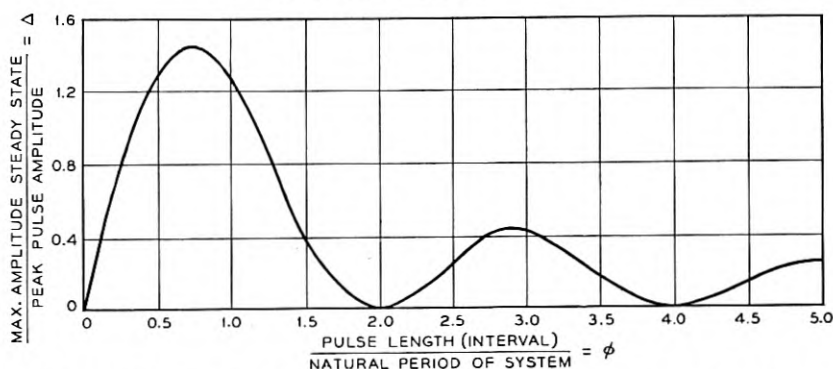

Fig. 5—Maximum amplitude as a function of frequency ratio-steady state triangular whip.

The inverse transform gives us

$$x = \frac{a\omega^2\omega_0}{\omega^2 - \omega_0^2} \left[\left(\frac{1}{\omega_0} \sin \omega_0 t - \frac{1}{\omega} \sin \omega t \right) + \left(\frac{1}{\omega_0} \sin \omega_0 \left(t - \frac{\pi}{\omega_0} \right) \right. \right.$$
$$\left. \left. - \frac{1}{\omega} \sin \omega \left(t - \frac{\pi}{\omega_0} \right) \right) u \left(t - \frac{\pi}{\omega_0} \right) \right]$$ (15)

and dividing this into two parts again, the transient and the steady state, we find for the transient,

$$x = \frac{a\omega^2\omega_0}{\omega^2 - \omega_0^2} \left[\frac{1}{\omega_0} \sin \omega_0 t - \frac{1}{\omega} \sin \omega t \right]$$

and substituting the dimensionless quantities

$$\delta = \frac{x}{a}, \qquad \frac{\pi/\omega_0}{T} = \varphi$$

and

$$\tau = \frac{t}{\pi/\omega_0}$$

we find

$$\delta = \frac{4\varphi^2}{4\varphi^2 - 1} \left(\sin \pi\tau - \frac{1}{2\varphi} \sin 2\pi\varphi\tau \right).$$ (16)

A plot of this equation as a family of curves for various values of φ is shown in Fig. 6. It is noted that, in general, this group of curves resembles those of Fig. 4 of the triangular whip.

The steady state is

$$x = \frac{a\omega^2 \omega_0}{\omega^2 - \omega_0^2} \left[\frac{1}{\omega_0} \sin \omega_0 t - \frac{1}{\omega}\sin \omega t \right.$$

$$\left. + \frac{1}{\omega_0} \sin \omega_0 \left(t - \frac{\pi}{\omega_0} \right) - \frac{1}{\omega}\sin \omega \left(t - \frac{\pi}{\omega_0} \right) \right] \tag{17}$$

and, in dimensionless quantities or expressed as a ratio of the pulse dimensions, we obtain

$$\delta_a = \frac{4\varphi}{1 - 4\varphi^2} \cos \pi\varphi \sin 2\pi\varphi(\tau - 1). \tag{18}$$

From (18) it follows that the maximum amplitude of the steady state is

$$\Delta = \frac{4\varphi \cos \pi\varphi}{1 - 4\varphi^2}. \tag{19}$$

A plot of this curve is shown in Fig. 7.

Shifted Cosine Whip.

The shifted cosine whip produces results of a similar nature. We have seen that the transform equation for this whip is (1.05)

$$F(s) = \frac{a\omega_0^2}{2s(s^2 + \omega_0^2)} (1 - \epsilon^{-2\pi s/\omega_0}). \tag{20}$$

Using equations (3) and (5) and transferring to dimensionless quantities, in which

$$\frac{x}{a} = \delta, \quad \frac{2\pi/\omega_0}{T} = \varphi = \frac{\omega}{\omega_0}, \quad \tau = \frac{t}{2\pi/\omega_0} = \frac{\omega_0 t}{2\pi}$$

we obtain

$$\delta = \frac{1}{2(\varphi^2 - 1)} \left(\cos 2\pi\varphi\tau - \varphi^2 \cos 2\pi\tau \right.$$

$$\left. - \cos 2\pi\varphi(\tau - 1)u(\tau - 1) + \varphi^2 \cos 2\pi(\tau - 1)u(\tau - 1) \right). \tag{21}$$

Since we are interested only in the transient displacement, (21) becomes

$$\delta = \frac{(1 - \cos 2\pi\varphi\tau) - \varphi^2(1 - \cos 2\pi\tau)}{2(1 - \varphi^2)} \tag{22}$$

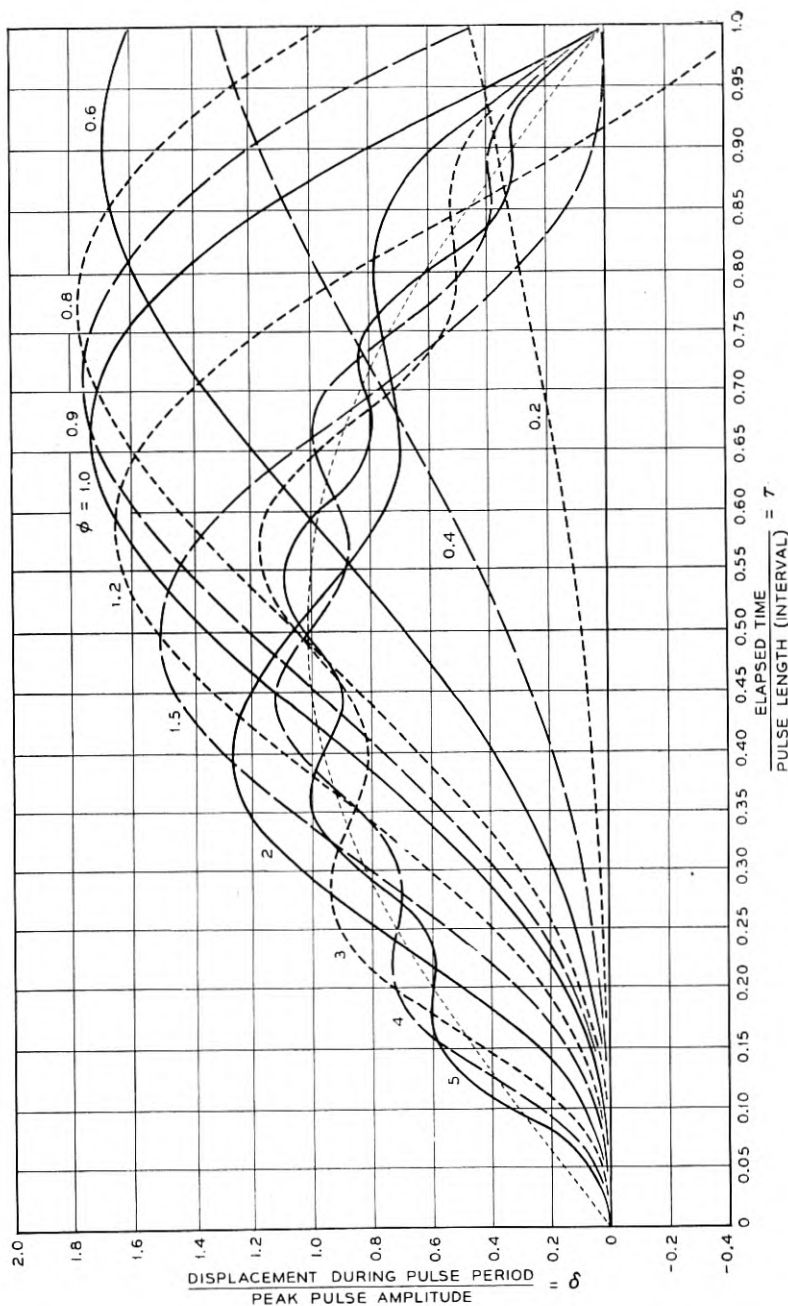A family of curves showing δ for various values of φ is shown in Fig. 8.

Fig. 6—Transient time displacement curves for various values of φ sine whip.

The steady state after the transient is (from Eq. 21)

$$\delta_a = \frac{1}{2(\varphi^2 - 1)} \left(\cos 2\pi\varphi\tau - \varphi^2 \cos 2\pi\tau \right.$$

$$\left. - \cos 2\pi\varphi(\tau - 1) + \varphi^2 \cos 2\pi(\tau - 1) \right)$$

which reduces to

$$\delta_a = \frac{\sin \pi\varphi}{1 - \varphi^2} \sin (2\pi\varphi\tau - \pi\varphi). \tag{23}$$
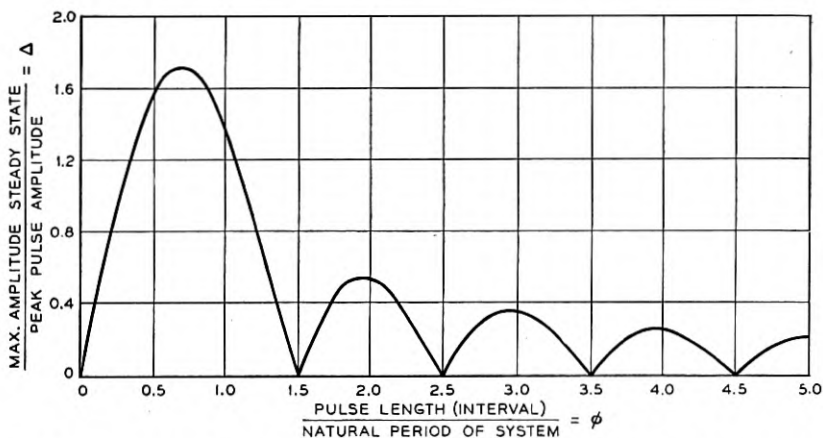

Fig. 7—Maximum amplitude as a function of frequency ration-steady state sine whip.

The maximum amplitude is

$$\Delta = \frac{\sin \pi\varphi}{1 - \varphi^2} \tag{24}$$

a plot of which is shown in Fig. 9.

Practical Considerations

Let us now consider the action of these various whips in terms of what they do to the system. The designer of shockmounts is primarily interested in the displacement across the mount or the relative displacement of base and mass.

In Fig. 10 the relative transient displacements for four systems are shown when subjected to a triangular whip. The natural frequencies are .4, 1.0, 1.5, and 2 times the frequency of the whip. From this it appears that the maximum relative displacement is approximately equal to the maximum
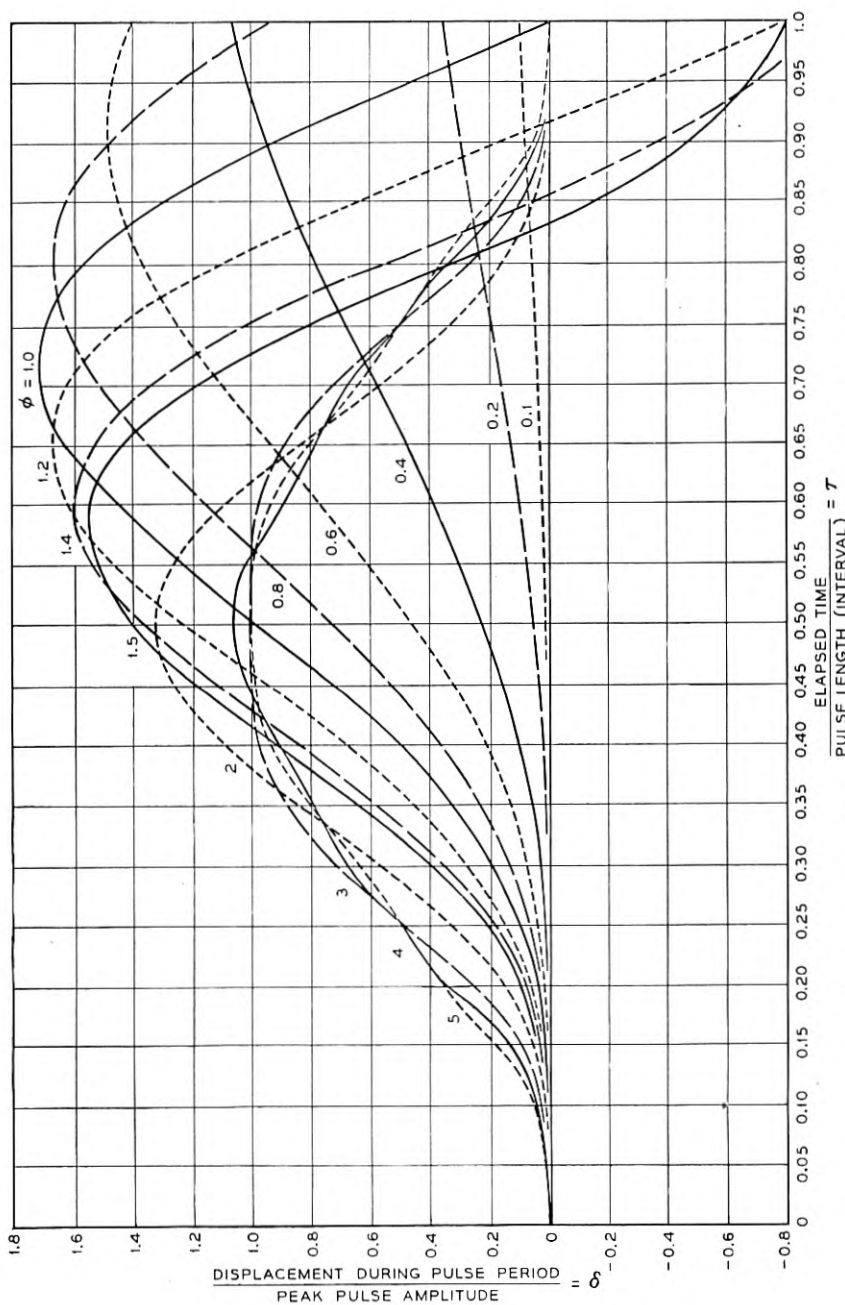
Fig. 8—Transient time displacement curves for various values of φ shifted cosine whip.

whip displacement.   It is also observed that the large relative displacements occur when the frequency of the system is smaller than the pulse frequency.

After the transient has passed, the relative steady-state displacement, which is of course equal to the absolute, obtains large values too.

From Fig. 5 we note that a maximum of 1.5 is reached for the triangular whip and up to 1.7 times for the sine whip (see Fig. 7) at a frequency of approximately $\frac{3}{4}$ of the whip.   Apparently even larger displacements across the mount occur after the transient has disappeared.

This is illustrated in Fig. 11 for the same systems as in Fig. 10.

As φ increases, which means if the frequency of the system increases with respect to the pulse frequency, the displacements across the mounts diminish,
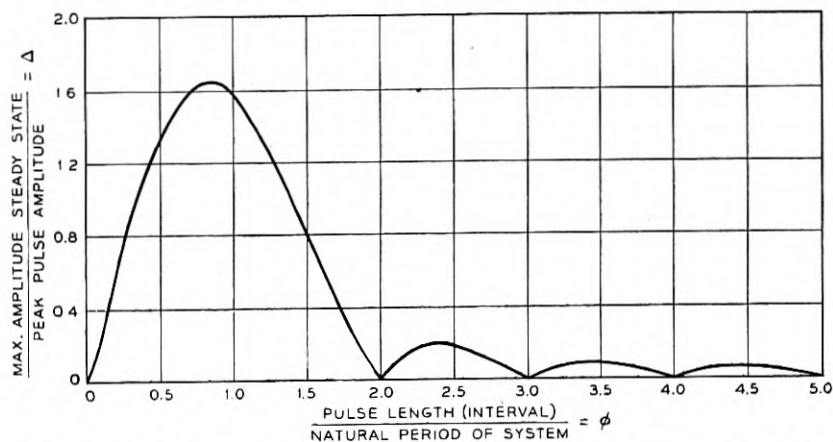

Fig. 9—Maximum amplitude as a function of frequency ratio-steady state shifted cosine whip.

while on the other hand the acceleration increases as will be shown later (see equation 39).

From this it seems advantageous to select a natural period of the system at least twice that of the pulse frequency.

The relative displacements are limited by practical considerations, such as available space between cabinets and bulk head, cable connections, personnel safety and others.

In the design of Bell Telephone Laboratories radar equipment, the relative displacement has been held to one-half inch, and the natural frequency in the neighborhood of 35 to 40 cycles per second or a period of 25 to 30 m.s.

The average of the heaviest shock administered to this type of equipment has a peak amplitude of 1.5 inch and a time interval of approximately 60 m.s.

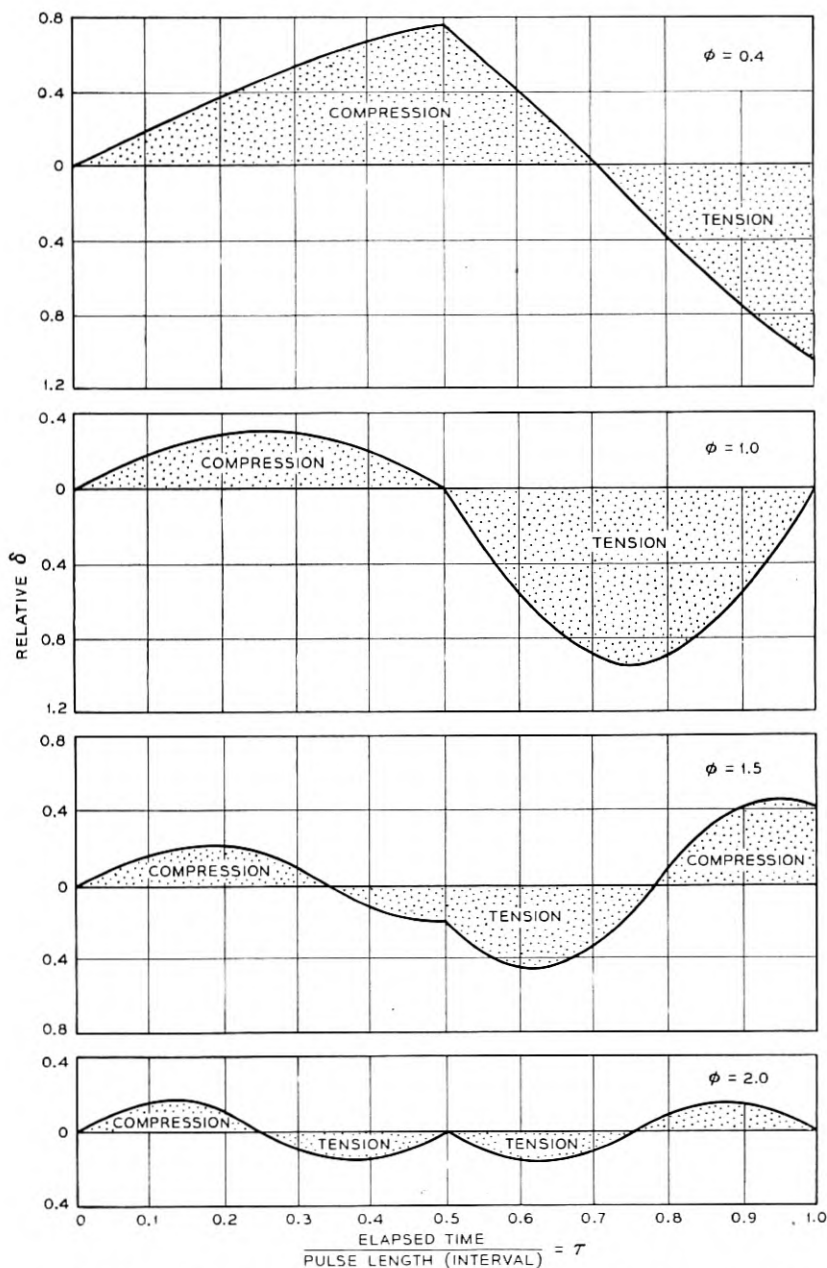From Fig. 5, we find that under these conditions a maximum relative dis-

Fig. 10—Transient time displacement curves across the mount for various values of φ triangular whip.
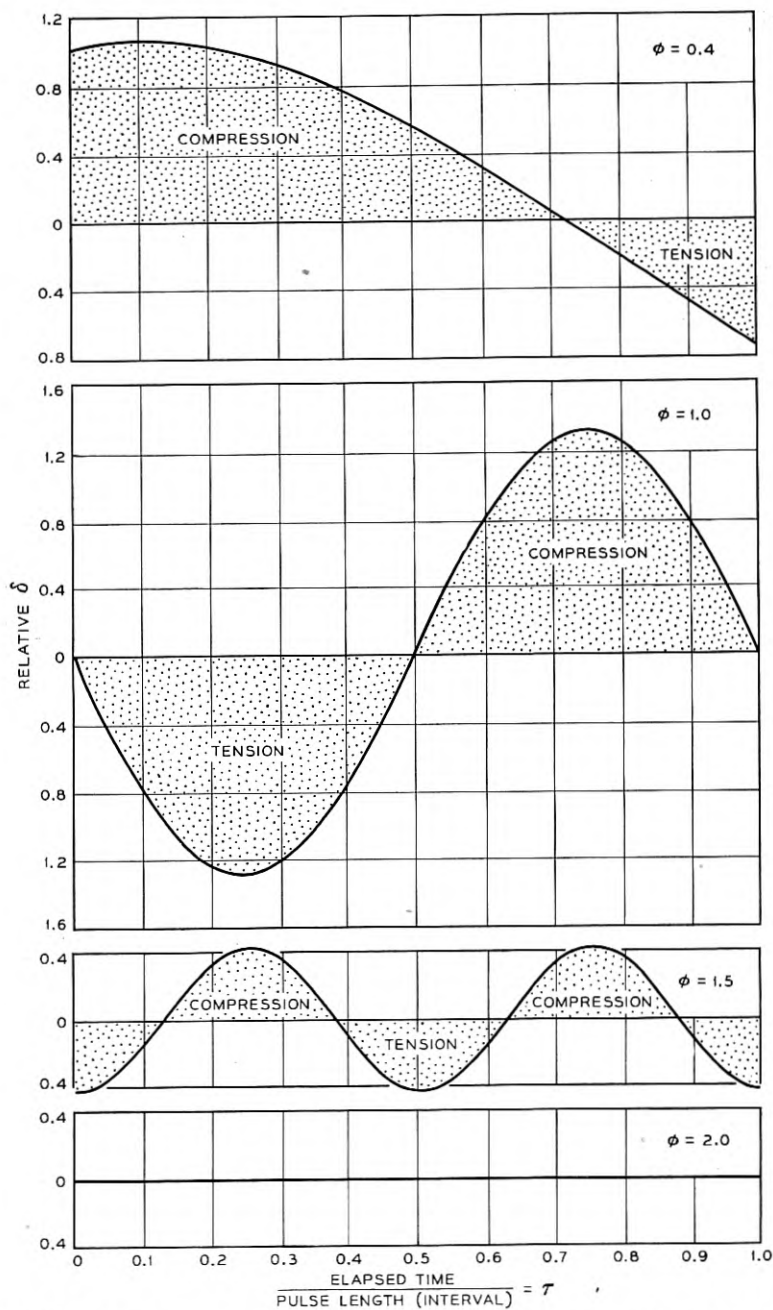
Fig. 11—Steady state time displacement curves across the mount.   Triangular whip.

placement of .42 times the peak pulse amplitude or approximately $\frac{5}{8}$ inch may be expected.

Taking into consideration that the shock mount has been designed with a certain amount of damping, it is thus possible to hold the relative displacement within the boundaries of its shock-absorbing capacity.
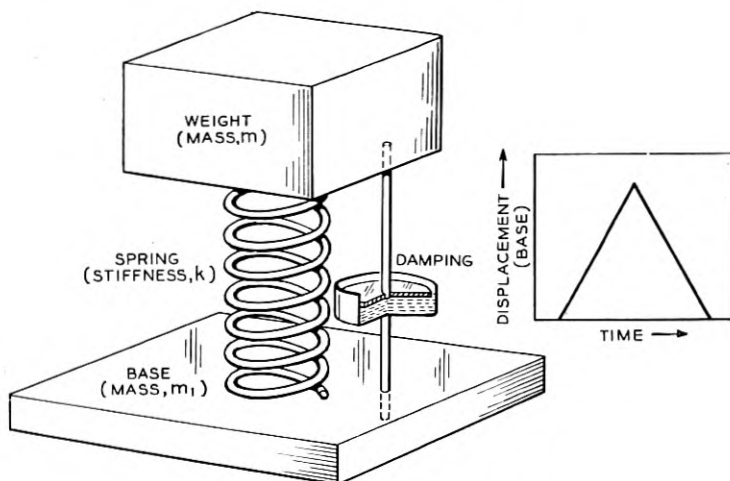

Fig. 12—System with damping.

Viscous Damping

The fundamental differential equation for a system with damping is (see Fig. 12).

$$\ddot{x} + 2\ell\dot{x} + \omega^2 x = 0 \tag{25}$$

If we let a whip operate on this system we obtain

$$\ddot{x} + 2\ell\dot{x} + \omega^2 x = \omega^2 x_1(t) \tag{26}$$

However, the sudden displacement of the base also produces an acceleration of the mass proportional to the velocity. If $x_1(t)$ is the displacement then $\dot{x}_1(t)$ may be represented to be the velocity and $2\ell\dot{x}_1(t)$ the acceleration. We have, then, for the completed equation

$$\ddot{x} + 2\ell\dot{x} + \omega^2 x = \omega^2 x_1(t) + 2\ell\dot{x}_1(t) \tag{27}$$

In the Laplacian terminology, if

$$x_1(t) = F(s)$$

then

$$\dot{x}_1(t) = sF(s) \quad \text{(initial value being zero)}$$

The Laplace transform of equation (27) is

$$X(s) = \frac{\omega^2 + 2\ell s}{s^2 + 2\ell s + \omega^2} F(s). \tag{28}$$

The solution of (28) is made easier if it is written in the form

$$X(s) = \frac{\omega^2 + 2\alpha s}{(s + \alpha)^2 + \beta^2} F(s) \tag{29}$$

in which

$$\alpha = \ell \quad \text{and} \quad \alpha^2 + \beta^2 = \omega^2.$$

Subjecting this system to a triangular whip, of which the Laplace transform is

$$F(s) = \frac{a}{b} \left(\frac{1 - \epsilon^{-bs}}{s} \right)^2$$

we have

$$X(s) = \frac{\omega^2 + 2\alpha s}{(s + \alpha)^2 + \beta^2} \frac{a}{b} \left(\frac{1 - \epsilon^{-bs}}{s} \right)^2 \tag{30}$$

the solution of which involves two transform pairs. The inverse transform gives us a solution of the transient as well as the steady state. It has been mentioned before that the steady state produces the maximum displacements across the mount; therefore it will be considered in more detail. We find that the steady state solution is

$$x_a(t) = \frac{a}{b} \frac{\epsilon^{-\alpha t}}{\beta} \left(-\sin \beta t + 2\epsilon^{\alpha b} \sin \beta(t - b) - \epsilon^{2\alpha b} \sin \beta(t - 2b) \right) \tag{31}$$

Which simplifies to

$$x_a(t) = \frac{\epsilon^{-\alpha t}}{\beta} \frac{a}{b} \sqrt{(A^2 + B^2)} \sin (\beta t - \theta) \tag{32}$$

Using dimensionless quantities

$$\eta = \frac{\ell}{\omega} = \frac{\alpha}{\omega} \quad \text{and} \quad \frac{x_a}{a} = \delta_a$$

and the substitution

$$\sqrt{1 - \eta^2} = \gamma,$$

we find that

$$b\beta = b\omega\gamma = \pi\varphi\gamma$$

Equation (32) may now be expressed as

$$\delta_a = \frac{\epsilon^{-\alpha t}}{\pi\varphi} \sqrt{(A^2 + B^2)} \sin(\omega\gamma t - \theta) \qquad \alpha t > 2\eta\pi\varphi \quad (33)$$

in which

$$\tan \theta = \frac{B}{A}$$

and

$$A = -1 + 2\epsilon^{\eta\pi\varphi} \cos \pi\varphi\gamma - \epsilon^{2\eta\pi\varphi} \cos 2\pi\varphi\gamma \qquad (34)$$

$$B = 2\epsilon^{\eta\pi\varphi} \sin \pi\varphi\gamma - \epsilon^{2\eta\pi\varphi} \sin 2\pi\varphi\gamma \qquad (35)$$
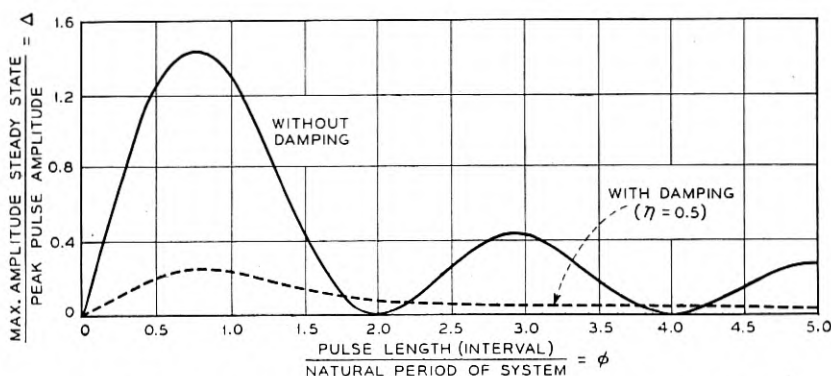

Fig. 13—Effect of damping on steady state amplitude for triangular whip.

From equation (33) we obtain the maximum displacement

$$\Delta = \frac{\epsilon^{-\alpha t}}{\pi\varphi} \sqrt{A^2 + B^2} \qquad \alpha t > 2\eta\pi\varphi \qquad (36)$$

in which

$$\alpha t = \frac{\eta}{\gamma} \left(\tan^{-1} \frac{\gamma}{\eta} + \tan^{-1} \frac{B}{A} \right) \qquad \alpha t > 2\eta\pi\varphi$$

In Fig. 13 a plot of equation (36) is shown for $\eta = .5$. This indicates that the peak value of Δ is .24 as compared to 1.48 when no damping is present.

Accelerations

The transient accelerations of the mass m during the whip action and the subsequent steady state may be found by examining the acceleration during the first part of a triangular whip. Designating the velocity of displacement

of the whip by v the expression for x may be formed from equation (7) by setting $t < b$.

$$x = \frac{a\omega^2}{b}\left(\frac{t}{\omega^2} - \frac{\sin \omega t}{\omega^3}\right), \qquad t < b \qquad (37)$$

and, since $\frac{a}{b} = v$

$$x = vt - \frac{v}{\omega}\sin \omega t \qquad (38)$$

whence

$$\ddot{x} = v\omega \sin \omega t$$

and the maximum acceleration is

$$A_0 = v\omega \qquad (39)$$

Let

$$\frac{A_0}{v\omega} = \lambda_0 \text{ then } \lambda_0 = 1$$

By proceeding in a similar manner with the next step of the whip the value of the acceleration ratio will be found to be

$$\lambda_0 = 3$$

and for the completed whip or steady state

$$\lambda_0 = 4$$

The expression $A_0 = \lambda_0 v\omega$ is an important factor in shock considerations. Thus we have a simple relation for the final maximum amplitude of the periodic acceleration of the mass m when subjected to a triangular whip; viz., it is four times the product of whip velocity and natural frequency of the system. The constant λ_0 depends upon the configuration of the whip; the velocity v indicates the intensity of the whip; while ω expresses the kind of response the system is capable of.

It is of interest to note that this maximum periodic value of A_0 will be produced only if the ratio of pulse frequency and natural frequency is of the correct value. It is difficult to produce shocks on existing equipment of exactly the same characteristics within narrow limits as to time duration and therefore it must expected that a considerable variation in damage may occur even though similar shocks are administered to identical test objects. For the same reason a shock of lower intensity may produce

more damage than a higher one because impulse amplitude as well as duration change at the same time.

Although damping is a highly desirable feature in a shock mount, the damping device may cause a certain amount of coupling between the mass and the base, and if too much damping is provided the transient acceleration of the mass may become excessive.

The analysis of this problem by means of the Laplace transforms is not difficult, for we can use results previously obtained. The transform equation for a system with damping, subjected to a whip, is

$$X(s) = \frac{\omega^2 + 2\alpha s}{(s + \alpha)^2 + \beta^2} \, F(s) \tag{40}$$

in which $F(s)$ represents the transform of the disturbance or excitation. Since we are interested in the effect of the damping or η upon the response, only the first part of the triangular whip will be considered.

In this case

$$x_1(t) = vt$$

and

$$\mathcal{L}[x_1(t)] = F(s) = \frac{v}{s^2}. \tag{41}$$

Substituting (41) in (40)

$$X(s) = \frac{v(\omega^2 + 2\alpha s)}{s^2[(s + \alpha)^2 + \beta^2]} = F_1(s) \tag{42}$$

If $X(s)$ is the transform of $x(t)$, a displacement, then the acceleration is $\ddot{x}(t)$ or $g(t)$, $(\ddot{x}(t) = g(t)$ by definition) and

$$\mathcal{L}[\ddot{x}(t)] = \mathcal{L}[g(t)] = s^2 X s$$

Substitution in (42) gives

$$s^2 \, X(s) = 2v\alpha \, \frac{s + \dfrac{\omega^2}{2\alpha}}{(s + \alpha)^2 + \beta^2} \tag{43}$$

Now $\mathcal{L}^{-1}[s^2 X(s)] = g(t)$
so that

$$g(t) = \frac{2v\alpha}{\beta} \left[\left(\frac{\omega^2}{2\alpha} - \alpha \right)^2 + \beta^2 \right]^{\frac{1}{2}} \epsilon^{-\alpha t} \sin(\beta t + \psi) \tag{44}$$
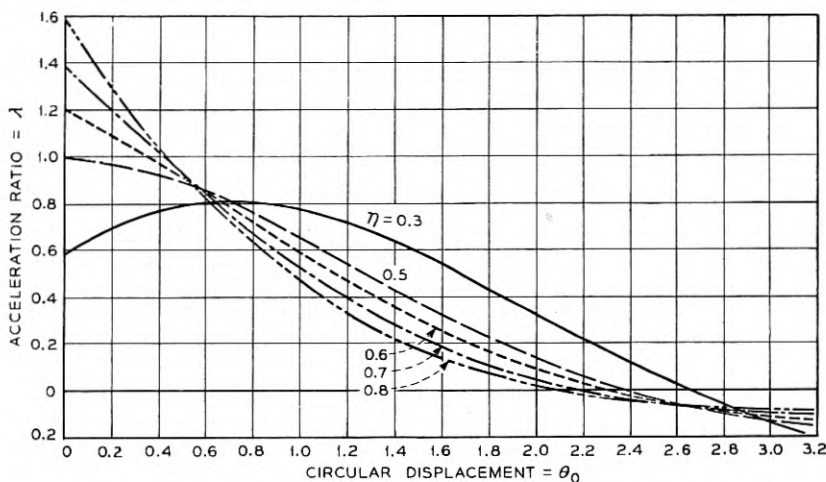
Fig. 14—Transient acceleration during initial part of triangular whip.

Letting

$$\frac{g(l)}{v\omega} = \lambda, \qquad \frac{\alpha}{\omega} = \frac{\ell}{\omega} = \eta, \qquad \beta = \omega \sqrt{1 - \eta^2} = \omega\gamma$$

and

$$\omega t = \theta_0$$

Substituting

$$\lambda = \frac{\epsilon^{-\eta\theta_0}}{\gamma} \sin(\lambda\theta_0 + \psi) \tag{45}$$

in which

$$\tan \psi = \frac{2\eta\gamma}{1 - 2\eta^2}$$

Figure 14 is a plot of λ against θ_0 for various values of η. It is noted that for $\eta = .5$ of critical damping the initial acceleration is equal to the undamped, λ being one.

The data presented here are also applicable to long duration pulses, because the final results have been given in dimensionless quantities, the units of measurement being those of the pulse.

Symbols Used

Mass .... m
Mass of base .... m_1
Spring stiffness .... k

Displacement mass...$x, x(t)$
Displacement base..$x_1, x_1(t)$
Force on base...$F, F(t)$
Velocity of base..v
Acceleration of base...$a_0, \ddot{x}_1$
Acceleration of mass m.......................................$\ddot{x}, \ddot{x}(t), g(t)$
Maximum acceleration of the mass m......................A_0

Maximum acceleration ratio..............................$\lambda_0 = \dfrac{A_0}{v\omega}$

Acceleration ratio..$\lambda = \dfrac{g(t)}{v\omega}$

Natural frequency of mass m (circular)....................ω, β_0
Circular (angular) displacement..............................$\omega t = \theta_0$
Frequency of sinusiode of which pulse consists (not pulse frequency).....ω_0
Peak pulse displacement.....................................a
Pulse period (triangular)....................................$2b$

"   "   (sine pulse).....................................$\dfrac{\pi}{\omega_0}$ $\Bigg\rbrace T_0$

"   "   (shifted cosine pulse)........................$\dfrac{2\pi}{\omega_0}$

Period of mass m...T

$\dfrac{\text{displacement during pulse period}}{\text{peak pulse amplitude}} = \ \dots \ \dfrac{x}{a} = \delta$

$\dfrac{\text{amplitude steady state}}{\text{peak pulse amplitude}} = \ \dots \ \delta_a$

$\dfrac{\text{max. amplitude steady state}}{\text{peak pulse amplitude}} = \ \dots \ \Delta$

$\dfrac{\text{elapsed time}}{\text{pulse length (interval)}} = \ \dots \ \dfrac{t}{2b}, \ \dfrac{t/\pi}{\omega_0}, \ \dfrac{t/2\pi}{\omega_0}, \ \dfrac{t}{T_0} = \tau$

$\dfrac{\text{pulse length (interval)}}{\text{natural period of system}} \ \dots \ \dfrac{T_0}{T} = \varphi$

Damping coefficient...ℓ, α

Critical damping ratio.......................................$\dfrac{\ell}{\omega} = \eta$

Transform of $x(t) = $.......................................$X(s)$
"   " $x_1(t) = $.......................................$X_1(s)$
"   " $F(t) = $..... $F_0(s)$
"   " $f(t) = $........ $F(s)$

$f(t)$ represents any function of t, without reference to its dimensional magnitude.

Maximally-flat Filters in Waveguide

By W. W. MUMFORD

Microwave radio relay repeaters require the use of band-pass filters which match closely the impedances of the interconnecting transmission lines and which suppress adjacent channels adequately. A type of structure called a *Maximally-Flat* filter meets these requirements.

The ladder network which gives a maximally-flat insertion loss characteristic is discussed and several methods of achieving its counterpart in microwave transmission lines are presented. Resonant cavities are used to simulate tuned circuits and the necessary formulas relative to this approximate equivalence are given.

Experimental data confirm the theory and show that this technique yields remarkable impedance matches.

INTRODUCTION

WE USUALLY associated the word *filter* with any device which is selective. The electric wave filter has that property which enables it to transmit energy in one band or bands of frequencies and to inhibit energy in other bands. Selectivity is the result of either selective absorption[1, 2*] or selective reflection. This paper discusses a special case of the classical lossless transducer which derives its selective properties entirely from selective reflection. The insertion loss of this type of filter can be analyzed in terms of the input reflection coefficient and the input standing wave ratio.

In many applications of lossless filters it is desirable to obtain a characteristic such that the insertion loss, and hence the reflection coefficient, is small over as wide a band as possible. A special case described here, referred to as a maximally-flat filter, has a loss characteristic such that a maximum number of its derivatives are zero at midband. While the maximally-flat type of characteristic does not give the smallest possible reflections over a finite pass band, it does give small reflections, and has added advantages of simplicity in design and in many cases less transient distortion than filters giving smaller reflections.

The desirable characteristics of maximally-flat filters have long been realized.[1, 3] Mr. W. R. Bennett[4] of these Laboratories derived the constants for a maximally-flat ladder network in the late 20's, and gave simple expressions for the element values. Butterworth,[5] Landon[6] and Wallman[7] have treated maximally-flat filter-amplifiers in which the filter sections are separated by amplifier tubes. Darlington[8] has considered the general case of four terminal filters which have insertion loss characteristics that can be prescribed, but he places the emphasis more on filters that have tolerable

---

* A list of selected references appears at the end of the paper.

ripples in the pass-band than on maximally-flat structures. The work of Bennett will be followed closely not only because it came first, but also because it is easy to understand.

Bennett expresses the values of the filter branches in terms of their cutoff frequencies, which in turn bear a relationship to the cutoff frequencies of the total filter. In the language of one who is familiar with microwave technique,[9, 10, 11, 12] the values of the filter branches can be expressed in terms of the loaded Q's of the cavities, which in turn bear a relationship to the loaded Q of the total filter. A simple mathematical expression connects the loaded Q to the cutoff wavelengths.

At low frequencies the band-pass maximally-flat filter is made up of resonant branches connected alternately in series and in parallel. The microwave analogue of this configuration is obtained by the use of shunt resonant cavities that are spaced approximately a quarter wavelength apart in the waveguide. Use is made of the impedance inverting property of a quarter wave line, thereby eliminating the necessity of using both series and parallel branches.

The resonant cavity in the waveguide resembles a shunt resonant tuned circuit,[13] but is different in several minor respects. An analysis of these differences reveals the corrective measures that are necessary in order that the simulation shall be sufficiently accurately attained.

The first part of the paper deals with the concepts of loaded Q and resonant filter branches of both the series and the parallel types. Admittance and impedance functions, as well as expressions for the insertion loss, are given using these terms, and the relationship between loaded Q and cutoff frequencies is stated. This concept of loaded Q is then introduced to describe the performance of a complete maximally-flat filter in terms of its cutoff frequencies. The insertion loss is then given as a simple expression containing the total Q and the resonant frequency. The Q's of all the branches are derived from the total Q in simple terms. The connection between the insertion loss and the input standing wave ratio is then discussed before turning to the actual design problem.

Next the paper deals with the application of the filter theory to waveguide technique. The limitations of the quarter-wave coupling lines are pointed out and the added selectivity due to them is derived.

Then the paper compares microwave resonant cavities with parallel-tuned circuits. Formulas are given which relate the geometrical configuration to the loaded Q, the resonant frequency and the excess phase of the cavities. Three types of cavities are treated: those using inductive posts, inductive irises and capacitive irises.

Finally, the measured results on a four-cavity maximally-flat filter in $1'' \times 2''$ waveguide are presented and compared with the original design points.

As a further confirmation of the theory, the experimental results on another and longer waveguide filter consisting of fifteen resonant cavities and fourteen connecting lines are given.   The conclusion is reached that maximally-flat waveguide filters can be designed to have excellent impedance match and off-band suppression qualities.

NOTATION

a	Width of waveguide.
b	Height of waveguide.
B	Normalized susceptance.
c	Velocity of light in free space.
C_r	Capacitance in the rth branch of a filter.
d	Width of iris opening.
d	Diameter of post in waveguide.
δ	A small number $\ll 1$.
ϵ	Base of natural logarithms.
f	Frequency.
f_0	Resonant frequency.
f_c	Frequency at half power point.
f_{cw}	Cutoff frequency of waveguide.
G	Terminating conductance of filter.
θ	$\dfrac{2\pi \ell}{\lambda}$
K	Susceptance parameter.
ℓ	Length of transmission line.
ℓ'	Length of line corresponding to excess phase of cavity.
ℓ_c	Length of line connecting two cavities.
λ_0	Resonant wavelength.
λ_c	Wavelength at half power point.
λ_g	Wavelength in transmission line.
λ_a	Wavelength in free space.
L_r	Inductance in r^{th} branch of a filter.
m	An integer, including zero.
n	Number of branches in filter.
P_0	Available power.
P_L	Power delivered to load.
Q	Loaded Q. The selectivity of a loaded circuit.
Q_r	Loaded Q of the rth branch.
Q_T	Loaded Q of the total filter.
R	Terminating resistance of the filter.
s	Distance from center of waveguide.
S	Voltage standing wave ratio.

τ Thickness of iris.
V_{max} Maximum voltage on transmission line.
V_{min} Minimum voltage on transmission line.
ω Angular frequency.
Ω Frequency parameter.
Y Admittance.
Y_0 Surge admittance of transmission line.
Z Impedance.
Z_0 Surge impedance of transmission line.
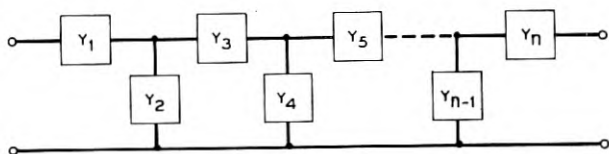
THE Y'S ARE USED TO DENOTE
GENERALIZED ADMITTANCE FUNCTIONS

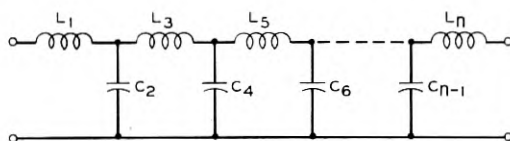Fig. 1—Block diagram of a filter consisting of a ladder network.

Fig. 2—Schematic diagram of a low-pass filter.

GENERAL

The art of designing filters which utilize lumped elements is well known. Desirable characteristics may be obtained by means of a ladder network of generalized admittances, such as is illustrated in Fig. 1. In particular a low-pass filter takes the configuration shown in Fig. 2, and a band-pass filter that of Fig. 3. In either case, certain frequency selectivity characteristics can be obtained when the individual branches are assigned definite values. The individual branches, L_1C_1, L_2C_2, in the bandpass filter consist of an inductance, L_r, and capacity, C_r, in series or shunt. For the specific case to be discussed in this paper, namely a filter consisting of lossless elements intended for insertion between a source having an internal resistance R and a receiver having the same resistance, analysis is simplified if a branch is described in terms of its resonant frequency and its loaded Q.* The

* The loaded Q of a resonant branch in such a filter is the reciprocal of its percentage band width measured to the half power points when that branch alone is fed by the same generator and has the same load resistance as that of the total filter.

resonant frequency of a branch is independent of the terminal resistance and is given by the relation

$$f_0 = \frac{1}{2\pi\sqrt{L_r C_r}} \tag{1}$$

The loaded Q of the branch, to be designated Q_r, is a function not only of the inductance and capacitance in the branch, but also of the resistance, R, of the terminations on the filter. For the series resonant branches, it is given by

$$Q_r = \frac{1}{2R}\sqrt{\frac{L_r}{C_r}} = \frac{\omega_0 L_r}{2R} \tag{2}$$

and for the parallel resonant branches

$$Q_r = \frac{R}{2}\sqrt{\frac{C_r}{L_r}} = \frac{\omega_0 C_r}{2}R. \tag{3}$$
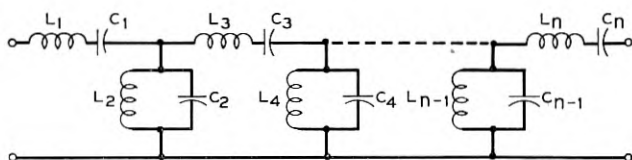
Fig. 3—Schematic diagram of a band-pass filter.

It may be noted that the loaded Q can be defined in terms of the insertion loss imposed by connecting the branch between a source and receiver each of resistance R. Analysis of such a circuit shows that

$$\frac{P_0}{P_L} = 1 + Q_r^2\left(\frac{f}{f_0} - \frac{f_0}{f}\right)^2 \tag{4}$$

where f is the frequency;

P_0 is the power available from a generator which has an internal resistance R;

P_L is the power delivered through the inserted branch to a load of resistance R.

At the cutoff frequency, f_c, defined as the frequency at which the power delivered to the load is half the available power, $\dfrac{P_0}{P_L} = 2$, whence

$$Q_r = \left|\frac{1}{\dfrac{f_c}{f_0} - \dfrac{f_0}{f_c}}\right| = \left|\frac{f_0}{f_{c_2} - f_{c_1}}\right|. \tag{5}$$

Written in terms of the wavelengths this becomes

$$Q_r = \frac{\dfrac{1}{\lambda_0}}{\dfrac{1}{\lambda_{c_2}} - \dfrac{1}{\lambda_{c_1}}}. \tag{6}$$

This equation is a convenient one to use later in the discussion on resonant cavities.

The normalized admittance of a single-shunt branch terminated by a resistance R can be expressed in terms of its resonant frequency and its Q; thus

$$YR = 1 + j2Q_r\left(\frac{f}{f_0} - \frac{f_0}{f}\right). \tag{7}$$

Similarly, the normalized impedance of a single-series branch terminated by a resistance R can be written

$$\frac{Z}{R} = 1 + j2Q_r\left(\frac{f}{f_0} - \frac{f_0}{f}\right). \tag{8}$$

The use of the term loaded Q thus has the advantage that expressions for normalized admittance and normalized impedance of shunt and series resonant circuits respectively are identical, as are also the corresponding expressions for their insertion loss functions.

Loss functions of complete filters can likewise be expressed in terms of a loaded Q defined for the complete filter. For example, the loss function of the particular type of filter called a "Maximally-flat" filter is given[4]

$$\frac{P_0}{P_L} = 1 + \left[\frac{\dfrac{f}{f_0} - \dfrac{f_0}{f}}{\dfrac{f_c}{f_0} - \dfrac{f_0}{f_c}}\right]^{2n} \tag{9}$$

where n is the number of resonant branches in the filter, and f_c is the cutoff frequency of the filter (half power points).

In consequence of the concept of loaded Q of the total filter, the loss function can be expressed as

$$\frac{P_0}{P_L} = 1 + \left[Q_T\left(\frac{f}{f_0} - \frac{f_0}{f}\right)\right]^{2n} \tag{10}$$

where the total Q_T of the filter is

$$Q_T = \left|\frac{1}{\dfrac{f_c}{f_0} - \dfrac{f_0}{f_c}}\right|. \tag{11}$$

For convenience, the bracketed term of equation 9 may be called Ω, a frequency parameter, whence

$$\Omega = \left[\frac{\dfrac{f}{f_0} - \dfrac{f_0}{f}}{\dfrac{f_c}{f_0} - \dfrac{f_0}{f_c}} \right] = Q_r \left(\frac{f}{f_0} - \frac{f_0}{f} \right) \tag{12}$$

and the loss function becomes
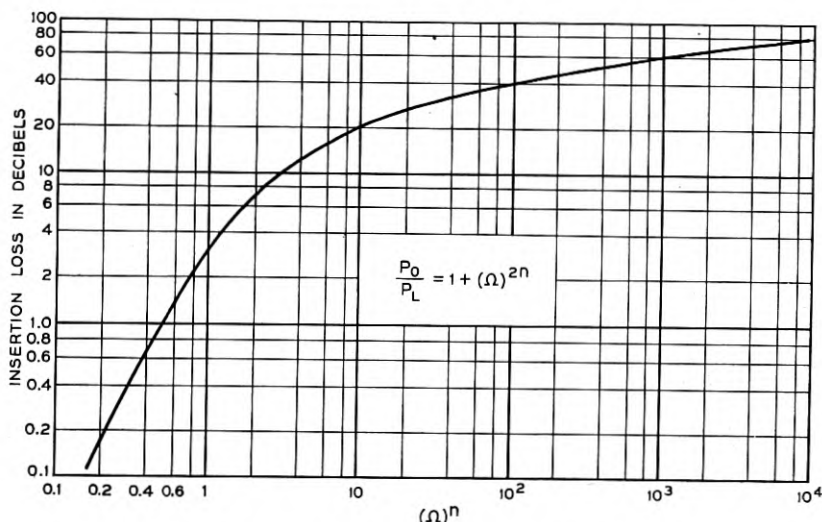
$$\frac{P_0}{P_L} = 1 + (\Omega)^{2n}. \tag{13}$$

Fig. 4—Insertion loss of maximally-flat filters.

MAXIMALLY-FLAT FILTERS

The loss function for maximally-flat filters as given in equation 13 is plotted in Fig. 4 where the insertion loss in db is used on the ordinate and Ω^n is used on the abscissa.

The ladder network which gives rise to this loss function consists of n resonant branches, as shown in Fig. 3, that are all tuned to the same frequency, but whose selectivities, or loaded Q's, are tapered from one end of the filter to the other according to the positive imaginary parts of the $2n$ roots of -1, according to the theories of Bennett[4] and Darlington.[8]   These roots are expressed thus

$$\sin\left(\frac{2r - 1}{2n}\right)\pi$$

where r is the number of the root, n is the total number of branches. Thus the selectivities of the branches follow the relation

$$Q_r = Q_T \sin \left(\frac{2r - 1}{2n} \right) \pi \tag{14}$$

where Q_T represents the selectivity of the total filter, and Q_r represents the required selectivity of the rth branch, e.g., the selectivities of the first, second and third branches are

$$Q_1 = Q_T \sin \frac{\pi}{2n}$$

$$Q_2 = Q_T \sin \frac{3\pi}{2n} \tag{15}$$

$$Q_3 = Q_T \sin \frac{5\pi}{2n}.$$

This type of filter is particularly practical when a filter is required to give more than a certain amount of insertion loss in an adjacent band, and less than another certain amount of insertion loss at the edges of the pass-band. Putting this information in equation 10 gives two equations containing two unknowns, Q_T, the selectivity of the total filter, and n, the number of branches needed to fulfill the stated requirements. The solution for n may be fractional, in which event the next higher integral value of n is chosen, and this value is used to determine the selectivity, Q_T, of the filter. From this, the selectivities of all the branches are determined in accordance with equation 14.

Standing Wave Ratio

An alternative way of specifying filter performance is to refer to the input impedance mismatch as a function of frequency. The impedance mismatch can be expressed in terms of the direct and the reflected waves and in terms of the standing wave ratio that exists along the transmission line that connects the properly terminated filter with its generator. The standing wave ratio and the insertion loss of a filter bear a definite relationship to each other if the filter is composed of purely reactive elements. This relationship is given by the formula

$$\frac{P_0}{P_L} = \frac{(S + 1)^2}{4S} \tag{16}$$

where S is the standing wave ratio, $\frac{V_{\text{max}}}{V_{\text{min}}}$, of the maximum voltage to the minimum voltage as measured along the transmission line.

When the filter characteristic is given by equation 13, the relationship between Ω, the frequency parameter, and the standing wave ratio can be expressed as

$$(\Omega)^n = \frac{S - 1}{2\sqrt{S}}.$$ (17)

This is shown graphically in Fig. 5, where the standing wave ratio is given in db $\left(20 \log_{10} \dfrac{V_{max}}{V_{min}}\right)$. This graph is used as an aid in the design of filters of
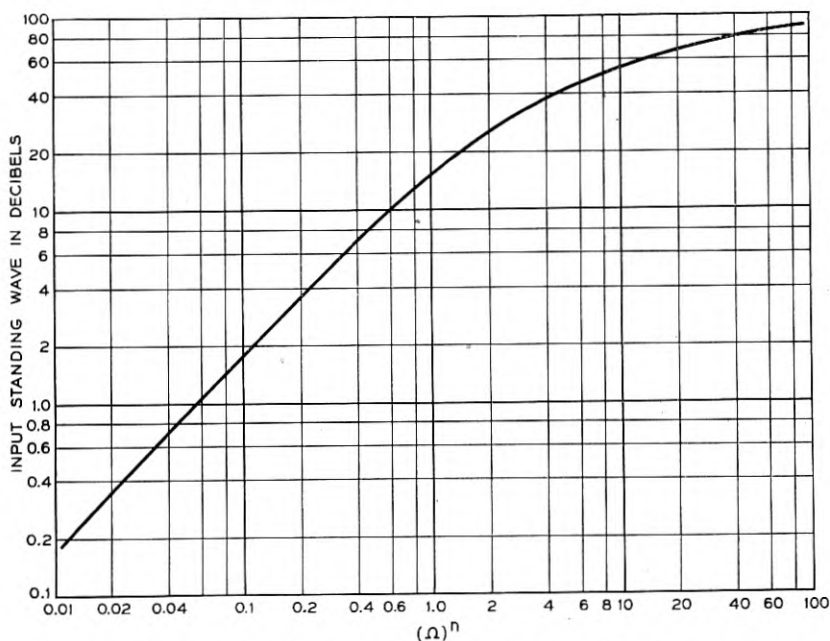

Fig. 5—Input standing wave ratio of maximally-flat filters.

this type, where the requirements are given in terms of the standing wave ratio. From this information the number of filter branches and the selectivity of the total filter can be determined, either from equation 17 or from Fig. 5.

DISTRIBUTED BRANCHES

It has been assumed that the mutual impedances of successive branches are all zero. At low frequencies this limitation may not be a serious one and the practical realization of the expected filter characteristics is accomplished by shielding properly one branch from another. However, as the

frequency is increased it becomes difficult to isolate the branches and unde-
sirable mutual impedances arise which complicate the problem.   In par-
ticular, in the microwave region, where waveguides are used, the physical
size of each branch may be large compared with the wavelength and it is
then impossible to lump all the branches at one place in the waveguide with-
out encountering the complicated effect of mutual impedances.

A practical way of circumventing this difficulty is to distribute the branch
circuits along the transmission line or waveguide at such distances that the
mutual impedances become negligible.   Then, however, the lengths of
transmission line act as transducers, but since their properties are well under-
stood and readily calculable this appears to be a practical solution.   As a
matter of fact, the impedance transforming properties of a length of trans-
mission line can be used to advantage.[9, 13, 14]   For instance, it is well
known that a quarter wavelength of lossless line transforms a load imped-
ance according to the relation

$$Z = \frac{Z_0^2}{Z_L} \tag{18}$$

where Z_0 is the surge impedance of the line and Z_L is the load impedance.

Hence if the load impedance consists of a series resonant circuit contain-
ing an inductance, a capacity and a resistance equal to Z_0 in series, the im-
pedance at the input end of the quarter wavelength of line is given

$$Z = \frac{Z_0}{\left[1 + j2Q \left(\frac{f}{f_0} - \frac{f_0}{f} \right) \right]}. \tag{19}$$

The input admittance is

$$Y = Y_0 \left[1 + j2Q \left(\frac{f}{f_0} - \frac{f_0}{f} \right) \right]. \tag{20}$$

As can be seen from equation 7, this is identical with the input admittance
of a parallel tuned circuit whose terminating conductance is

$$G = Y_0. \tag{21}$$

The quarter-wave line likewise transforms a parallel circuit to a series
circuit, as is illustrated in Fig. 6.   This property of the quarter-wave line
thus makes it possible to simulate a ladder network of alternate series and
shunt branches by spacing shunt branches (or series branches) at quarter
wavelength intervals along a transmission line, as illustrated in Fig. 7.
The resonant frequencies and the selectivities of the branches are chosen as
before.

Sometimes in practice a quarter wavelength may not be sufficient spacing to avoid mutual impedances arising between adjacent elements, in which event the connecting line may be increased to a higher odd multiple of quarter wavelength.   This accentuates the frequency sensitivity of the connect-
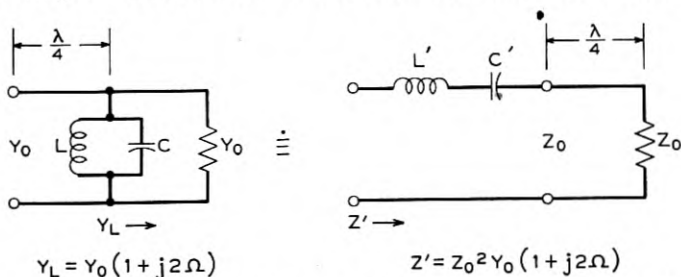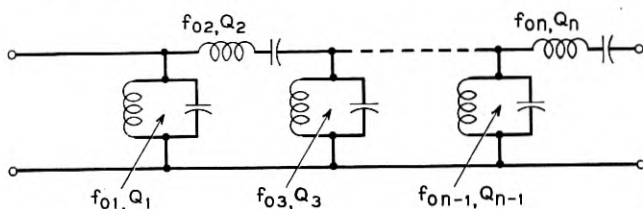

$$Y_L = Y_0(1 + j2\Omega) \qquad\qquad Z' = Z_0^2 Y_0(1 + j2\Omega)$$

Fig. 6—Illustrating the impedance inverting property of a quarter wavelength of transmission line.

LUMPED CONSTANT FILTER USING SERIES & SHUNT ELEMENTS

LUMPED CONSTANT FILTER USING ONLY SHUNT ELEMENTS
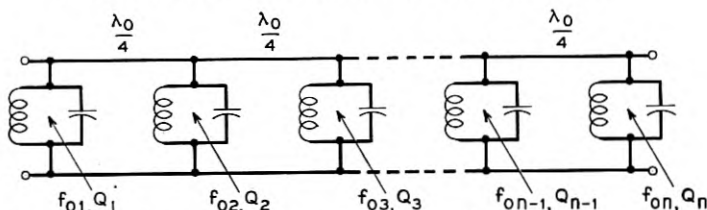
Fig. 7—Simulation of ladder network by shunt branches at quarter wave intervals.

ing line, but this effect can be taken into account by decreasing the selectivities of the branches themselves by appropriate amounts.   In narrow-band filters this may be negligible, but in broad-band filters it may be considerable, as shown in the following analysis.

SELECTIVITY OF CONNECTING LINES

Consider a length of transmission line having a surge impedance $Z_0 = \dfrac{1}{Y_0}$ and terminated in a parallel resonant circuit containing an inductance, a

capacitance and a resistance equal to Z_0,* as in Fig. 6. The terminating admittance is given by the relation (See Eq. 7 and 9)

$$Y_L = Y_0(1 + j2\Omega). \tag{22}$$

The input admittance at the end of the length of line, ℓ, (nominally a quarter wavelength long) is given by the relation

$$\frac{Y}{Y_0} = \frac{(1 + j2\Omega)\cos\theta + j\sin\theta}{\cos\theta + j(1 + j2\Omega)\sin\theta} \tag{23}$$

where

$$\theta = \frac{2\pi\ell}{\lambda}$$

$$\ell = \text{length of line}$$

$$\lambda = \text{wavelength}$$

$$\Omega = Q\left(\frac{f}{f_0} - \frac{f_0}{f}\right)$$

letting

$$\theta = \frac{\pi}{2}(1 + \delta) = \frac{\pi}{2} + \frac{\pi\delta}{2} \tag{24}$$

$$\cos\theta = -\sin\frac{\pi\delta}{2} \doteq -\frac{\pi\delta}{2} \tag{25}$$

$$\sin\theta = \cos\frac{\pi\delta}{2} \doteq 1 \tag{26}$$

where δ is a number small compared with 1. Then the admittance becomes

$$\frac{Y}{Y_0} \doteq j\frac{\pi\delta}{2} + \frac{1}{1 + j\left(2\Omega + \frac{\pi\delta}{2}\right)}. \tag{27}$$

This is the normalized input admittance of a circuit as shown in Fig. 8, where each end of an ideally inverting line is shunted by a tuned circuit whose normalized admittance is $j\frac{\pi\delta}{2}$.

From Eq. 24, setting $\frac{2\pi\ell}{\lambda_0} = \frac{\pi}{2}$, it follows that

$$\delta = \pm\left(\frac{f}{f_0} - 1\right) \doteq \left(\frac{f}{f_0} - \frac{f_0}{f}\right)(\tfrac{1}{2}). \tag{28}$$

* More generally, the terminating admittance can assume any value without affecting the result.

From equation 7, the admittance of the circuit is expressed in terms of its selectivity, thus

$$j\frac{\pi\delta}{2} = j2Q\left(\frac{f}{f_0} - \frac{f_0}{f}\right). \tag{29}$$

Solving for the selectivity of this circuit, from Equations 28 and 29:

$$Q = \frac{\pi}{8}. \tag{30}$$

The selectivity of the coupling line can hence be counteracted by subtracting $\frac{\pi}{8}$ from the selectivities of the branches associated with it, provided
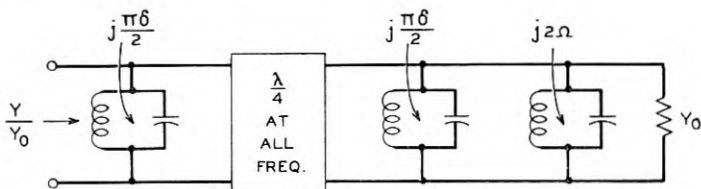

Fig. 8—Schematic diagram illustrating that the selectivity of a quarter wavelength of line can be represented by adding a tuned circuit to each end of an ideally inverting impedance transformer.

the coupling line is a quarter wavelength long. If it becomes necessary to use $\frac{3}{4}$ wavelength coupling lines, the selectivity of the line is tripled and $\frac{3\pi}{8}$ is subtracted from the selectivities of the associated branches.

RESONANT CAVITIES

The foregoing analysis reviews the principles of the design of filters which use lumped-constant circuits distributed along a transmission line. These principles can be applied to the design of filters in waveguides, coaxial lines, or any other types of transmission lines, provided that these lines are sufficiently lossless, the band is sufficiently narrow and the branches themselves are realizable. In the microwave region the first two provisions are usually met without difficulty, as is also the third provision when circuits with distributed constants are used. It may be difficult to construct a coil and a condenser circuit for microwaves, but easy to construct a resonant cavity which displays some of the desirable properties of the tuned circuit. Resonant cavities are similar to lumped tuned circuits in two respects.[12, 13] They transmit a band of frequencies and they introduce a phase shift. An approximate equivalence is demonstrated in Appendix I, and is illustrated in Fig. 9, which depicts a resonant cavity as being nearly identical with a

tuned circuit situated across the middle of a short length of transmission line.   This short length of transmission line is added in order to account for an excess of phase shift associated with the resonant cavity, but it can readily be absorbed in the connecting line which otherwise would have been an odd quarter wavelength long.

The similarity between resonant cavities and resonant lumped circuits enables one to use the known art of designing lumped element filters to de-
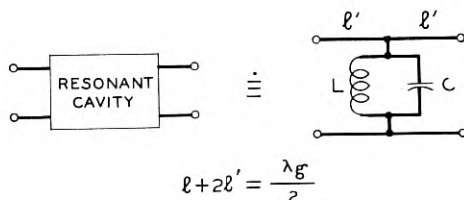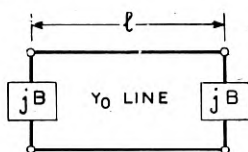

$$\ell + 2\ell' = \frac{\lambda_g}{2}$$

Fig. 9—A resonant cavity is approximately equivalent to a resonant circuit shunted across a short length of transmission line.

$$TAN \frac{2\pi \ell}{\lambda_0} = \frac{2}{B}$$

$$Q = \frac{ARC\ TAN \dfrac{2}{B}}{2\ ARC\ SIN \dfrac{2}{\sqrt{B^4 + 4B^2}}} \doteq \frac{\sqrt{B^4 + 4B^2}}{4}\ ARC\ TAN \frac{2}{B}$$

Fig. 10—The resonant wavelength and the loaded Q of a cavity depend upon the normalized susceptance of the end obstacles and their separation.

sign filters which use resonant cavities, provided that the selectivity, the resonant frequency and the excess phase shift of the resonant cavity are known.

Resonant Wavelength and Loaded Q of Cavities

These properties can best be derived by considering one of the usual types of cavities, which consists of two obstacles or discontinuities separated by a length of transmission line.   Such a cavity is shown schematically in Fig. 10.   The obstacles at each end are assumed to be equal, and to have an unvarying susceptance BY_0, where Y_0 is the surge admittance of the con-

necting transmission line. This type of cavity is resonant when the relation is satisfied[9, 10]

$$\tan \frac{2\pi \ell}{\lambda_0} = \frac{2}{B} \tag{31}$$

where λ_0 is the resonant wavelength in the transmission line,

    ℓ is the length of the cavity

    B is the normalized susceptance of the end obstacles.

This resonance occurs at any number of wavelengths, but the 1st or 2nd longest wavelength at which resonance occurs is in the region which is usually of greatest interest.

The selectivity in this region is determined also by the value of the normalized susceptance, B, of the obstacles, and is given by the relation (See Appendix I)

$$Q = \frac{\arctan \dfrac{2}{B}}{2 \arcsin \dfrac{2}{\sqrt{B^4 + 4B^2}}} . \tag{32}$$

This selectivity is based upon the wavelength, not the frequency parameter. In terms of the wavelength in the transmission line this is

$$Q = \left| \frac{\dfrac{2\pi \ell}{\lambda_{g0}}}{\dfrac{2\pi \ell}{\lambda_{gc1}} - \dfrac{2\pi \ell}{\lambda_{gc2}}} \right| \doteq \left| \frac{\lambda_{g0}}{\lambda_{gc1} - \lambda_{gc2}} \right| \tag{33}$$

where λ_{g0} is the wavelength of resonance in the transmission line and λ_{gc} is the wavelength at the half power points. If the phase velocity in the transmission line does not vary with frequency, then the selectivity can be expressed simply in terms of either the wavelength or the frequency since

$$\frac{f}{f_0} - \frac{f_0}{f} = \frac{\lambda_0}{\lambda} - \frac{\lambda}{\lambda_0} . \tag{34}$$

However, when the velocity in the transmission line varies with frequency, equation 34 does not hold true, and the expression relating the two parameters is more complicated. In the case of the rectangular waveguide

$$\lambda_g = \frac{c}{\sqrt{f^2 - f_{cw}^2}} \tag{35}$$

where c is the velocity of light in vacuum, f_{cw} is the cutoff frequency of the waveguide, $f_{cw} = \dfrac{c}{2a}$ and a is the width of the waveguide.

It can be shown readily that the frequency parameter can be expressed in terms of the wavelength, thus

$$\left(\frac{f}{f_0} - \frac{f_0}{f} \right) = \left(\frac{\lambda_{g0}}{\lambda_g} - \frac{\lambda_g}{\lambda_{g0}} \right) \left(\frac{\lambda_a}{\lambda_g} \right) \left(\frac{\lambda_{a0}}{\lambda_{g0}} \right) \tag{36}$$

where λ_a is the wavelength in free space.

For narrow percentage bands, this reduces to the approximate relation

$$\left(\frac{f}{f_0} - \frac{f_0}{f} \right) \doteq \left(\frac{\lambda_{g0}}{\lambda_g} - \frac{\lambda_g}{\lambda_{g0}} \right) \left(\frac{\lambda_{a0}}{\lambda_{g0}} \right)^2. \tag{37}$$
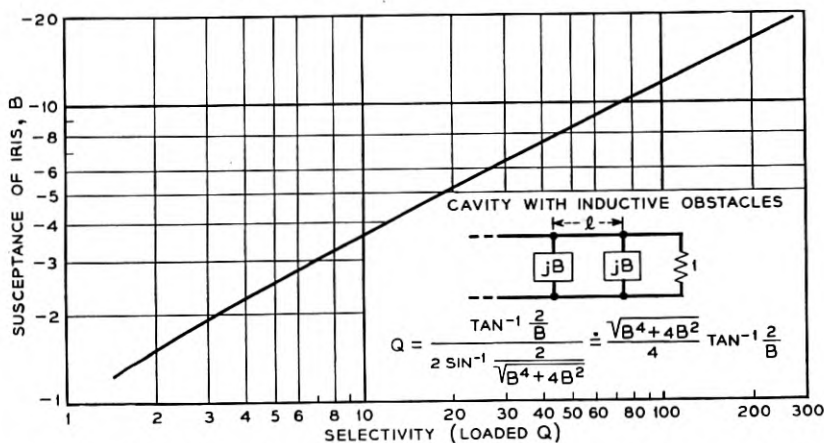

Fig. 11—The relation between loaded Q and normalized susceptance. (Inductive obstacles)

This states, in effect, that the percentage bandwidth is greater in terms of wavelength than in terms of frequency, by the square of the ratio of the wavelengths in the guide and in free space. The selectivity in terms of the frequencies and wavelength ratio thus becomes

$$Q \doteq \frac{1}{\left(\frac{f_2}{f_0} - \frac{f_0}{f_c} \right)} \cdot \left(\frac{\lambda_{a0}}{\lambda_{g0}} \right)^2 = \frac{f_0}{(f_{c2} - f_{c1})} \cdot \left(\frac{\lambda_{a0}}{\lambda_{g0}} \right)^2 \tag{38}$$

This is the selectivity that is plotted as a function of B in Figures 11 and 12.

EXCESS PHASE AND CONNECTING LINES

The excess phase of this type of cavity is taken into account by adding the lengths of line, ℓ' (see Fig. 9), which have a length given by the relation (See Appendix I)

$$\tan \frac{4\pi \ell'}{\lambda_{g0}} = - \left(\frac{2}{B} \right). \tag{39}$$

Combining Eq. 31 and Eq. 39 and solving for ℓ' in terms of ℓ

$$\ell' = \frac{\lambda_{g0}}{4} - \frac{\ell}{2} \tag{40}$$

where ℓ is the length of the cavity and λ_{g0} is the resonant wavelength in the line.
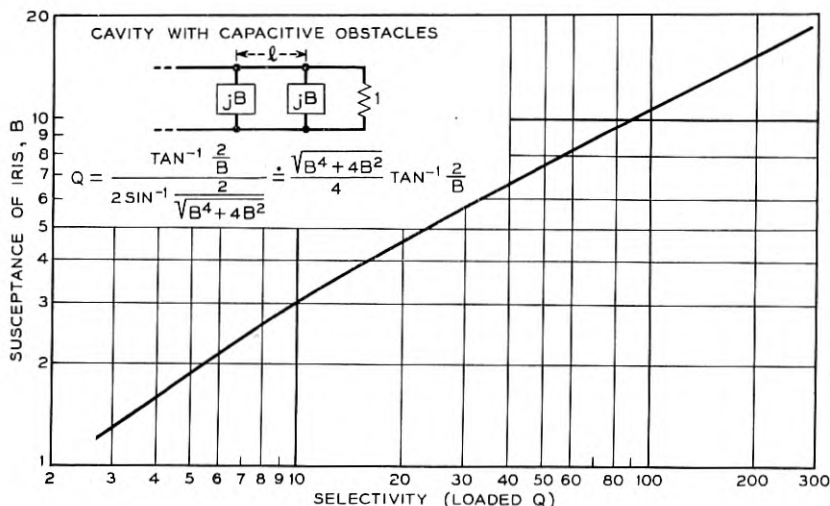

Fig. 12—The relation between loaded Q and normalized susceptance. (Capacitive obstacles)

Thus, when this length, corresponding to the excess phase of the cavity resonator, is absorbed in the length of line connecting two cavities together, the correct total connecting length becomes

$$\ell_c = (2m + 1) \frac{\lambda_{g0}}{4} - \ell'_1 - \ell'_2$$

$$= \frac{\ell_1 + \ell_2}{2} - \frac{\lambda_g}{4} + m \frac{\lambda_g}{2} \tag{41}$$

where ℓ_1 and ℓ_2 are the lengths of the cavities and m is any integer including zero.

Obstacles in Waveguides

The three properties of the cavity—the resonant frequency, the selectivity and the excess phase—are given in Equations 31, 32 and 39, regardless of the sign of the normalized susceptance, B. In the case where the obstacles are inductive, B is negative; and where the obstacles are capacitive, B is positive.

Further explanation is needed to distinguish between these two important cases. First consider the case where inductive obstacles are used. Tan $\frac{2\pi\ell}{\lambda_{g0}}$ is negative and the cavity length lies between a quarter and a half wavelength (plus any multiple of half wavelength). The selectivity, as given by equation (32), is plotted on Fig. 11 for the fundamental mode. The excess phase is positive, and the added lengths, ℓ', of Fig. 9 are positive. The connecting lines between two such cavities are then slightly less than a quarter wavelength (or odd multiple thereof).

Next consider the case where the obstacles are capacitive. Tan $\frac{2\pi\ell}{\lambda_{g0}}$ is positive and the cavity length lies between zero and a quarter wavelength (plus any multiple of half wavelengths). The selectivity as given by equation (32) is plotted in Fig. 12 for cavity lengths lying between a half wavelength and three quarters wavelength. The excess phase is negative and the added lengths, ℓ_1' of Fig. 9 are negative. The connecting lines between two such cavities are then slightly longer than a quarter wavelength (or odd multiple thereof).

SUSCEPTANCE OF OBSTACLES

The Equations (31), (32) and (39) give the resonant wavelength, the selectivity (in terms of wavelength) and the excess phase as functions of the normalized susceptance of the obstacles which form the ends of the cavity, and a knowledge of this susceptance as a function of the geometrical configuration of the obstacle is necessary to complete the design of the filter. At low frequencies, conventional coils and condensers can be used to form the discontinuities in the transmission line; while at high frequencies, transmission line stubs can be used.[14] In the microwave region, where waveguides are employed, obstacles having the shapes shown in Figures 13, 14, and 15 can be used.[15]

INDUCTIVE VANES

Figure 13 shows a plane metallic obstacle, transversely located across a rectangular waveguide, with a centrally located rectangular opening extending completely across the waveguide in a direction parallel to the electric vector. For thin obstacles, the normalized susceptance can be calculated from the approximate formula,[15]

$$B \doteq -\frac{\lambda_g}{a} \cot^2 \frac{\pi d}{2a} \qquad (42)$$

where λ_g is the wavelength in the waveguide, a is the width of the waveguide, and d is the width of the iris opening.

When the iris is constructed of material of finite thickness, τ, the expression for the susceptance is more complicated,[10, 11] and the equivalent circuit becomes a four-terminal network with both shunt and series elements. The equivalent shunt susceptance of this network can be obtained experimentally by measuring the insertion loss of the iris, from which a curve such as shown in Fig. 16 can be computed. These data* were taken for irises .050″ thick in waveguide having internal dimensions of 0.872″ × 1.872″ in the frequency range around 4000 mc. The ordinate is a parameter, K, from which the normalized susceptance is calculated:
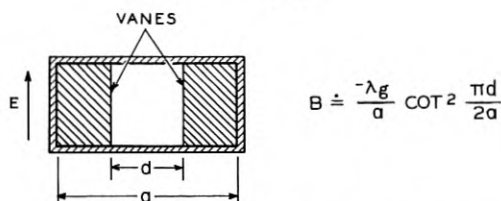
$$B = K \left(\frac{\lambda_g}{2a}\right). \tag{43}$$

$$B \doteq \frac{-\lambda_g}{a} \cot^2 \frac{\pi d}{2a}$$

Fig. 13—One type of inductive obstacle in rectangular waveguide.

$$B \doteq \frac{4b}{\lambda_g} \log_\epsilon \csc \frac{\pi d}{2b}$$
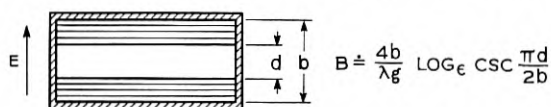
Fig. 14—One type of capacitive obstacle in rectangular waveguide.

$$B \doteq \frac{2\lambda_g}{a} \cdot \frac{1}{\log_\epsilon \left(\frac{4a}{\pi d \epsilon^2}\right)}$$
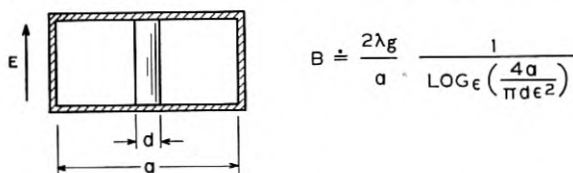
Fig. 15—Another type of inductive obstacle consists of a cylindrical post.

Along the abscissa is plotted the ratio of iris opening to width of the waveguide.

It can be demonstrated that for values of K from -1 to -20, the equivalent iris opening is approximately the actual opening less the thickness of the metal sheet. For practical purposes, when the susceptance lies between -1.5 and -30, it is often sufficient to use the approximation,

$$B \doteq - \frac{\lambda_g}{a} \cot^2 \left(\frac{\pi(d - \tau)}{2a}\right) \tag{44}$$

where τ is the thickness of the iris.

* Data supplied by Mr. L. C. Tillotson of Bell Telephone Laboratories.

Capacitive Irises

The normalized susceptance of infinitely thin capacitive obstacles, as illustrated in Fig. 14, may be calculated by the approximate relation[15]

$$B \doteq \frac{4b}{\lambda_g} \log_\epsilon \operatorname{cosec} \frac{\pi d}{2b} \tag{45}$$

where b is the height of the waveguide, λ_g is the wavelength in the waveguide, and d is the width of the iris opening.

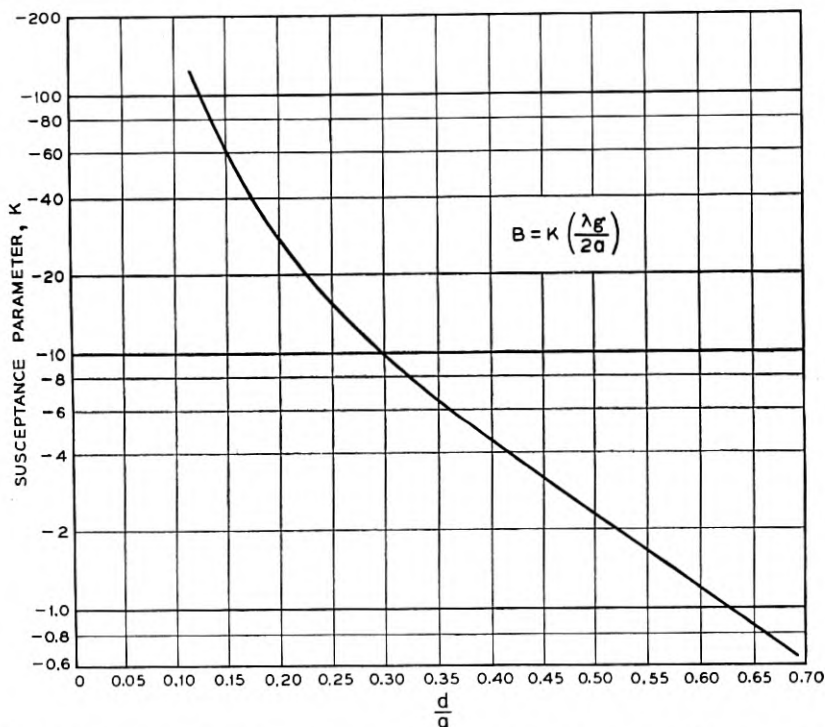$$B = K \left(\frac{\lambda g}{2a} \right)$$

Fig. 16—Experimentally determined curve of normalized susceptance of inductive irises.

As with the inductive vanes, the normalized susceptance is a function of the iris thickness and may be calculated from the approximate formula[15]

$$B \doteq B_0 + \frac{2\pi\tau}{\lambda_g} \left(\frac{b}{d} - \frac{d}{b} \right) \tag{46}$$

where B_0 is the normalized susceptance of the infinitely thin iris, and τ is the iris thickness.

For best results, the irises should be designed from experimentally determined curves, however.

INDUCTIVE POSTS

The normalized susceptance of the round cylindrical inductive post, centrally located in the waveguide parallel to the electric vector, may be calculated from the approximate formula[11, 15, 16]

$$B = - \frac{2\lambda_g}{a} \frac{1}{\log_\epsilon \left(\frac{4a}{\pi d \epsilon^2} \right)} \tag{47}$$

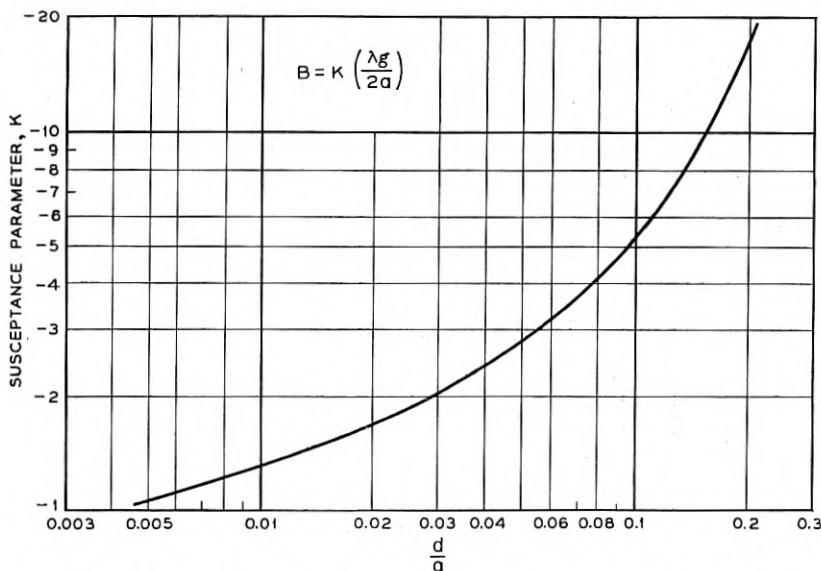where a is the width of the guide, and d is the post diameter.

Fig. 17—Experimentally determined curve of normalized susceptance of inductive posts

The experimentally determined values of susceptance are somewhat less than the values calculated by the formula (47). The difference is less than 20% when $\frac{d}{a}$ is less than 0.08. A curve of experimentally determined values is plotted in Fig. 17, the data being taken in rectangular waveguide 0.872″ × 1.872″ at a frequency near 4000 mc.*

The normalized susceptance of posts is also a function of their position in the waveguide, the susceptance decreasing as the posts are moved off center. This feature may be used when it is desired to make all the posts in a filter

* Data supplied by Mr. A. E. Bowen of Bell Telephone Laboratories.

from stock of a given diameter. The expression for the normalized susceptance of off-center posts is given by the relation[11, 16]

$$B \doteq -\frac{2\lambda_g}{a} \frac{1}{\sec^2 \dfrac{\pi s}{a} \left[\log_\epsilon \left(\dfrac{4a}{\pi d\epsilon^2} \cos \dfrac{\pi s}{a} \right) \right]} \tag{48}$$

where s is the distance off center.

EXPERIMENTAL DATA

The principles of waveguide filter design as outlined in the foregoing have been used in several applications. For example the channel branching filters in the New York-Boston microwave radio relay link consist of two resonant cavities separated by the equivalent of $\frac{3}{4}$ wavelength sections of waveguide. The transmitting modulators in this relay system also use two-chamber filters to separate the wanted sideband from the unwanted sideband. The transmission band in each of these applications was 10 mc
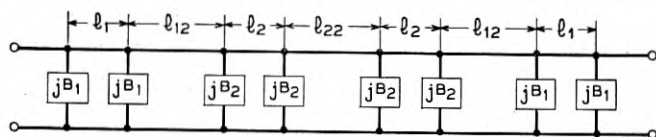

Fig. 18—Diagram of a transmission line filter consisting of four resonant cavities and three connecting lengths of line.

and the image frequency or the unwanted sideband which was to be reflected was 130 mc away.

In another case the requirements were that the standing wave ratio should be less than 0.64 db over a band of 20 mc and more than 28 db 30 mc on each side of the midband frequency. The design formulae indicated that a filter consisting of four cavities would be needed. These, then, would take the general configuration shown in Fig. 18, where the first and last cavities are formed by the obstacles jB_1 and the length of line ℓ_1, while the two middle cavities are formed by the obstacles jB_2 and the length ℓ_2. The lengths ℓ_{12} and ℓ_{22} correspond to the transforming sections of transmission line which connect the cavities together. The loaded Q's required to meet the specifications turned out to be $Q_1 = 12.25$ and $Q_2 = 30.0$, after allowance had been made for the selectivities of the $\frac{3}{4}$ wavelength connecting sections. Assuming that the cavities would be formed with inductive obstacles, as shown schematically in Fig. 19, the susceptances to obtain these selectivities were obtained from Fig. 11 based on equation 32. This gave

$$B_1 = -4.08$$
$$B_2 = -6.36$$

These susceptances were realized with centrally located round posts, for which the data of Fig. 17 has been plotted, and this filter was constructed according to the calculated dimensions which are shown in Fig. 20. Each of the four cavities was tuned separately to resonance near midband by adjusting a capacitive plug located in the center of each. The characteristic then obtained is plotted in Fig. 21, which shows that the standing wave
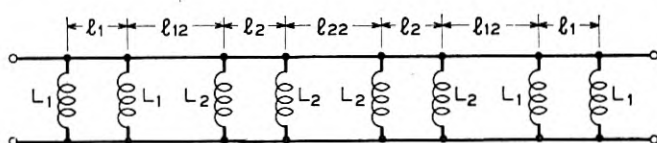

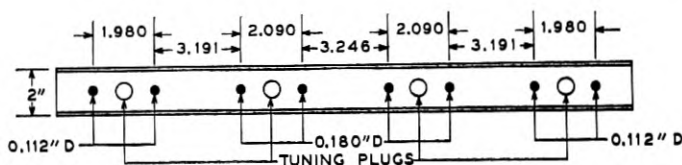Fig. 19—A four-cavity filter which utilizes inductive obstacles.

Fig. 20—The calculated dimensions for a four-cavity maximally-flat filter in 0.872" x 1.872" rectangular waveguide.
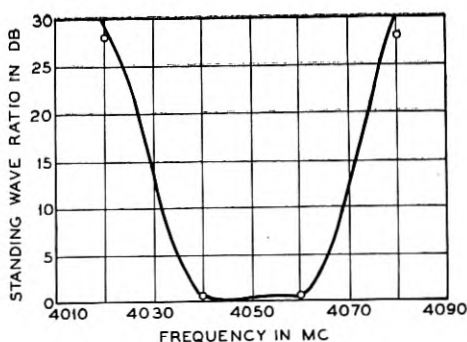

Fig. 21—Measured characteristic of four-cavity filter of Figure 20.

ratio met the design points quite well. These are shown as circles in the figure. The insertion loss of this filter was less than 0.7 db over a 25-mc band and less than 0.3-db at midband.

Another maximally-flat waveguide filter consisting of fifteen resonant cavities gave an insertion loss of two decibels at midband, 4-db loss at 20-mc bandwidth and 40-db loss at 30-mc bandwidth. The input standing wave ratio was less than 1.0 db over a 20-mc band. Its characteristics are plotted in Figs. 22 and 23. This excellent performance is remarkable in

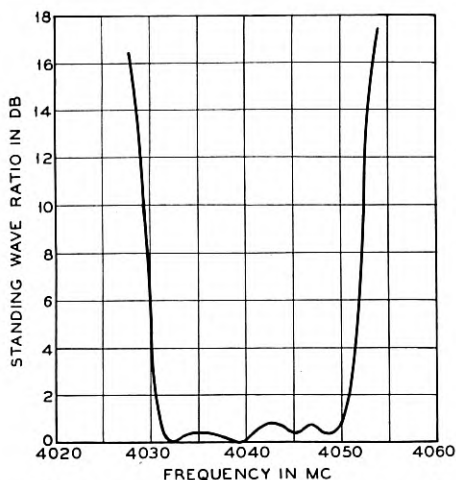Fig. 22—Measured standing wave ratio of maximally-flat filter consisting of fifteen resonant cavities.
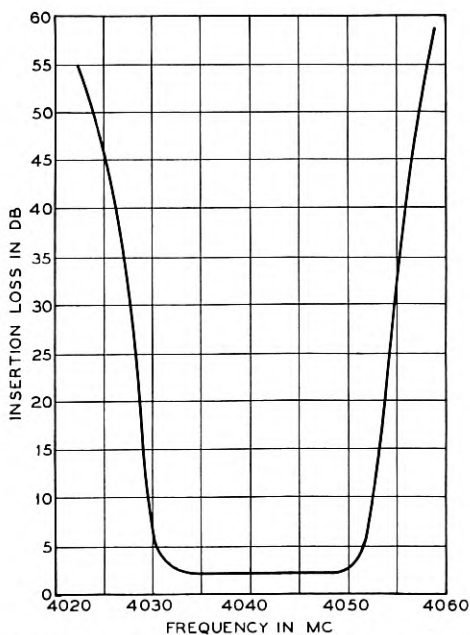

Fig. 23—Measured insertion loss of the fifteen-cavity filter.

view of the difficulties that might be encountered in constructing and aligning a filter consisting of 75 discontinuities and 29 lengths of waveguide. Its physical length (over 80″) may be seen in the photograph of Fig. 24.
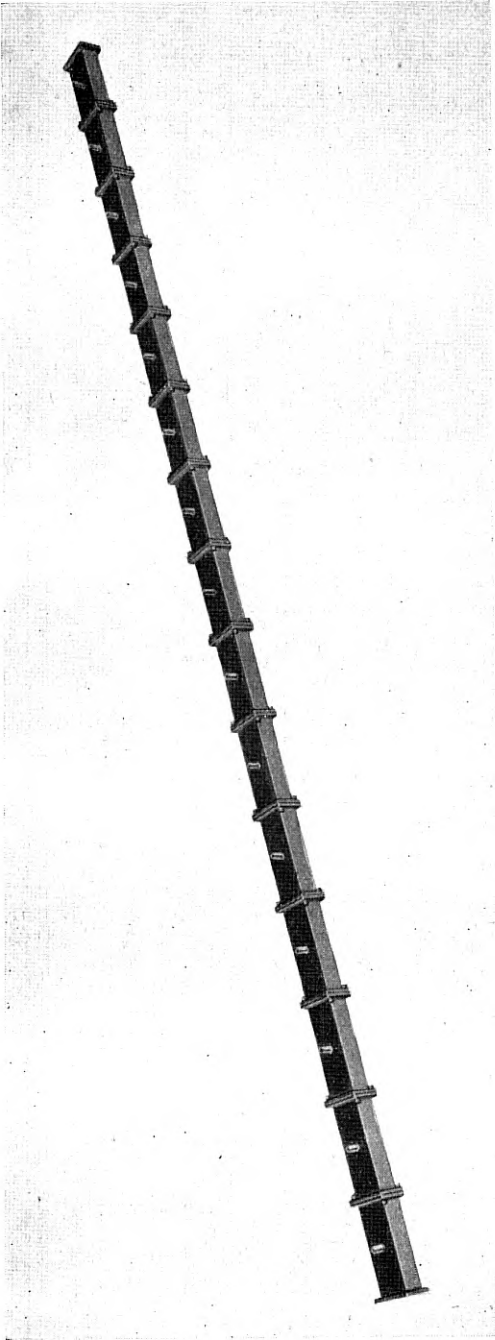
Fig. 24—The fifteen cavity filter.

The theoretical treatment of maximally-flat filters presented here has ignored the dissipation in the elements. Better agreement between expected and observed characteristics would be obtained if this had been taken into account. The observation of .3-db loss and 2-db loss in the four-cavity and the fifteen-cavity maximally-flat filters is indicative of the amounts of added insertion loss to be expected because of dissipation in the elements. In addition to the increased loss at midband, we should expect a rounding of the insertion loss characteristic near the cutoff frequencies, and a broadening of the standing wave characteristic at frequencies well beyond cutoff. In many applications, however, these effects can be ignored.

CONCLUDING REMARKS

In the foregoing, the design of maximally-flat band-pass filters has been treated in detail. The treatment of other types of band-pass and band-rejection filters is beyond the scope of the present paper, although much of the material presented here may be of use in designing such filters. In fact, almost any filter consisting of a ladder network of inductive and capacitive elements in series and in shunt can be simulated in waveguides by following these principles. Emphasis on the maximally-flat filter has been deliberate for two reasons: it gives a type of transmission characteristic that is useful in microwave work; it is simple to design.

ACKNOWLEDGEMENT

REFERENCES

1. E. L. Norton, Constant Resistance Networks with Applications to Filter Groups, *B. S. T. J.*, Vol. XVI, pp. 178–193, April 1937.
2. W. D. Lewis and L. C. Tillotson, *B. S. T. J.*, Vol. XXVII, #1, pp. 83–95, January 1948.
3. E. L. Norton, U. S. Patent #1,788,538, January 13, 1931.
4. W. R. Bennett, U. S. Patent #1,849,656, March 15, 1932.
5. S. Butterworth, *Wireless Engineer*, Vol. VII, #85, pp. 536–541, October 1930.
6. V. D. Landon, *R.C.A. Review*, Vol. V, pp. 347–362 and pp. 481–497, 1940–41.
7. Henry Wallman, *M.I.T. Radiation Laboratory Report* #524, February 23, 1944.
8. S. Darlington, *Journal of Math. and Phys.*, Vol. XVIII, pp. 257–353, September 1939.

9. R. M. Fano and A. W. Lawson, *Proc. I.R.E.*, Vol., Vol. 35, #1, pp. 1318–1323, November 1947.
10. Wilbur L. Pritchard, *Journal of Applied Physics*, Vol. XVIII, #10, pp. 862–872, October 1947.
11. M.I.T. Wave Guide Handbook, *Supplement Rad. Lab. Rpt.* 41, Sec. 21a, (January 23, 1945).
12. A. L. Samuel, J. W. Clark and W. W. Mumford, Gas Discharge Transmit-Receive Switch. *B. S. T. J.*, Vol. XXV, #1, pp. 48–101, January 1946.
13. S. A. Schelkunoff, Representation of Impedance Functions in Terms of Resonant Frequencies. *Proc. I.R.E.*, Vol. XXXII, pp. 83–90, February 1944.
14. W. P. Mason and R. A. Sykes, *B. S. T. J.*, Vol. XVI, pp. 275–302, July 1937.
15. Sperry Microwave Transmission Design Data, Publication No. 23–80, Sperry Gyroscope Co.
16. S. A. Schelkunoff, *Quarterly of Applied Math.*, Vol. I, #1, pp. 78–85, April 1943.
17. G. C. Southworth, Hyper-Frequency Wave Guides, *B. S. T. J.*, Vol. XV, pp. 284–309, April 1936.

APPENDIX I

A cavity resonator, consisting of a length of transmission line, ℓ, at each end of which there is an unvarying susceptance, jB, is approximately equivalent to a tuned circuit, consisting of an inductance, L, and a capacity, C, in parallel located at the center of a short length of transmission line, $2\ell'$, when these two conditions are satisfied:

(1) The square root of L over C is equal to the surge impedance of the transmission line divided by twice the loaded Q of the cavity.

(2) The sum of the lengths of the two transmission lines ℓ and $2\ell'$ is equal to a half wavelength at resonance.

The first of these conditions follows from equation 3 of the text above, and the proof of the second condition will be given in the following analysis, based on the schematic drawing of Figures 9 and 10. In this analysis, the loaded Q of the cavity is derived in terms of the susceptance of the obstacles at its ends.

Since the cavity and the tuned circuit are both symmetrical it is adequate to consider but one half of each in establishing the equivalence. Then by setting the short circuit admittance of one equal to the other and setting the open circuit admittance of one equal to the other, the necessary relationships are derived.

The following symbols will be used in addition to those used in the text:

$$Y_{sc} = \text{Normalized admittance, short circuited.}$$

$$Y_{oc} = \text{Normalized admittance, open circuited.}$$

The subscripts 1 and x refer to the cavity and the equivalent tuned circuit respectively.

$$\theta_1 = \frac{2\pi}{\lambda_g} \cdot \frac{\ell}{2}$$

$$\theta_x = \left\lceil \frac{2\pi}{\lambda_g} \cdot \ell' \right.$$

The short-circuited admittances of half the cavity and half the tuned circuit are

$$Y_{sc1} = j(B_1 - \cot \theta_1) \tag{A1}$$

$$Y_{scx} = -j \cot \theta_x \tag{A2}$$

while the open-circuited admittances are

$$Y_{oc1} = j(B_1 + \tan \theta_1) \tag{A3}$$

$$Y_{ocx} = \frac{j \left(\dfrac{B_x}{2} + \tan \theta_x \right)}{1 - \dfrac{B_x}{2} \tan \theta_x}. \tag{A4}$$

Putting $Y_{sc1} = Y_{sc2}$

$$\tan \theta_x = \frac{1}{\cot \theta_1 - B_1}. \tag{A5}$$

Putting A5 in A4 and setting $Y_{oc1} = Y_{ocx}$

$$B_1 + \tan \theta_1 = \frac{\dfrac{B_x}{2} + \dfrac{1}{\cot \theta_1 - B_1}}{1 - \dfrac{B_x}{2} \dfrac{1}{\cot \theta_1 - B_1}}. \tag{A6}$$

Solving for B_x we have

$$B_x = -B_1(B_1 \sin 2\theta_1 - 2 \cos 2\theta_1) \tag{A7}$$

which becomes

$$B_x = \sqrt{B_1^4 + 4B_1^2} \sin \frac{2\pi\ell}{\lambda_{g0}} \left(\frac{\lambda_{g0}}{\lambda_g} - 1 \right) \tag{A8}$$

where

$$\frac{2\pi\ell}{\lambda_{g0}} = \text{arc} \tan \frac{2}{B_1}. \tag{A9}$$

Equation A9 gives the requirements for resonance.

The expression for the loaded Q is

$$Q = \frac{\dfrac{2\pi\ell}{\lambda_{g0}}}{\dfrac{2\pi\ell}{\lambda_{gc2}} - \dfrac{2\pi\ell}{\lambda_{gc1}}}. \tag{A10}$$

The cutoff wavelengths are obtained when B_x is equal to ± 2 and we have from equation A8

$$\frac{2\pi\ell}{\lambda_{gc1}} = \frac{2\pi\ell}{\lambda_{g0}} - \text{arc sin} \frac{2}{B_1\sqrt{B_1^2 + 4}}, \tag{A11}$$

$$\frac{2\pi\ell}{\lambda_{gc2}} = \frac{2\pi\ell}{\lambda_{g0}} + \text{arc sin} \frac{2}{B_1\sqrt{B_1^2 + 4}}, \tag{A12}$$

from which we obtain

$$Q = \frac{\text{arc tan} \dfrac{2}{B}}{2 \text{ arc sin} \dfrac{2}{\sqrt{B^4 + 4B^2}}} \doteq \frac{\sqrt{B_1^4 + 4B_1^2}}{4} \text{arc tan} \frac{2}{B}. \tag{A13}$$

This gives the loaded Q of the cavity in terms of the susceptance of the end obstacles.

To derive the length corresponding to the excess phase of the cavity, let the short-circuited admittances be equal by equating equations A1 and A2, and let the wavelength be the resonant wavelength of the cavity, and we have

$$B_1 - \cot \theta_{10} = - \cot \theta_{xo}. \tag{A14}$$

From equation A9

$$B_1 = 2 \cot 2\theta_{10} \tag{A15}$$

so that

$$2 \cot 2\theta_{10} - \cot \theta_{10} = -\cot \theta_{x0}. \tag{A16}$$

But

$$2 \cot 2\theta_{10} - \cot \theta_{10} = -\tan \theta_{10} \tag{A17}$$

hence

$$\tan \theta_{10} = \cot \theta_{x0} \tag{A18}$$

or

$$\theta_{10} + \theta_{x0} = \frac{\pi}{2} \tag{A19}$$

That is

$$\frac{2\pi}{\lambda_{g0}} \cdot \frac{\ell}{2} + \frac{2\pi\ell'}{\lambda_{g0}} = \frac{\pi}{2}$$

whence

$$\ell + 2\ell' = \frac{\lambda_{g0}}{2} \qquad (A20)$$

which proves the second condition mentioned above, namely, that the sum of the lengths of the transmission lines in the cavity and its equivalent circuit is equal to a half wavelength.

The normalized admittance of the cavity terminated in the surge admittance of the guide can be written in terms of its loaded Q and a wavelength variable as

$$YR \doteq 1 + j2Q\left[2\left(\frac{\lambda_{g0}}{\lambda_g}\right) - 1\right]. \qquad (A21)$$

This expression is obtained from equations A8 and A13 by making the assumption that the bandwidth is narrow so that the sine of the angle in equation A8 can be replaced by the angle. This admittance is referred to a point slightly inside the cavity, i.e. a distance ℓ' inside.

The similarity between this expression and the corresponding one for the parallel resonant circuit consisting of lumped elements is evident. (See eq. 7 of the text.)

$$YR = 1 + j2Q\left[\frac{f}{f_o} - \frac{f_o}{f}\right] \qquad (A22)$$

In the case of the cavity the bracketed term is a wavelength variable; in the case of the tuned circuit it is a frequency variable.

The loss function for maximally-flat filters in waveguides becomes

$$\frac{P_0}{P_L} \doteq 1 + \left[Q_r 2\left(\frac{\lambda_{g0}}{\lambda_g} - 1\right)\right]^{2n}. \qquad (A23)$$

The loaded Q's of the cavities taper sinusoidally from one end of the filter to the other so that

$$Q_r = Q_T \sin\left(\frac{2r-1}{2n}\right)\pi. \qquad (A24)$$

Transient Response of an FM Receiver

By MANVEL K. ZINN

INTRODUCTION

THIS paper develops various formulas for the response of an FM receiver to signal or noise input voltages of arbitrary form. The principal object in view is to obtain a more complete understanding of how an FM receiver responds to transient voltages, such as those arising from ignition interference, but the more general aspects of the theory have other applications as well. In particular, general formulas are given for the response of a linear circuit to an applied voltage, or current, of variable frequency. The Fourier transforms, or frequency spectra, of the response, and the envelope thereof, are determined.

Two examples are given: (1) the audio response of an FM receiver to a very large impulse and (2) the response, including harmonic distortion, to a sinusoidal signal wave.

The element of an FM receiver that demands most discussion is the balanced frequency detector. The greater part of the paper accordingly deals with that important element. The general problem can be stated as follows: A limiter and frequency detector are transmitting a steady unmodulated carrier wave to an audio output circuit. At time, $t = 0$, frequency modulation of arbitrary form is applied to the carrier (either by signal modulation or a superposed noise transient). What is the audio output voltage that results?

FREQUENCY DETECTOR

Except for the greater bandwidth, the amplifiers and selective circuits between the antenna and the limiter of an FM receiver are similar to those of an AM receiver in their transmission features. If the selective circuits have a bandwidth ample to accommodate the maximum frequency swing of the FM transmitter, and if the transmission over the band is substantially "flat" and the phase shift nearly linear with frequency, the amplifiers will introduce little distortion. The limiter and frequency detector are therefore regarded as the distinctive elements of an FM receiver meriting theoretical discussion.

The literature contains descriptions of frequency detectors of several types together with adequate analyses of the action of the circuits based on the variable impedance concept.[1] The more generally used circuits can be

---

[1] See Items 3 to 6 in list of references attached.

reduced to the circuit shown schematically in Fig. 1, which can be taken to illustrate a generic form of frequency detector. Z_1 and Z_2 are two resonant impedances tuned to different frequencies, one above, the other below, the carrier frequency.[2] For example, the simplest version of Z_1 and Z_2 could be, for each, a parallel combination of R, L and C. Across each of these impedances is connected a rectifier with load circuit so proportioned that the rectification is substantially linear. The rectifiers are poled so that their low-frequency outputs are opposed, thereby obtaining cancellation of even-order demodulation products. With this arrangement, the low-frequency output voltage V_o, which is applied to the audio amplifier, is substantially proportional to the difference between the envelopes of the voltage drops across Z_1 and Z_2.

The resistance elements of the impedances, Z_1 and Z_2, each include a shunting resistance equal to half the load resistance of the associated rectifier, which therefore determines, to some extent, the Q of the tuned circuit. The output diode load, $R_o C_o$, has negligible impedance at the carrier frequency. Under these conditions, the low-frequency output voltage across the two-rectifier load impedances is

$$V_o = \eta \,([V_1] - [V_2])$$

where η = detection efficiency (nearly unity)
V_1, V_2 = high-frequency voltages across Z_1, Z_2, respectively (Fig. 1)
$[V]$ = envelope of V.

All this is in accord with the accepted understanding of the operation of a properly designed linear rectifier working at an efficiency approaching 100 per cent.

The amplitudes of the voltages, V_1 and V_2, across the resonant impedances, Z_1 and Z_2, of Fig. 1 are shown in Fig. 2. In the practical engineering analysis of this frequency detector circuit, employing the idea of impedance that varies in step with the instantaneous frequency, the two voltages of Fig. 2 are subtracted (owing to the opposed polarities of the rectifiers) to obtain the over-all voltage-frequency characteristic shown in Fig. 3. Then it is inferred, by physical intuition, that if the instantaneous frequency of the carrier is varied at the input, the output voltage wave will vary as indicated by the curve of Fig. 3. Strictly speaking, this is a false assumption, but where the rate of variation of the instantaneous frequency is at an audio signal frequency far below the carrier frequency, the error in the assumption is of no importance, whereas the simplification in thinking accomplished

---

[2] The term *carrier frequency* will be used to designate the value of the unmodulated received frequency after all heterodyne conversions. (This frequency is equal to the mid-band frequency of the last intermediate frequency amplifier ahead of the limiter, if tuning is perfect.)

by it is considerable. It is only where the rate of variation of the instantaneous frequency is high, as it can be in the case of a large noise transient caused by impulse excitation, that the error in the assumption in question
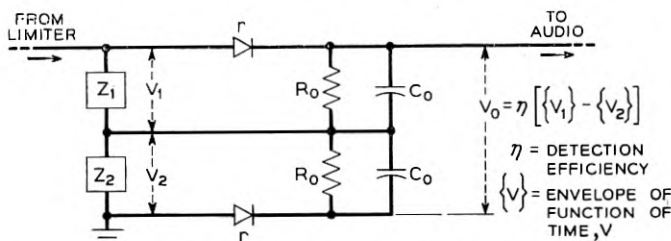
Fig. 1—Circuit of a balanced frequency detector.

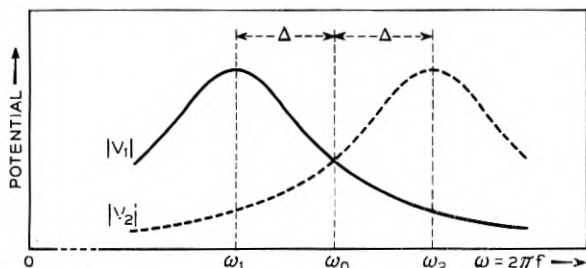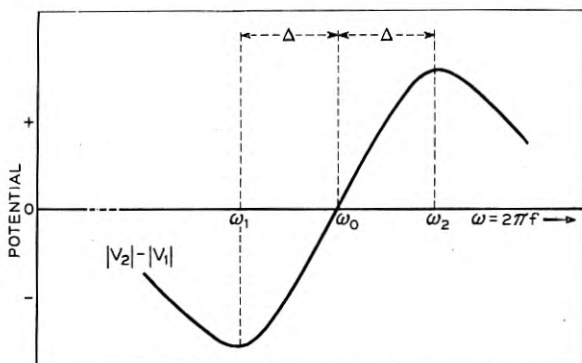Fig. 2—Voltages across tuned circuits of frequency detector.

Fig. 3—Output voltage of frequency detector.

can become serious. A particularly subtle error that can arise from the assumption is to fall into the habit of regarding the characteristic curve of Fig. 3 as a frequency transmission curve of the sort obtained by measuring the ratio of output to input of a linear network over a range of frequencies.

The curve of Fig. 3 is not such a transmission curve, because the principle of superposition does not apply and a frequency conversion is involved.

Owing to the considerations discussed above, the analysis to follow avoids the assumption of variable impedance associated with the varying instantaneous frequency. This does not imply that the assumption, as employed by various writers, is considered seriously erroneous, but, rather, that it seems preferable to develop the theory without invoking the assumption, provided that this can be done without falling into unmanageable complications. Briefly, the procedure in the work to follow is to determine directly the envelopes of the voltages V_1 and V_2 as functions of time, one envelope then being subtracted from the other to obtain the output wave.
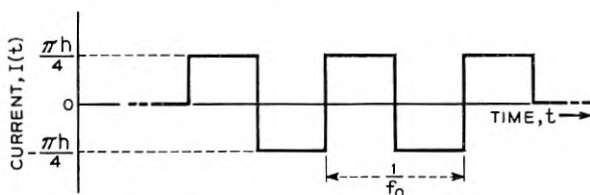
Fig. 4—Current wave out of limiter.

GENERAL THEORY

When a carrier is being received, the limiter can be regarded as substantially a constant current source having an internal shunt admittance small compared to the admittance of the tuned impedance elements, Z_1 and Z_2, of the frequency detector. If the limiting is severe, as it should be for good operation, the current delivered by the limiter is a rectangular wave as illustrated in Fig. 4. When this current is driven through the impedances, Z_1 and Z_2, the voltage drops, V_1 and V_2, that arise across these elements are substantially sinusoidal in form, owing to the selectivity, which practically extinguishes all harmonics of the carrier frequency. We therefore take the current input to be sinusoidal in the first place, namely

$$I(t) = h \cos 2\pi f_o t$$

This is the unmodulated current, $\pi h/4$ being the current cutoff point of the limiter and f_o the frequency of the carrier. When the carrier is modulated in frequency, we write

$$I(t) = h \cos [2\pi f_o t + \theta(t)] \qquad (1)$$

where $\theta(t)$ is the phase angle varying with time. The instantaneous frequency then is

$$f(t) = \frac{1}{2\pi} \frac{d}{dt} [2\pi f_o t + \theta(t)] = f_o + \frac{1}{2\pi} \theta'(t). \qquad (2)$$

In the transmission of signals by frequency modulation, the instantaneous radian frequency deviation, $\theta'(t)$, is made to vary in proportion to the signal amplitude, so that $\theta(t)$ then varies in proportion to the time integral of the signal amplitude.

As a preliminary step to the discussion of the frequency detector itself, we require a formula for the voltage drop across an impedance $Z(f)$ when the frequency-modulated current (1) flows through it. The point of view usually adopted is to regard the impedance as a composite function of time, viz., $Z[f(t)]$, and to say that the voltage across it is

$$V(t) = I(t)Z[f(t)] = I(t)Z\left[f_0 + \frac{1}{2\pi}\theta'(t)\right]. \tag{3}$$

This quasi-stationary viewpoint gives results that are nearly correct if the rate of change, $\theta''(t)/2\pi$, of the variable frequency is not too large. The magnitude of the error has been determined in a paper by Carson and Fry.[3] In the present paper, impedance is a function of frequency that is independent of time, as in the classic theory of linear systems. The frequent use of the term "instantaneous frequency," as defined by (2), does not imply a departure from this point of view.

In the following, $H(t)$ is, in general, the voltage response as a function of time, of a network to a unit impulse of current applied at time $t = 0$. In the case of a two-terminal impedance element, $H(t)$ is the voltage drop across the element when a unit impulse of current is sent through it. Then, if the frequency modulated current (1) flow through the impedance, the voltage drop is

$$V(t) = h \int_0^\infty \cos\left[\omega_0(t - \tau) + \theta(t - \tau)\right]H(\tau)\,d\tau \tag{4}$$

where $\omega_0 = 2\pi f_0$. $\theta(t)$ can have any form as a function of time. $V(t)$ can be written,

$$V(t) = \frac{h}{2}e^{i\omega_0 t}\int_0^\infty e^{-i\omega_0\tau + i\theta(t-\tau)}H(\tau)\,d\tau$$

$$+ \frac{h}{2}e^{-i\omega_0 t}\int_0^\infty e^{i\omega_0\tau - i\theta(t-\tau)}H(\tau)\,d\tau. \tag{5}$$

In the frequency detector problem, the result finally desired is the envelope of the voltage wave. It will clarify the discussion to explain first what is meant by an envelope. If the voltage is of the form

$$V(t) = c(t)\cos\left[\omega_0 t + \phi(t)\right]$$

$$= a(t)\cos\omega_0 t - b(t)\sin\omega_0 t$$

$$= \tfrac{1}{2}[a(t) + ib(t)]e^{i\omega_0 t} + \tfrac{1}{2}[a(t) - ib(t)]e^{-i\omega_0 t} \tag{6}$$

[3] Item 1 in the bibliography. See formula 21 in that paper.

the complex function,

$$[V(t)] = c(t) \, e^{i\phi(t)} = a(t) + ib(t) \tag{7}$$

is here called the "envelope function" of the voltage with respect to the radian frequency ω_0, $c(t)$ being a real amplitude modulation factor, which is the envelope[4] itself, as usually conceived, and exp $[i\phi(t)]$ a complex frequency modulation factor, in which $\phi'(t)$ is the instantaneous deviation of the radian frequency from the reference value, ω_0. If such a modulated voltage wave is applied to an ideal linear detector, the output voltage across the load circuit of the latter is the real envelope, $c(t) = [a^2(t) + b^2(t)]^{1/2}$. This concept of an envelope function provides a convenient generalization of modulation ideas. Both amplitude modulation and frequency modulation vary the envelope function, but in different ways. In amplitude modulation, the real magnitude, $c(t)$, is varied while the angle ϕ is constant, whereas, in frequency modulation, c is constant and it is the angle, $\phi(t)$, that is varied.

It will be seen that (5) is in precisely the same form as (6), so that we can write the envelope function of $V(t)$ immediately, as follows:

$$[V(t)] = a(t) + ib(t) = h \int_0^\infty e^{-i\omega_0\tau + i\theta(t-\tau)} H(\tau) \, d\tau. \tag{8}$$

The conjugate envelope function then is

$$[\overline{V(t)}] = a(t) - ib(t) = h \int_0^\infty e^{i\omega_0\tau - i\theta(t-\tau)} H(\tau) \, d\tau. \tag{9}$$

The spectrum of the envelope function is also of interest. To obtain the spectrum, which we shall call, $F_0(f)$, we find the Fourier transform (hereafter abbreviated, F.T.) of both sides of (8), viz.:

$$F_0(f) = \int_{-\infty}^\infty [V(t)]e^{-i\omega t} \, dt = h \int_{-\infty}^\infty e^{-i\omega t} \int_0^\infty e^{-i\omega_0\tau + i\theta(t-\tau)} \cdot H(\tau) \, d\tau \, dt. \tag{10}$$

It is permissible to reverse the order of integration of τ and t, obtaining

$$F_0(f) = h \int_0^\infty e^{-i\omega_0\tau} H(\tau) \int_{-\infty}^\infty e^{-i\omega t + i\theta(t-\tau)} \, dt \, d\tau. \tag{11}$$

The F.T. of $h \exp [i\theta(t)]$ will be designated, $\Psi(f)$, i.e.

$$\Psi(f) = h \int_{-\infty}^\infty e^{i\theta(t) - i\omega t} \, dt. \tag{12}$$

---

[4] The "envelope", so defined, is an engineering concept and is not quite the same thing as the envelope of mathematics, which is always tangent to a curve or set of curves.

Putting $t - \tau$ in place of t in place of t as the variable of integration in (12) we have

$$\Psi(f) = he^{i\omega\tau} \int_{-\infty}^{\infty} e^{-i\omega t + i\theta(t-\tau)} \, dt. \tag{13}$$

Thus it is seen that the inner integral of (11) is equal to $e^{-i\omega\tau}\Psi(f)$ and the equation becomes

$$F_0(f) = \Psi(f) \int_0^{\infty} H(\tau)e^{-i(\omega+\omega_0)\tau} \, d\tau. \tag{14}$$

Now the F.T. of $H(t)$ is $Z(f)$, i.e.

$$Z(f) = \int_{-\infty}^{\infty} H(t)e^{-i\omega t} \, dt. \tag{15}$$

Therefore

$$Z(f + f_0) = \int_{-\infty}^{\infty} H(t)e^{-i(\omega+\omega_0)t} \, dt. \tag{16}$$

This differs from the integral in (14) only in the lower limit of integration. But since $H(t)$ is the response to an impulse applied at time $t = 0$, $H(t) = 0$ for $t < 0$ and the two integrals are therefore equal. Putting (16) in (14) we have, finally

$$F_0(f) = \int_{-\infty}^{\infty} [a(t) + ib(t)]e^{-i\omega t} \, dt = \Psi(f)Z(f + f_0). \tag{17}$$

The F.T. of the conjugate envelope function, $a - ib$, is

$$\bar{F}_0(-f) = \int_{-\infty}^{\infty} [a(t) - ib(t)]e^{-i\omega t} \, dt = \bar{\Psi}(-f)\bar{Z}(-f + f_0) \tag{18}$$

where symbols with the superbar denote the complex conjugates of unbarred symbols. Since $Z(f)$ is the F.T. of a real variable, $H(t)$, it must assume conjugate values for positive and negative values of f, i.e., $Z(f) = \bar{Z}(-f)$ and therefore $Z(f + f_0) = \bar{Z}(-f + f_0)$. Consequently, (18) could be written

$$\bar{F}_0(-f) = \bar{\Psi}(-f)Z(f + f_0) \tag{19}$$

(17) and (18) are the final solutions in frequency functions corresponding to the solutions (8) and (9) in time functions. The formulas in frequency functions have the advantage of compactness, which makes them easy to remember.

We require also the F.T. of the voltage itself, $V(t)$, which we shall call $F(f)$. From (6)

$$F(f) = \int_{-\infty}^{\infty} V(t)e^{-i\omega t} \, dt = \frac{1}{2} \int_{-\infty}^{\infty} (a + ib)e^{-i(\omega-\omega_0)t} dt$$

$$+ \frac{1}{2} \int_{-\infty}^{\infty} (a - ib)e^{-i(\omega+\omega_0)} \, d^t t \tag{20}$$

and from (17) and (18) this evidently is

$$F(f) = \tfrac{1}{2}\Psi(f - f_0)Z(f) + \tfrac{1}{2}\bar{\Psi}(-f - f_0)\bar{Z}(-f) \tag{21}$$

or, since $Z(f) = \bar{Z}(-f)$

$$F(f) = \tfrac{1}{2}Z(f)\,[\Psi(f - f_0) + \bar{\Psi}(-f - f_0)]. \tag{22}$$

Anyone familiar with the rules of Fourier transforms could write down this frequency function in the first place and then proceed to find the time functions by the reverse of the process just carried out. But the time functions are more closely related to the physics of the problem and therefore provide a more fundamental starting point for its solution.

It will be appreciated that, although the above discussion has been phrased to apply to the problem of finding the voltage drop across an impedance when a frequency modulated current flows through it, the formulas also give the current through an admittance when a frequency-modulated voltage is applied across it. They also give the output voltage or current of a four-terminal network when a frequency-modulated current or voltage is applied at the input. These various applications of the formulas obviously can be made by placing definitions on Z and H appropriate to the particular problem.

The next step is to assume suitable values of the impedance $Z(f)$ and various forms of the frequency modulation function θ and to employ these particular values in the general formulas 8, 9, 17 and 18.

BALANCED FREQUENCY DETECTOR

The impedance can be defined, in general, as a rational algebraic function, viz.:

$$Z(i\omega) = \frac{(i\omega - a_1)(i\omega - a_2) \cdots (i\omega - a_m)}{(i\omega - p_1)(i\pi - p_2) \cdots (i\omega - p_n)} = \frac{P(i\omega)}{Q(i\omega)}. \tag{23}$$

Writing the polynominals P and Q in this way as the products of their factors exhibits the a's as the zeros of Z and the p's as the poles. The latter determine the frequencies of free vibration of the network. For the network to be stable, the p's must all have negative real parts. The a's and p's are either real or occur in conjugate complex pairs. By the partial fraction rule, the expression can be broken up into a series of simple fractions; thus

$$Z(i\omega) = \frac{A_1}{i\omega - p_1} + \frac{A_2}{i\omega - p_2} + \cdots. \tag{24}$$

If the poles are all simple, the A's are given by

$$A_j = \frac{P(p_j)}{Q'(p_j)}. \tag{25}$$

For the present purpose, only a pair of terms of (24) need be considered. This will provide a specific solution of the balanced frequency detector for the case, previously used for illustration, where the impedances are two simple resonant circuits of parallel R, L and C. At the same time, this solution can be extended to more complicated circuits by superposing a number of such elementary solutions, as is clearly possible with the type of impedance development indicated by (24).

The impedance of R, L and C in parallel, written in the form of (23) and (24), is

$$Z(i\omega) = \frac{i\omega}{C} \frac{1}{(i\omega - p_1)(i\omega - p_2)} = \frac{k}{i\omega - p_1} + \frac{\bar{k}}{i\omega - p_2}$$

$$= \frac{k}{i\omega + \gamma} + \frac{\bar{k}}{i\omega + \bar{\gamma}} \qquad (26)$$

where

$$-p_1 = \gamma = \alpha + i\beta$$

$$-p_2 = \bar{\gamma} = \alpha - i\beta$$

$$k = \frac{1}{2C}\left(1 - \frac{i\alpha}{\beta}\right)$$

$$\bar{k} = \frac{1}{2C}\left(1 + \frac{i\alpha}{\beta}\right)$$

$$\alpha = \frac{1}{2RC}, \qquad \beta = \sqrt{\frac{1}{LC} - \frac{1}{4R^2C^2}} = \sqrt{\omega_c^2 - \alpha^2}, \qquad \omega_c = \frac{1}{\sqrt{LC}}.$$

The voltage response of the circuit to a unit impulse of current is then

$$H(t) = \int_{-\infty}^{\infty} \left(\frac{k}{i\omega + \gamma} + \frac{\bar{k}}{i\omega + \bar{\gamma}}\right) e^{i\omega t}\, df = ke^{-\gamma t} + \bar{k}e^{-\bar{\gamma}t}, \quad t > 0. \qquad (27)$$

To find the envelope function of the voltage drop when the frequency modulated current

$$I(t) = \frac{h}{2}\left(e^{i\omega_0 t + i\theta(t)} + e^{-i\omega_0 t - i\theta(t)}\right) \qquad (1)$$

is applied to the circuit, we make use of the general formula, (17), which states that the spectrum, or Fourier transform, of this envelope function is

$$F_0(f) = \int_{-\infty}^{\infty} [a(t) + ib(t)]e^{-i\omega t}\, dt = \Psi(f)Z(f + f_0) \qquad (17)$$

where $\Psi(f)$ is the F.T. of $h \exp [i\theta(t)]$ and $Z(f)$ is the impedance, (26), in this case.   The envelope function then is

$$
\begin{aligned}
a(t) + ib(t) &= \int_{-\infty}^{\infty} \Psi(f)Z(f + f_0)e^{i\omega t} \, df \\
&= hke^{-(i\omega_0 + \gamma)t} \int_{-\infty}^{t} e^{(i\omega_0 + \gamma)\tau + i\theta(\tau)} \, d\tau \qquad (28) \\
&\quad + h\bar{k}e^{-(i\omega_0 + \bar{\gamma})t} \int_{-\infty}^{t} e^{(i\omega_0 + \bar{\gamma})\tau + i\theta(\tau)} \, d\tau.
\end{aligned}
$$

This result is obtained by employing the convolution formula[5], which states that if F_1 and F_2 are F.T.'s of G_1 and G_2, respectively, then the F.T. of F_1F_2 is

$$
\int_{-\infty}^{\infty} F_1(f)F_2(f)e^{i\omega t} \, df = \int_{-\infty}^{\infty} G_1(\tau)G_2(t - \tau) \, d\tau. \qquad (29)
$$

(The upper limit of the integrals in (28) is t instead of ∞ for the reason that $H(t)$ is zero for $t < 0$.)   The result could have been obtained equally well without using the Fourier transforms by substituting (27) in (8).   When $\theta(t)$ is specified mathematically in the infinite interval $(-\infty, \infty)$ these formulas give the resultant of the steady state and transient oscillations. Various problems can be solved by specifying particular forms of variation for $\theta(t)$.   Two examples follow: (1) where the instantaneous frequency, $\theta'(t)$, is an impulse and (2), where $\theta'(t)$ is a sinusoidal wave, as for elementary signal transmission.

Example 1: Impulse Modulation

Ignition interference comprises a sequence of sharp impulses, each of duration very brief compared to the interval between them, so that the transient in the receiver produced by one impulse dies away before the next one arrives.   It is therefore sufficient to consider the disturbance caused by a single impulse.

If the receiver is perfectly tuned, an impulse produces, in the tuned circuits, a transient of the same nominal frequency[6] as the signal carrier. When superposed on the carrier, the interfering transient alters, or modulates, both the amplitude and phase of the carrier.   The amplitude modulation is wiped out by the limiter, but the phase modulation remains to produce noise in the output.   The phase shift caused by the transient is a random variable, because it depends upon the time of arrival of the impulse, and this is entirely fortuitous.

---

[5] See pair 202 of Item 10 in the bibliography.
[6] By "nominal frequency" is meant the frequency as determined by counting zeros of the wave.   The transient actually comprises a spectrum of frequencies spread over the band of the tuned circuits, of course.

It is of engineering interest to determine the noise produced by a very large impulse, exceeding greatly the amplitude of the signal carrier.   When such a large impulse arrives, it causes a sudden jump, or discontinuity, in the phase of the carrier.   The excursion of the instantaneous frequency corresponding to the phase jump is indefinitely large and the problem accordingly cannot be solved satisfactorily by means of the usual assumption of quasi-stationary frequency.   The problem of large impulsive interference provides, therefore, the principal justification for the more exact method of analysis here employed.   In the paragraph following, the problem is restated in terms providing a suitable basis for mathematical analysis.

We assume, as before, that the limiter is delivering to the frequency detector a steady carrier current of constant amplitude h and frequency f_0. At time $t = 0$ a brief disturbance occurs specified by the statement that the instantaneous frequency, $\theta'(t)$, of the current suddenly executes an impulse of moment Θ.   That is: $\theta'(t)$ is zero at all times except at $t = 0$, when it goes to infinity and back to zero again in such a way that the area of the impulse so formed is Θ.   The carrier current amplitude then remains constant but the phase, $\theta(t)$, of the carrier takes a sudden jump of Θ radians at $t = 0$.   What is the voltage output of the frequency detector?

The general formula (28) gives directly the envelope function of the voltage across the impedance (26) for a phase function $\theta(t)$.   In this formula we have now to put $\theta(t) = 0$ before time $t = 0$ and Θ, after $t = 0$.   We do this by dividing the interval of integration into two parts, $(-\infty, 0)$ and $(0, t)$; thus

$$a(t) + ib(t) = hke^{-(i\omega_0+\gamma)t} \left(\int_{-\infty}^{0} e^{(i\omega_0+\gamma)\tau}\, d\tau + e^{i\Theta} \int_{0}^{t} e^{(i\omega_0+\gamma)\tau}\, d\tau \right)$$

$$+ h\bar{k}e^{-(i\omega_0+\bar{\gamma})t} \left(\int_{-\infty}^{0} e^{(i\omega_0+\bar{\gamma})\tau}\, d\tau + e^{i\Theta} \int_{0}^{t} e^{(i\omega_0+\bar{\gamma})\tau}\, d\tau \right)$$

$$= hk\, \frac{(1 - e^{i\Theta})e^{-(i\omega_0+\gamma)t} + e^{i\Theta}}{i\omega_0 + \gamma} + h\bar{k}\, \frac{(1 - e^{i\Theta})e^{-(i\omega_0+\bar{\gamma})t} + e^{i\Theta}}{i\omega_0 + \bar{\gamma}} . \quad (30)$$

Let the radian frequency interval by which the applied frequency ω_0 is set off from the resonant frequency ω_c be

$$\Delta = \omega_0 - \omega_c \quad (31)$$

as indicated on the curves of Fig. 2.   When α/ω_c is small compared to unity, as it is in practical circuits, β is very nearly equal to ω_c.   (See the formulas following equations (26).)   Then

$$i\omega_0 + \gamma = i\omega_0 + \alpha + i\omega_c = \alpha - i\Delta + 2i\omega_0$$

and

$$i\omega_0 + \bar{\gamma} = i\omega_0 + \alpha - i\omega_c = \alpha + i\Delta. \quad (32)$$

From this it is evident that the first term of (30) contains the demodulation sum product of frequency on the order of $2\omega_0$. This frequency will be suppressed by the diode load circuit and consequently the second term of (30) is an adequate representation of the envelope function. Therefore we write

$$a(t) + ib(t) = h\bar{k} \frac{(1 - e^{i\Theta})e^{-(i\omega_0+\bar{\gamma})t} + e^{i\Theta}}{i\omega_0 + \bar{\gamma}} \tag{33}$$

and with the above approximations this is very nearly equal to

$$a(t) + ib(t) = \frac{h}{2C} \frac{(1 - e^{i\Theta})e^{-(\alpha+i\Delta)t} + e^{i\Theta}}{\alpha + i\Delta}. \tag{34}$$

One deduction that can be made immediately from this formula is that the frequency of the oscillation in the output of the rectifier caused by the phase jump at the input is Δ, the radian frequency interval by which the applied carrier frequency differs from the resonant frequency. The oscillation is heavily damped, however, because α, while being very small compared to ω_c, is comparable in magnitude with Δ in circuits commonly used.

The angle of the complex envelope function (34) represents merely a phase shift of the carrier frequency ω_0. We are interested only in the magnitude of the function, viz.:

$$c(t) = [a^2(t) + b^2(t)]^{1/2}. \tag{35}$$

After some algebraic work, the desired formula comes out of (34) in the following form:

$$c(t) = \frac{h}{2C} \frac{\left[1 - 2m(t)\sin\left(\Delta t + \frac{\Theta}{2}\right) + m^2(t)\right]^{1/2}}{(\alpha^2 + \Delta^2)^{1/2}}, t > 0$$

where

$$m(t) = 2e^{-\alpha t}\sin\frac{\Theta}{2} \tag{36}$$

The discussion so far has dealt with a single impedance (or network) and has been concerned with obtaining formulas for the voltage across the impedance, and the envelope thereof, when a frequency-modulated current is sent through it. It is necessary now to refer to the construction of the balanced frequency detector, which is the particular object of our study. Figure 1 shows two impedances having the variation with frequency sketched in Fig. 2. The carrier current is driven through the two impedances in series and linear rectifiers are connected across each in such polarity that their low-frequency output voltages are opposed. We assume that the output

voltage of each rectifier is the envelope of the voltage existing across its associated impedance. Therefore, to find the total output of the balanced frequency detector, we have to find the difference between the envelopes of these voltages.

It is necessary to specify the two impedances more precisely. It appears that the best operation is obtained if the frequency of the carrier is midway between the resonant frequencies of the two impedances. That is

$$\Delta = \omega_0 - \omega_1 = \omega_2 - \omega_0$$

where ω_1, ω_2 are the resonant frequencies of Z_1, Z_2, (previously written as ω_c, for any impedance). Furthermore it appears that the two impedances should have identical values of C and very nearly the same damping constants. The design of the detector circuit is accordingly specified by

$$C_1 = C_2 = C$$
$$R_1 = R_2 = R$$
$$L_1 = 1/\omega_1^2 C$$
$$L_2 = 1/\omega_2^2 C$$

and then

$$\alpha_1 = \alpha_2 = \alpha = 1/2RC$$
$$k_1 = k_2 = k = 1/2C \qquad (a/\omega_0 \ll 1)$$
$$\sqrt{\frac{L_1}{L_2}} = \frac{\omega_2}{\omega_1} = \frac{\omega_0 + \Delta}{\omega_0 - \Delta}. \tag{37}$$

All the quantities are assumed to be substantially constant over the significant frequency range.

With the circuit constants so proportioned, it can be seen from (36) that the envelope of the voltage across Z_1 differs from that across Z_2 only in the sign of Δ. Therefore, the output voltage of the balanced frequency detector, when the instantaneous frequency variation is an impulse of moment Θ at $t = 0$, is

$$V_0(t) = c_2(t) - c_1(t)$$
$$= \frac{h}{2C} (\alpha^2 + \Delta^2)^{-1/2} \left(\left[1 + 2m \sin\left(\Delta t - \frac{\Theta}{2}\right) + m^2 \right]^{1/2} \right.$$
$$\left. - \left[1 - 2m \sin\left(\Delta t + \frac{\Theta}{2}\right) + m^2 \right]^{1/2} \right), \qquad t > 0 \tag{38}$$
$$= 0, \qquad t < 0, \quad \text{where } m = 2e^{-\alpha t} \sin\frac{\Theta}{2}.$$

On Fig. 5 is given a plot of this function for a value $\alpha/\Delta = 1$ of the relative damping. Calculations for other values of α/Δ show that the output oscillates only weakly for $\alpha/\Delta = \frac{1}{2}$ and is nearly dead-beat for $\alpha/\Delta = 2$
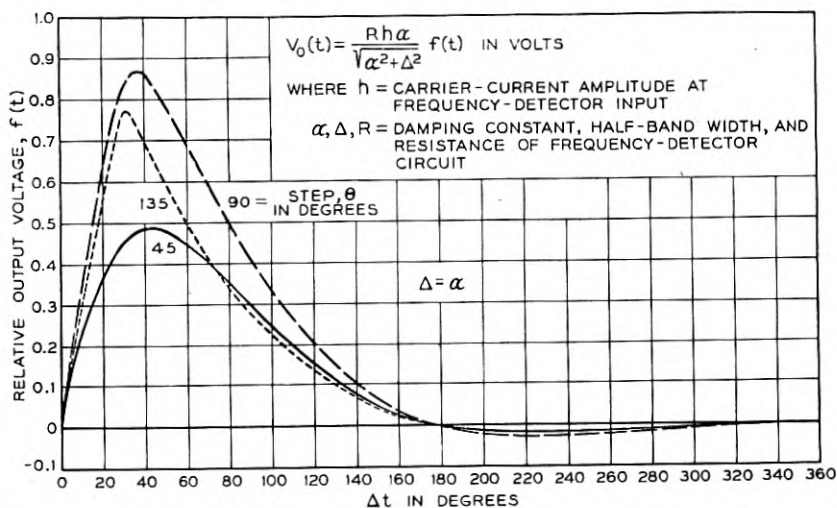

Fig. 5—Transient response of a balanced frequency detector for a step Θ in the carrier phase.

Example 2: Signal Reception

If the carrier is frequency-modulated by a signal

$$s(t) = S \cos qt \tag{39}$$

and the frequency modulation factor of the transmitter is μ, the phase of the carrier wave is made to vary in accordance with the relation

$$\theta(t) = \mu \int_{-\infty}^{t} s(t) \, dt = \frac{\mu S}{q} \sin qt = x \sin qt \tag{40}$$

μS is then the radian frequency deviation of the transmitter and $\mu S/q$, which is the ratio of this frequency deviation to the frequency of the signal, is commonly referred to as the "frequency deviation ratio." This factor, which is denoted by x in the above equation, enters as a fundamental parameter in all FM theory.

To find the envelope function of the voltage wave produced across the impedance (26), when the frequency-modulated carrier is received at the frequency detector, we put (40) in (28). To effect the integration, the expansion

$$e^{ix \sin qt} = \sum_{n=-\infty}^{\infty} J_n(x) e^{inqt} \tag{41}$$

is used, $J_n(x)$ being the Bessel coefficient of the first kind, of the nth order and with the argument x. For brevity, $J_n(x)$ will be written J_n. Also, the first term of (28) is to be omitted, because, as was shown in the preceding example, it represents frequency sum terms which are filtered out by the diode output circuit. Then we have

$$a(t) + ib(t) = h\bar{k}e^{-(i\omega_0+\bar{\gamma})t} \int_{-\infty}^{t} e^{(i\omega+\bar{\gamma})\tau} \sum_{n=-\infty}^{\infty} J_n e^{inq\tau} d\tau. \qquad (42)$$

When the integration is carried out, the result is

$$a(t) + ib(t) = h\bar{k} \sum_{n=-\infty}^{\infty} \frac{J_n e^{inqt}}{i\omega_0 + \bar{\gamma} + inq} = h\bar{k} \sum_{n=-\infty}^{\infty} \frac{J_n e^{inqt}}{\alpha + i\Delta + inq}. \qquad (43)$$

To obtain the magnitude of $a + ib$, which is the envelope required, we multiply the above Fourier series for $a + ib$ by that for $a - ib$, obtaining a double summation, which can be written as follows:

$$c^2(t) = a^2(t) + b^2(t) = c_0 + \sum_{n=1}^{\infty} (c_n e^{inqt} + \bar{c}_n e^{-inqt})$$

$$= a_0 + 2 \sum_{n=1}^{\infty} a_n \cos nqt \qquad (44)$$

where a_n is the real part of the complex coefficient c_n and $a_0 = c_0$.
The coefficients are given by

$$c_n = \frac{h^2}{4C^2} \sum_{m=-\infty}^{\infty} \frac{J_m J_{m+n}}{(\alpha - i\Delta - imq)[\alpha + i\Delta + i(m+n)q]}$$

$$\bar{c}_n = \frac{h^2}{4C^2} \sum_{m=-\infty}^{\infty} \frac{J_m J_{m+n}}{(\alpha + i\Delta + imq)[\alpha - i\Delta - i(m+n)q]}. \qquad (45)$$

Obtaining this result involves use of the relation

$$J_{-n}(x) = (-)^n J_n(x). \qquad (46)$$

From (45)

$$a_n = \frac{h^2}{4C^2} \sum_{m=-\infty}^{\infty} \frac{J_m J_{m+n}[\alpha^2 + (\Delta + mq)(\Delta + mq + nq)]}{[\alpha^2 + (\Delta + mq)^2][\alpha^2 + (\Delta + mq + nq)^2]}. \qquad (47)$$

Finally, we have to obtain, as before, the difference between the envelopes of the voltages across the two impedances of the balanced frequency detector; that is, we have to determine

$$V_0(t) = c_2(t) - c_1(t) \qquad (48)$$

where $c_1(t)$ is given by (44) as it stands and $c_2(t)$ is obtained from the same expression merely by reversing the sign of Δ. The complete solution for

the output voltage of the frequency detector, when a phase variation, $\theta'(t) = xq \cos qt$, is impressed on the carrier at the input, then is

$$V_0(t) = \left[a_0 + 2 \sum_{n=1}^{\infty} a_{n2} \cos nqt \right]^{1/2} - \left[a_0 + 2 \sum_{n=1}^{\infty} a_{n1} \cos nqt \right]^{1/2} \quad (49)$$

where a_{n1} is given by (47) and a_{n2} is given by the same formula with the sign of Δ reversed.

An approximation that is permissible when the frequency swing xq does not approach the available frequency range Δ is

$$V_0(t) = \sum_{n=1}^{\infty} A_n \cos nqt \quad (50)$$

where

$$A_n = \frac{a_{n2} - a_{n1}}{\sqrt{a_0}}, \qquad n \text{ odd}; = 0, n \text{ even}. \quad (51)$$

The table following gives the results of a computation of the first four coefficients from formulas (45) and (51) for the case of a frequency deviation ratio, $x = 5$, for $q/2\pi = 3000$ cycles per second, for $\Delta/2\pi = 30,000$ cycles per second and for $\alpha/\Delta = \frac{1}{2}, 1$ and 2.

Coefficient	$\alpha/\Delta = .5$	1.0	2.0
A_0	0	0	0
A_1	.848	.478	.191
A_2	0	0	0
A_3	.0312	−.00438	−.00281

Note: To obtain volts, multiply all values by $\dfrac{Rh\alpha}{(\alpha^2 + \Delta^2)^{1/2}}$

The coefficients for even values of n vanish, which confirms what can be inferred from physical considerations, namely, that the balanced construction of the frequency detector eliminates the d.c. component and all even harmonics. From the ratio of A_3 to A_1 we obtain the following ratios, expressed in db's, of the third harmonic distortion to the fundamental signal for the three circuit designs:

α/Δ	$20 \log 10 \, | A_3/A_1 |$
.5	−28.7 db
1.0	−40.8
2.0	−36.6

The results for the sinusoidal signal, when considered in conjunction with those for the impulse modulation, also permit certain conclusions regarding signal-to-noise ratios for impulsive interference in FM reception.

Ratio of Noise to Signal

It may be helpful, in conclusion, to attempt a theoretical estimate of the ratio of noise to signal in the audio output under the condition of severe impulsive interference.

The ratio of the peak value of the pulse to the signal amplitude at the frequency detector output is given by the ratio of the peak values of $f(t)$, as plotted in figure 5, to the values of A_1 in the table above. To obtain a result of practical significance, however, the effect of the audio circuit should be taken into account. In the absence of specific information on the structure of this circuit, we assume that the peak value of a pulse at its output is equal to the area, or moment, of the pulse at its input times twice the audio cutoff frequency. This is true for an ideal "square cutoff" filter and not seriously in error for actual circuits. The area of the largest pulse at the frequency detector output is approximately $2\Delta/(\alpha^2 + \Delta^2)$ and the value of A_1, the signal fundamental amplitude, can be approximated by

$$A_1 = \frac{2\Delta\, x\, q}{\alpha^2 + \Delta^2} \tag{52}$$

(For the example above, this approximation gives $A_1 = .8$, $.5$ and $.2$ as compared to the exact values, $.848$, $.478$ and $.191$.) In this way we arrive at the following estimate of the peak ratio of noise to signal in the audio output:

$$\frac{\text{Max. value of largest pulse}}{\text{Signal amplitude}} = \frac{\omega_a}{\pi\, x\, q} \tag{53}$$

where ω_a is the cutoff-frequency of the audio circuit, q the signal frequency and x the frequency deviation ratio. Then xq is the "frequency swing" of the transmitter, i. e., the maximum departure of the instantaneous frequency from its mean value. It is to be noted that this formula is free from the detector circuit parameters, α, Δ, R, and indicates that, to a first approximation, at least, the maximum ratio of noise to signal depends only upon the audio circuit cutoff frequency and the FM swing. Furthermore, this establishes a ceiling for the interference that will not be exceeded no matter how large the impulses may be.

Bibliography

1. Variable Frequency Electric Circuit Theory with Application to the Theory of Frequency-Modulation, John R. Carson and Thornton C. Fry in *Bell System Technical Journal*, Vol. XVI, No. 4, October 1937.
2. The Detection of Frequency Modulated Waves, J. G. Chaffee in *Proc. I.R.E.*, Vol. 23, May 1935. (*Bell Tel. Sys.* Monograph B-863)
3. Effects of Tuned Circuits upon a Frequency Modulated Signal, Hans Roder in *Proc. I.R.E.*, Vol. 25, December 1937.
4. The Reception of Frequency-Modulated Radio Signals, Victor J. Andrew in *Proc. I.R.E.*, Vol. 20, May 1932.

5. The Phase Discriminator, K. R. Sturley in *Wireless Engineer*, February 1944.
6. Radio Engineers Handbook, F. E. Terman, First Ed., pp. 585–588.
7. Motor Car Ignition Interference, C. C. Eaglesfield in *Wireless Engineer*, *23*, 1946.
8. Interference Problems in Frequency Modulation, F. L. H. M. Stumpers in *Philips Research Reports*, *2*, 1947.
9. On the Calculation of Impulse Noise Transients in Frequency Modulation Receivers, F. L. H. M. Stumpers in *Philips Research Reports*, *2*, 1947.
10. Fourier Integrals for Practical Applications, George A. Campbell and Ronald M. Foster in *Bell System Technical Journal*, October 1928—Monograph B-584.

Transverse Fields in Traveling-Wave Tubes

By J. R. PIERCE

Traveling-wave tubes will have gain even if the r-f field at the mean position of the electron stream is purely transverse. The addition of a longitudinal magnetic focusing field reduces the gain due to transverse fields and increases the electron velocity for optimum gain.

ALL slow electromagnetic waves have both longitudinal and transverse electric field components. Sometimes either the longitudinal or the transverse field may go to zero along a line or plane parallel to the direction of propagation. For instance, for the slow mode of propagation there is no transverse field on the axis of a helically-conducting sheet. Still, over any plane normal to the direction of propagation there are bound to be both longitudinal and transverse field components.

If a very strong longitudinal magnetic field is used in connection with a traveling-wave tube, the transverse motions of electrons may be so restricted as to be of little importance. With weak focusing fields, however, the transverse motion of electrons may be important in producing gain. The transverse fields can force the electrons sidewise, and thus change the longitudinal fields acting on them in such a way as to abstract energy from the electron stream.[1] This is closely analagous to the action of the longitudinal fields in displacing electrons forward or backward into regions of greater or lesser longitudinal field.

The purpose of this paper is to analyze the behavior of traveling-wave tubes in which transverse fields are important. The attack will be similar to that used previously.[2]

1. CIRCUIT THEORY

In this paper we shall consider only the electric field associated with the slow mode of propagation along the circuit having a speed close to the electron speed, and we shall neglect other field components attributable to local space charge. The writer believes the results so obtained to be valid at low currents but in error at high currents, and an acceptable guide at currents usually encountered.

In an earlier paper[2] a relation was found between the longitudinal field E_z excited in a mode of propagation of a transmission system and the longitud-

---

[1] See, for instance, J. R. Pierce and W. G. Shepherd, "Reflex Oscillators," *B. S. T. J.*, Vol. 26, No. 3, pp. 666–670 (July, 1947).

[2] J. R. Pierce, "Theory of the Beam-Type Traveling-Wave Tube," *Proc. I. R. E.*, Vol. 35, pp. 111–123, Feb. 1947.

inal exciting current q. Both E_z and q vary as $(\exp j\omega t)(\exp -\Gamma z)$. The relation is

$$E_z = q \frac{\Gamma_0}{\psi_0^*(\Gamma^2 - \Gamma_0^2)}. \tag{1}$$

Here Γ_0 is the propagation constant of the transmission mode considered and is defined in such a sense that for unattenuated propagation, $\Gamma_0 = j\beta_0$ where β_0 is a positive number. The quantity ψ_0 is defined as

$$\psi_0 = \frac{2P}{E_z E_z^*}. \tag{2}$$

Here P is complex power transmitted by the mode and E_z is the field associated with the mode.

In generalizing (1), let us consider the combination of equations (1) and (2)

$$P^* = \tfrac{1}{2} q E_z^* \frac{\Gamma_0}{\Gamma^2 - \Gamma_0^2}. \tag{3}$$

Now, suppose there is motion of the electrons not only in the z direction but in a direction normal to the z direction, which we will call the y direction. We shall have two extra first-order terms of the same general nature as qE_z^*, which contribute to the power, giving

$$P^* = \frac{1}{2}\left(q_z E_z^* + (-I_0)y \frac{\partial E_z^*}{\partial y} + q_y E_y^* \right) \frac{\Gamma_0}{\Gamma^2 - \Gamma_0^2}. \tag{4}$$

Here q_z is the a-c convection current in the z direction, $-I_0$ is the d-c convection current in the z direction (assumed to be the only d-c convection current), y is a small displacement, q_y is the convection current in the y direction and E_y is the field in the y direction.

We will now specialize this expression. Suppose we consider a two-dimensional transverse magnetic wave propagating in the z direction with a phase velocity v such that $v^2 \ll c^2$. Then over a restricted region the electric field can be represented quite accurately as the gradient of a scaler potential of

$$V = \exp(-\Gamma z)(A \exp(j\Gamma y) + B \exp(-j\Gamma y)). \tag{5}$$

Here A and B are constants. Using our notation, in which the field is understood to include the factor $\exp(-\Gamma z)$, we obtain

$$E_z = \Gamma(A \exp(j\Gamma y) + B \exp(-j\Gamma y)) \tag{6}$$

$$\frac{\partial E_z}{\partial y} = j\Gamma^2(A \exp(j\Gamma y) - B \exp(-i\Gamma y)) \tag{7}$$

$$E_y = -j\Gamma(A \exp(j\Gamma y) - B \exp(-j\Gamma y)). \tag{8}$$

In other words

$$\frac{\partial E_z}{\partial y} = -\Gamma E_y \,. \tag{9}$$

This relation will also be approximately correct remote from the axis in an axially symmetrical tube.   Here we let y represent a displacement in the r direction.

We may also define a quantity α so that

$$E_y = j\alpha E_z \tag{10}$$

$$\alpha = \frac{-(A \exp{(j\Gamma y)} - B \exp{(-j\Gamma y)})}{Ay \exp{(j\Gamma_y)} + B \exp{(-j\Gamma y)}} \,. \tag{11}$$

For an active mode, such as the one we consider, the chief component of $j\Gamma$ is a positive real number.   Hence, for large positive values of y, the quantity α approaches a value

$$\alpha = 1 \,. \tag{12}$$

This is characteristic of a plane symmetrical field far from the axis and also of an axially symmetrical field far from the axis.

Using (9) and (12) we rewrite (4)

$$P^* = \tfrac{1}{2} E_z^* [q_z - j\alpha^* (\Gamma^* I_0 y + q_y)] \tag{13}$$

We see from this that, according to our assumptions, for the mode considered,

$$E_z = (q_z - j\alpha^* (\Gamma^* I_0 y + q_y)) \frac{\Gamma_0}{\psi_0^* (\Gamma^2 - \Gamma_0^2)} \,. \tag{14}$$

We will henceforward assume that α and ψ are so nearly real that we can regard them as real quantities, giving

$$E_z = [q_z - j\alpha (\Gamma^* I_0 y + q_y)] \frac{\Gamma_0}{\psi_0 (\Gamma^2 - \Gamma_0^2)} \,. \tag{15}$$

This is, then, the circuit equation which we will use.

2. Electronics Equations

We will assume an unperturbed motion of velocity u_0 in the z direction, parallel to a uniform magnetic field of strength B.   Products of a-c quantities will be neglected.

In the x direction, perpendicular to the y and z direction

$$\frac{d\dot{x}}{dt} = -\eta B \dot{y}. \tag{16}$$

Assume that $\dot{x} = 0$ at $y = 0$.   Then

$$\dot{x} = -\eta By. \tag{17}$$

In the y direction we have

$$\frac{d\dot{y}}{dt} = \eta(B\dot{x} - j\alpha E_z). \tag{18}$$

Now

$$\frac{d\dot{y}}{dt} = \frac{\partial \dot{y}}{\partial t} + \frac{\partial \dot{y}}{\partial z}\frac{dz}{dt} \tag{19}$$

$$\frac{d\dot{y}}{dt} = u_0(j\beta - \Gamma)\dot{y} \tag{20}$$

$$\beta = \frac{\omega}{u_0}. \tag{21}$$

We obtain from (20) and (18), and (17)

$$(j\beta - \Gamma)\dot{y} = -u_0\beta_0^2 y - \frac{j\eta\alpha E_z}{u_0} \tag{22}$$

$$\beta_0 = \frac{\eta B}{u_0}. \tag{23}$$

We may note that ηB is the electron cyclotron frequency.   Now,

$$\dot{y} = \frac{\partial y}{\partial t} - \frac{\partial y}{\partial z}\frac{dz}{dt}$$

$$\dot{y} = u_0(j\beta - \Gamma)y. \tag{24}$$

From (24) and (22) we obtain

$$y = \frac{-j\eta\alpha E_z}{u_0^2[(j\beta - \Gamma)^2 + \beta_0^2]} \tag{25}$$

$$\dot{y} = \frac{-j\eta\alpha(j\beta - \Gamma)E_z}{u_0[(j\beta - \Gamma)^2 + \beta_0^2]}. \tag{26}$$

We will have for q_y

$$q_y = -I_0\frac{\dot{y}}{u_0} \tag{27}$$

$$q_y = \frac{j\eta\alpha I_0(j\beta - \Gamma)E_z}{u_0^2[(j\beta - \Gamma)^2 + \beta_0^2]}. \tag{28}$$

It is easily shown that

$$\dot{z} = \frac{\eta E_z}{u_0(j\beta - \Gamma)}. \tag{29}$$

If ρ_0 is the d-c linear charge density and ρ the a-c linear charge density

$$\rho_0 = -\frac{I_0}{u_0}. \tag{30}$$

If q_z is the z component of convention current, we have

$$q_z = \rho_0 \dot{z} + u_0 \rho$$
$$= -\frac{I_0 \dot{z}}{u_0} + u_0 \rho. \tag{31}$$

We also have

$$\frac{\partial q_z}{\partial z} = -\frac{\partial \rho}{\partial t} \tag{32}$$

$$\Gamma q_z = j\omega\rho.$$

From (31) and (32) we obtain

$$q_z = \frac{-j\beta I_0 \dot{z}}{(j\beta - \Gamma)}. \tag{33}$$

Thus

$$q_z = \frac{j\eta\beta I_0 E_z}{u_0^2(j\beta - \Gamma)^2}. \tag{34}$$

3. Combined Equation

Combining (34), (28) and (25) with (15), we obtain

$$1 = \frac{\eta I_0}{u_0^2} \frac{\Gamma_0}{\psi_0(\Gamma^2 - \Gamma_0^2)} \left[\frac{j\beta}{(j\beta - \Gamma)_0^2} - \frac{\alpha^2(\Gamma^* - (j\beta - \Gamma))}{[(j\beta - \Gamma) + \beta_0^2]} \right]. \tag{35}$$

We now introduce new parameters

$$K = \frac{1}{\beta^2\psi_0} = \frac{E_z E_z^*}{2\beta^2 P} \tag{36}$$

$$C^3 = \left(\frac{KI_0}{4V_0} \right). \tag{37}$$

Here P_0 is the power transmitted by the circuit for a field strength E_z. K has the dimensions of impedance. V_0 is the voltage specifying the electron velocity u_0

$$u_0^2 = 2\eta V_0. \tag{38}$$

From (36)–(38) and (35) we see

$$1 = \frac{2\beta^2 C^3 \Gamma_0}{(\Gamma^2 - \Gamma_0^2)} \left[\frac{j\beta}{(j\beta - \Gamma)^2} - \frac{\alpha^2(\Gamma^* - (j\beta - \Gamma))}{[(j\beta - \Gamma)^2 + \beta_0^2]} \right]. \tag{39}$$

We now make the approximation that

$$-\Gamma = -j\beta + \delta. \tag{40}$$

Where $|\delta| \ll |\beta|$. Neglecting higher order terms,

$$\frac{\Gamma^2 - \Gamma_0^2}{\Gamma_0} = 2j\beta^3 C^3 \left[\frac{1}{\delta^2} + \frac{\alpha^2}{\delta^2 + \beta_0^2} \right]. \tag{41}$$

4. Purely Transverse Field Along the Path

We can imagine a case in which α approaches infinity and the quantity

$$D^3 = \alpha^2 C^3 = \frac{E_y E_y^*}{\beta^2 P} \frac{I_0}{8V_0} \tag{42}$$

remains finite. In this case we have

$$\frac{\Gamma^2 - \Gamma_0^2}{\Gamma_0} = \frac{2j\beta^3 D^3}{\delta^2 + \beta_0^2}. \tag{43}$$

We will let

$$-\Gamma_0 = -j\beta - j\beta Db - \beta Dd. \tag{44}$$

Here b is a parameter describing the difference in speed between the electrons and the unperturbed wave and d is a loss parameter.

Assuming $bD \ll 1$ and $dD \ll 1$, and letting $\beta D(x + jy) = \delta$, $\qquad$ (45) we find

$$(x^2 - y^2 + f^2)(y + b) + 2xy(x + d) = -1 \tag{46}$$

$$(x^2 - y^2 + f^2)(x + d) - 2xy(y + b) = 0 \tag{47}$$

where

$$f^2 = \frac{\beta_0^2}{\beta^2 D^2}. \tag{48}$$

If would be difficult to work with all of the parameters b, f and d. However, it scarcely seems that the attenuation parameter d should enter into any unusual phenomena due to the presence of the magnetic field. Accordingly, let us investigate (46) and (47) for $d = 0$. We then obtain

$$x^2(3y + b) + (f^2 - y^2)(y + b) = -1 \tag{46a}$$

$$x[x^2 + (f^2 - y^2) - 2y(y + b)] = 0. \tag{47a}$$

From the $x = 0$ solution of (47a) we obtain

$$x = 0 \tag{49}$$

$$b = \frac{1}{y^2 - f^2} - y. \tag{50}$$

If is found that this solution obtains for large and small values of b. For very large and very small values of b, either $y \doteq -b$ (51) or $y \doteq \pm f$ (52) The wave given by (50) is a *circuit* wave; that given by (51) represents the travel down the tube of electrons oscillating in the magnetic field with cyclotron frequency.
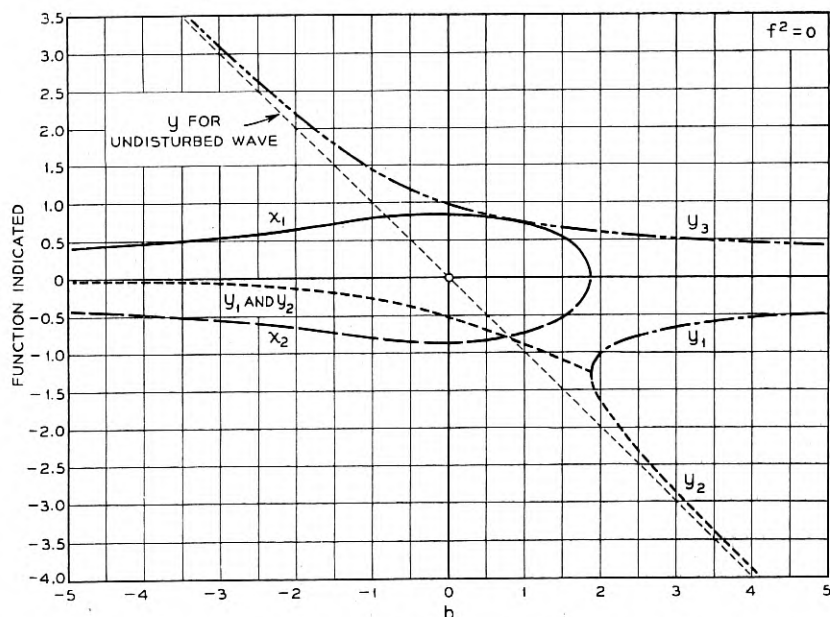

Fig. 1—Plot of parameters giving velocity and attenuation of the three forward waves vs. a parameter b proportional to electron speed with respect to the undisturbed wave. A positive value of x means an increasing wave; a positive value of y means a wave traveling faster than the electrons. This plot is for $f^2 = 0$ (no magnetic field).

In an intermediate range of b, we have from (47a)

$$x = \pm \sqrt{2y(y + b) - (f^2 - y^2)} \tag{53}$$

and

$$b = -2y \pm \sqrt{f^2 - 1/2y}. \tag{54}$$

For a given value of f^2 we can assume values of y and obtain values of b. Then, x can be obtained from (52) or (53). In Figs. 1–6, x and y are plotted vs. b for $f^2 = 0, .5, 1, 2, 4$ and 10. It should be noted that x_1, the parameter expressing the rate of increase of the increasing wave, has a maximum at larger values of b as f is increased (as the magnetic focusing field is increased). Thus, for higher magnetic focusing fields the electrons must be shot into the
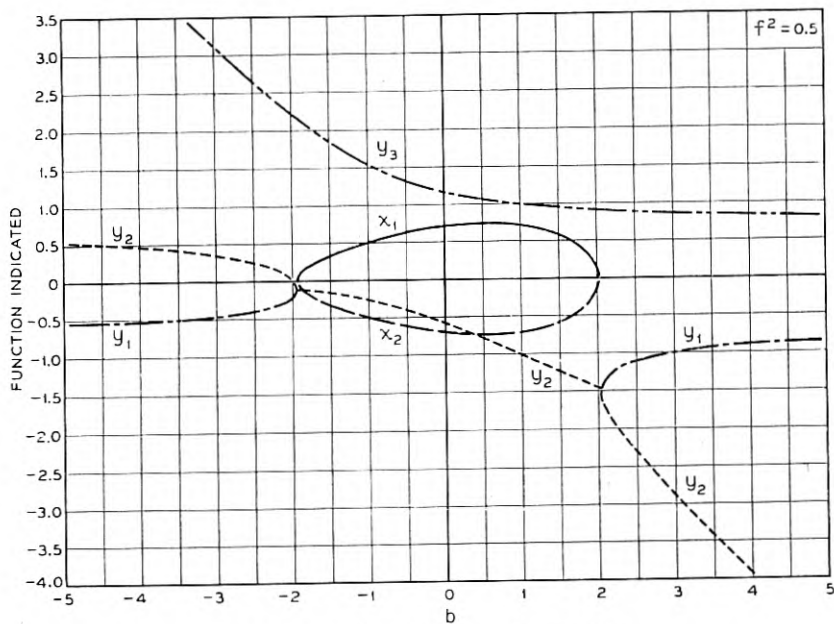
Fig. 2—Propagation parameters for $f^2 = 0.5$.
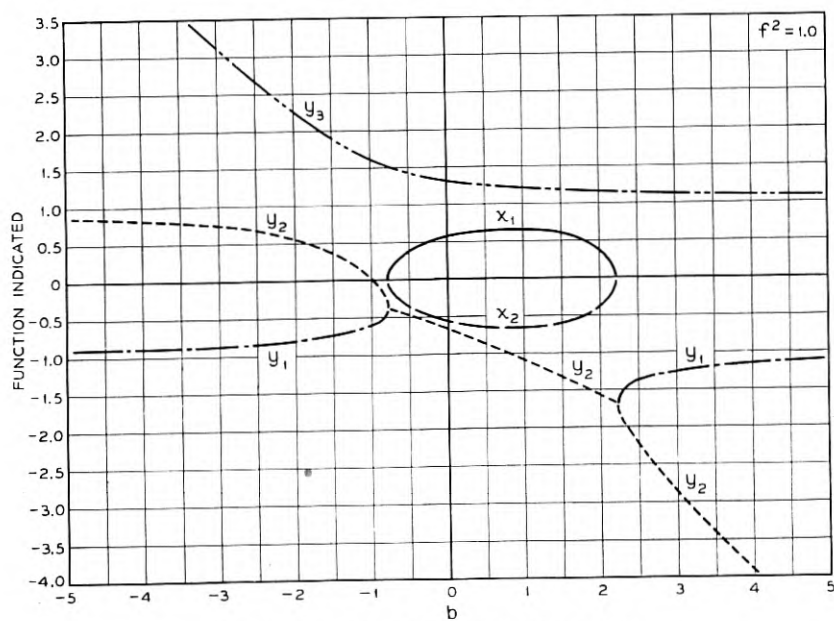
Fig. 3—Propagation parameters for $f^2 = 1.0$.
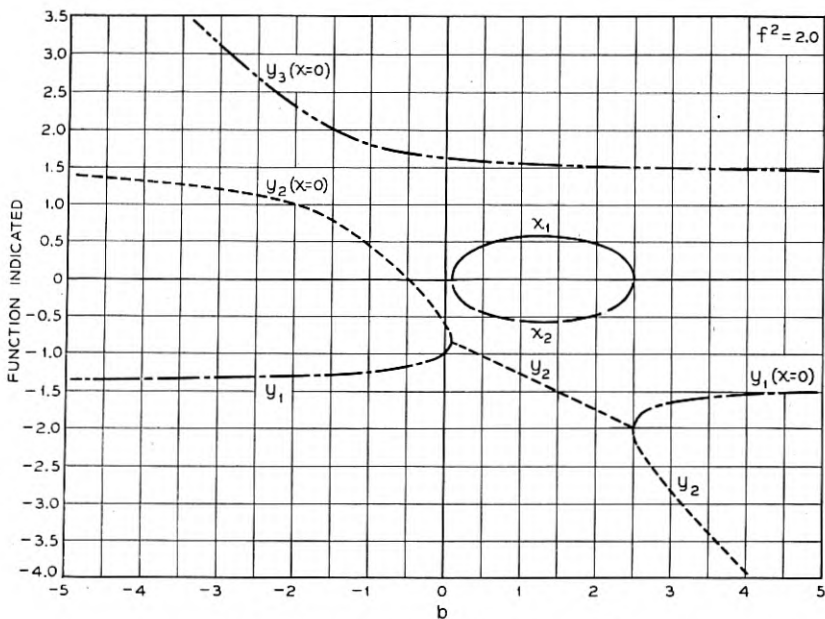
Fig. 4—Propagation parameters for $f^2 = 2.0$.
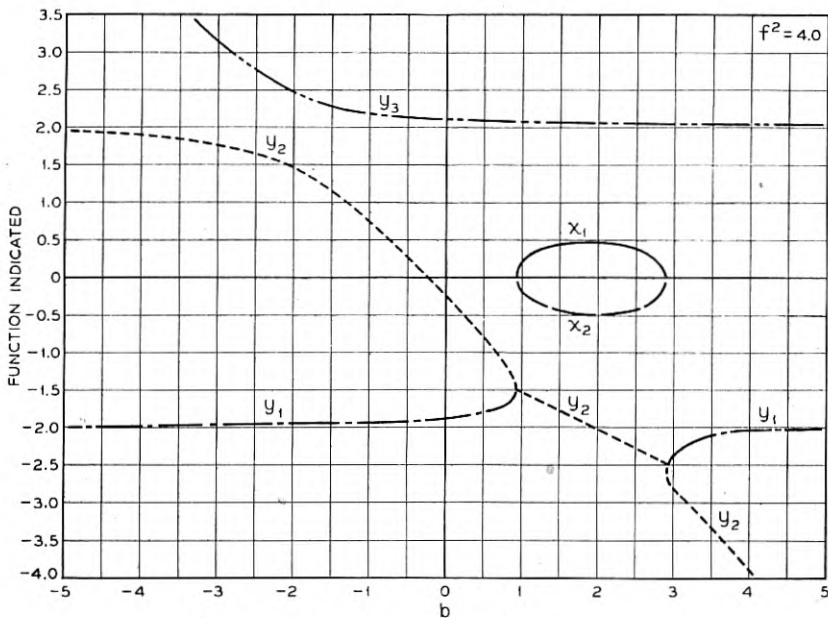
Fig. 5—Propagation parameters for $f^2 = 4.0$.
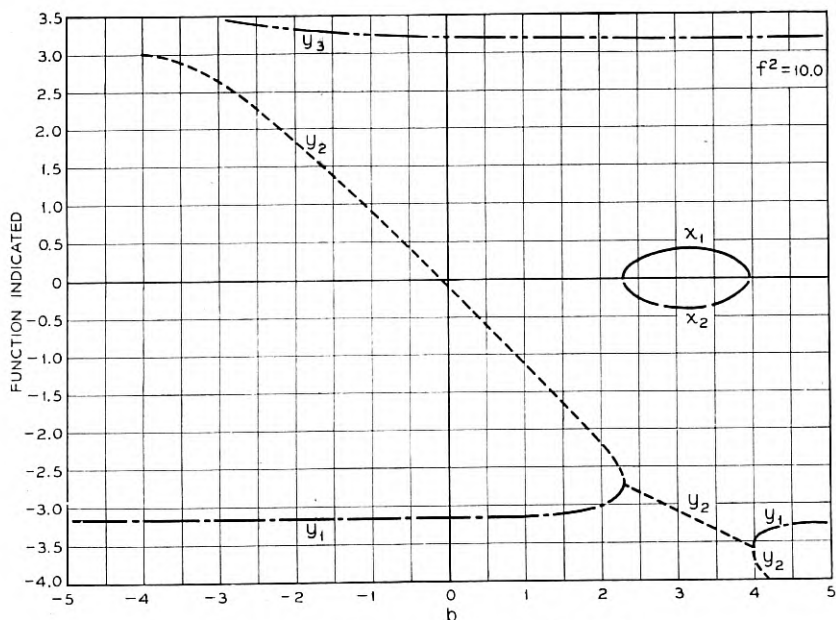
Fig. 6—Propagation parameters for $f = 10.0$.
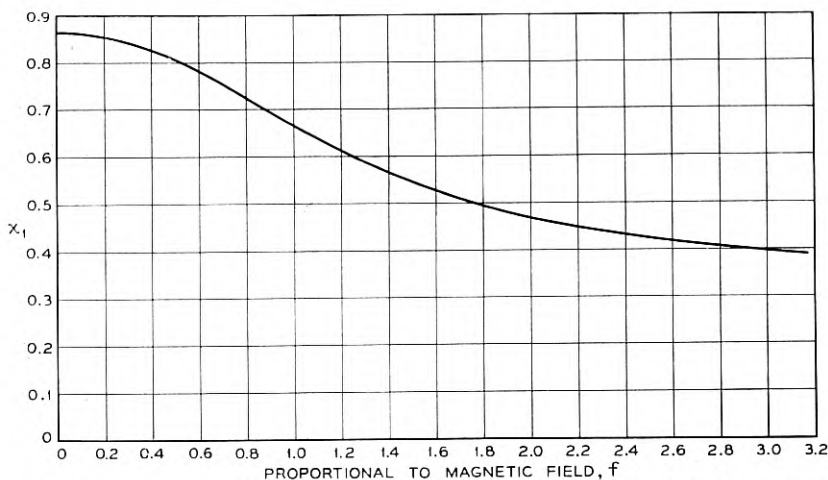
Fig. 7—Parameter x giving rate of increase of increasing wave vs. f, which is proportional to magnetic field strength.

circuit faster to get optimum results than for low fields. In Fig. 7, the maximum positive value of x is plotted vs. f. The plot serves to illustrate the effect on gain of increasing the magnetic field.

Let us consider an example.   Suppose

$$\lambda = 7.5 \text{ cm}$$

$$D = .03$$

These values are chosen because there is a longitudinal field tube which operates at 7.5 cm with a value of C (which corresponds to D) of about .03.   The table below shows the ratio of the maximum value of x_1 to the maximum value of x_1 for no magnetic field.

Magnetic Field in Gauss	f	x_1/x_{10}
0	0	1
50	1.17	.71
100	2.34	.50

A field of 50 to 100 gauss should be sufficient to give useful focusing action. Thus, it may be desirable to use magnetic focusing fields in deflection traveling wave tubes.   This will be more especially true in low-voltage tubes, for which D may be expected to be higher than .03.

5. Mixed Fields

In tubes designed for use with longitudinal fields, the transverse fields far off the axis approach in strength the longitudinal fields.   The same is true of transverse field tubes far off the axis.   Thus, it is of interest to consider equation (41) for cases in which α is neither very small nor very large, but rather is of the order of unity.

If the magnetic field is very intense so that β_0^2 is large, then the term containing α^2, which represents the effect of transverse fields, will be very small and the tube will behave much as if the transverse fields were absent.

Consideration of both terms presents considerable difficulty as (41) leads to 5 waves (5 values of δ) instead of 3.   The writer has attacked the problem only for the special case of $b = d = 0$.   In this case we obtain from (41)

$$\delta = -j\beta^3 C^3 \left[\frac{1}{\delta^2} + \frac{\alpha^2}{\delta^2 + \beta_0^2} \right]. \tag{55}$$

In work which is given as an appendix, Dr. L. A. MacColl has shown that the two "new" waves (waves introduced when $\alpha = 0$) are unattenuated and thus unimportant and uninteresting (unless, as an off-chance, they have some drastic effect in fitting the boundary conditions).

Proceeding from this information, we will find the change in δ as β_0^2 is increased from zero.   From (51) we obtain

$$d\delta = -j\beta^3 C^3 \left[-\frac{2d\delta}{\delta^3} - \frac{2\alpha^2 \delta d\delta}{(\delta^2 + \beta_0^2)^2} - \frac{2\alpha^2 d\beta_0^2}{(\delta^2 + \beta_0^2)^2} \right]. \tag{56}$$

Now, if $\beta_0 = 0$

$$-j\beta^3 C^3 = \frac{\delta^3}{(1 + \alpha^2)}. \tag{57}$$

Using this in connection with (56) for $\beta_0 = 0$ we obtain

$$d\delta = -\frac{2\alpha^2}{3\delta} d\beta_0^2. \tag{58}$$

For the increasing wave

$$\delta_1 = \beta(.866 - j.5). \tag{59}$$

Hence, for this wave

$$d\delta_1 = \frac{2}{9}(-.866 + j.5) \frac{d\beta_0^2}{\beta}. \tag{60}$$

This shows that applying a small magnetic field tends to decrease the gain. This does not mean, however, that the gain with a longitudinal and a transverse field and a magnetic field is less than the gain with the longitudinal field alone. To see this, we can assume that not β_0 but α^2 is small. Differentiating (55) we obtain

$$d\delta = -j\beta^3 C^3 \left[\frac{-2d\delta}{\delta^3} - \frac{2\alpha^2 \delta d\delta}{(\delta^2 + \beta_0^2)^2} - \frac{d\alpha^2}{(\delta^2 + \beta_0^2)} \right]. \tag{61}$$

If $\alpha = 0$

$$-j\beta^3 C^3 = \delta^3 \tag{62}$$

$$d\delta = \frac{1}{3} \frac{\delta^3 d\alpha^2}{(\delta^2 + \beta_0^2)}. \tag{63}$$

If β_0^2 is zero, a small transverse field (small increase in α^2) increases the magnitude of δ without changing the phase angle. If $\beta_0^2 \gg |\delta|$, then

$$d\delta = \frac{-j\beta^3 C^3}{\beta_0^2} d\alpha^2 \tag{64}$$

and the change in δ is purely imaginary. For the increasing wave, the change in δ as a transverse field is added will range from an increase in the real part for small magnetic fields to no change in the real part for large magnetic fields.

APPENDIX

STUDY OF THE ALGEBRAIC EQUATION

$$\delta = -j\beta^3 C^3 \left[\frac{1}{\delta^2} + \frac{\alpha^2}{\delta^2 + \beta_0^2} \right] \tag{1A}$$

$$\delta^3(\delta^2 + \beta_0^2) + j\beta^3 C^3(\delta^2 + \beta_0^2 + \alpha^2\delta^2) = 0$$

$$\delta^5 + \beta_0^2\delta^3 + j\beta^3 C^3(1 + \alpha^2)\delta^2 + j\beta_0^2\beta^3 C^3 = 0$$

$$\left(\frac{\delta}{\beta_0}\right)^5 + \left(\frac{\delta}{\beta_0}\right)^3 + j\left(\frac{\beta}{\beta_0}\right)^3 C^3(1 + \alpha^2)\left(\frac{\delta}{\beta_0}\right)^2 + j\left(\frac{\beta}{\beta_0}\right)^3 C^3 = 0 \qquad (2A)$$

Write

$$\frac{\delta}{\beta_0} = z$$

$$\left(\frac{\beta}{\beta_0}\right)^3 C^3 = a \qquad (3A)$$

$$\left(\frac{\beta}{\beta_0}\right)^3 C^3 a^2 = b$$

Then

$$z^5 + z^3 + j(a + b)z^2 + ja = 0 \qquad (4A)$$

a is assumed to be positive, and b is assumed to be real and non-negative. For $b = 0$ we have

$$(z^3 + ja)(z^2 + 1) = 0 \qquad (5A)$$

$$z = j, -j, ja^{1/3}, ja^{1/3} e^{2\pi j/3}, ja^{1/3} e^{4\pi j/3} \qquad (6A)$$

We have

$$[5z^4 + 3^2 z + 2j(a + b)z]\frac{\partial z}{\partial b} + jz^2 = 0$$

$$\frac{\partial z}{\partial b} = \frac{-jz^2}{5z^4 + 3z^2 + 2j(a + b)z} \qquad (7A)$$

From this we draw the following conclusion. Suppose that for a certain value of b the five roots are distinct, and that among them there is a purely imaginary root. Then as b varies, in the neighborhood of its initial value, that root remains purely imaginary.

In particular, consider b as increasing from the initial value 0. As long as the five roots remain distinct, there are exactly three purely imaginary roots.

In order to have a real root $z = x$, we would have to have simultaneously

$$x^5 + x^3 = 0$$

$$(a + b)x^2 + a = 0 \qquad (8A)$$

This is impossible (with $a > 0$). Hence there is never a real root.

In particular, as b increases from 0, no root can cross the real axis. Hence, as b increases from 0, as long as the roots remain distinct, there are two purely imaginary roots above the real axis, one purely imaginary root below the real axis, and two complex roots below the real axis.

Since there is no term in z^4 in the equation, the sum of all the roots is 0. Hence the two complex roots must be located symmetrically with respect to the imaginary axis.

First order variations of the roots with b can be calculated at once by means of the equation

$$\frac{\partial z}{\partial b} = \frac{-jz^2}{5z^4 + 3z^2 + 2j(a + b)z} \tag{9A}$$

In principle, higher-order variations can be calculated by carrying the differentiation to higher orders. However, the formulae get wonderfully complicated.

A very practical way of solving the equation is the following:

The three imaginary roots can be found by plotting a curve. If we let $z = jy$, (4A) becomes

$$y^5 - y^3 + (a + b)y^2 - a = 0 \tag{10A}$$

For the imaginary roots y is real and we have merely to plot the left-hand side of (10A) vs. y to find the roots. Denote them by z_1, z_2, z_3, which are now regarded as known numbers. These roots satisfy the equation

$$(z - z_1)(z - z_2)(z - z_3) \equiv z^3 - (z_1 + z_2 + z_3)z^2 + (z_1z_2 + z_1z_3 + z_2z_3)z$$

$$- z_1z_2z_3 \equiv z^3 + \alpha_1z^2 + \alpha_2z + \alpha_3 = 0 \tag{11A}$$

The two complex roots satisfy some equation

$$z^2 + \beta_1z + \beta_2 = 0 \tag{12A}$$

The β's are at present unknown. When we find them we can at once calculate the complex roots. We must have

$$(z^3 + \alpha_1z^2 + \alpha_2z + \alpha_3)(z^2 + \beta_1z + \beta_2) \equiv z^5 + z^3 + j(a + b)z^2 + ja \tag{13A}$$

Comparing the coefficients of z^4 and z^0, we get the equations

$$\alpha_1 + \beta_1 = 0$$

$$\alpha_3\beta_2 = ja \tag{14A}$$

which give us the β's.

Suppose that the magnetic field is very small, so that $\beta_0 \ll \beta$. Then unless α is very small, both a and b in (10A) will be very large numbers, and we find that two of the imaginary roots are given approximately by

$$y = \pm \left(\frac{a}{a + b}\right)^{1/2} \tag{15A}$$

As $\beta_0 \rightarrow 0$ the other three roots are given by

$$z = [-j(a + b)]^{1/3} \tag{16A}$$

These three roots correspond to the waves found for traveling-wave tubes with a purely longitudinal field. The roots according to (15A) represent such a combination of deflection and bunching as to produce no induced current in the circuit. The roots of (15A) are "extra" roots attributable to the consideration of transverse fields and transverse electron motion.

For the roots given by (15A), $\delta/\beta \rightarrow 0$ as $\beta_0 \rightarrow 0$. Thus in this case it is convenient to form the solution of two parts, one varying as

$$e^{-j\beta z} \sin \left(\frac{a\beta_0}{a + b} \right) z$$

and the other varying as

$$e^{-j\beta z} \cos \left(\frac{a\beta_0}{a + b} \right) z$$

As $\beta_0 \rightarrow 0$, the first of these approaches the form

$$z e^{-j\beta z}$$

and the second approaches the form

$$e^{-j\beta z}$$

Again, these "extra" waves produce no induced current in the circuit.

Two additional pieces of information:

As $a \rightarrow 0$, b a remaining fixed, the roots approach the limiting values

$$0, 0, 0, j, -j.$$

As $a \rightarrow \infty$, ba remaining fixed, two of the roots approach the limiting values

$$\pm j \sqrt{\frac{a}{a + b}},$$

the other roots behave as

$$j(a + b)^{1/3}, j(a + b)^{1/3} e^{2\pi j/3}, j(a + b)^{1/3} e^{4\pi j/3}$$

Much of the preceding discussion depends upon the roots remaining distinct. The condition that two or more of the roots coincide, which is a relation between a and b, can be written out, but it has not as yet been reduced to a compact and intelligible form.

Abstracts of Technical Articles by Bell System Authors

Pulse Code Modulation.[1] H. S. BLACK and J. O. EDSON. A radically new modulation technique for multichannel telephony has been developed which involves the conversion of speech waves into coded pulses. An 8-channel system embodying these principles was produced. The method appears to have exceptional possibilities from the standpoint of freedom from interference, but its full significance in connection with future radio and wire transmission may take some time to reveal.

Modulation in Communication.[2] F. A. COWAN. Any signaling system requires some means for introducing a change in conditions at the sending end which may be recognized at the receiving end. The process by which the conditions are changed has come to be called modulation. There are many varieties of forms of change as well as a large number of conditions which are subject to change in response to the signals to be transmitted.

In early systems for communication at a distance the signal information might have been impressed upon a rising column of smoke, a light, a stone tablet, or a sheet of parchment. For modern communication wide use is made of systems in which the signals change the magnitude or condition of electric energy.

Starting with the electric telegraph a little more than a hundred years ago this medium of communication has grown steadily more important and more complex. To meet a variety of needs many systems of modulation have been developed and papers describing them in detail are available in the technical literature. Various aspects of the modulation processes have been analyzed carefully and presented and some of the earlier conceptions have acquired a classical textbook status. Recent trends have placed emphasis on modulation systems which more readily may be understood when viewed in a somewhat different manner. It is the purpose of this paper to present certain conceptions which may facilitate the understanding of the various systems of modulation and permit an improved perspective.

Frequency Division Techniques for a Coaxial Cable Network.[3] R. E. CRANE, J. T. DIXON and G. H. HUBER. A description is given of developments employing frequency division techniques by which the telephone-message-carrying potentialities of the coaxial cable system are realized. By these methods 480 high quality telephone messages are prepared for

[1] *Trans. A. I. E. E,* vol. 66, 1947 (pp. 895–899).
[2] *Trans. A. I. E. E.,* vol. 66, 1947 (pp. 792–796).
[3] *Trans. A. I. E. E.,* vol. 66, 1947 (pp. 1451–1459).

transmission over the line and restored to original condition at main terminal points. At intermediate points appropriate groups of channels may be removed, inserted, bridged, or relocated in the frequency spectrum of the line.

Experimental Studies of a Remodulating Repeater.[4] W. M. GOODALL. This paper describes tests made on an experimental broad-band microwave f.m. repeater. A superheterodyne receiving unit is used with a microwave reflex-oscillator transmitting unit to form a repeater. An experimental setup for testing this repeater in a circulating-pulse system is described. Oscillograms showing the performance of the repeater on a multilink basis are discussed.

An Electronic Regenerative Repeater for Teletypewriter Signals.[5] R. B. HEARN. The important factor in teletypewriter signal transmission over circuits is the relative position on a time scale of the code pulses. If this timing is preserved, wide amplitude variations can be experienced without errors resulting. Correctly timed signal pulses at the transmitting end of a circuit are not necessarily properly timed at the receiving end, as the transmission path may shift the timing of some transitions with respect to others. However, if the signals are not too badly changed or distorted, it is possible to retime them at an intermediate point and send them on in their original form.

Many arrangements have been devised for automatically retiming and retransmitting teletypewriter signals. These arrangements are known as regenerative repeaters. A few of these have been designed to make use of electronic timing arrangements and the purpose of this paper is to describe such an electronic regenerative repeater, known as repeater *TG-29*, designed originally for use by the Armed Forces.

Submarine Detection by Sonar.[6] A. C. KELLER. Sonar, the only effective method of detecting completely submerged submarines was a major factor in the defeat of the *U*-boat and the winning of the Battle of the Atlantic. A majority of the 996 enemy submarines sunk during World War II was detected and located by sonar. The word sonar is formed from the phrase SOund Navigation And Ranging and applies broadly to under water sound devices for listening, echo ranging, and locating obstacles.

The QJA sonar system, one of those which got into active service during World War II, is described here. This equipment was designed by Bell Telephone Laboratories and manufactured by the Western Electric Company.

[4] *Proc. I. R. E.*, May 1948 (pp. 580–583).
[5] *Trans. A. I. E. E.*, vol. 66, 1947 (pp. 904–911).
[6] *Trans. A. I. E. E.*, vol. 66, 1947 (pp. 1217–1230).

Measurement of High Q Cavities at 10,000 Megacycles.[7]   R. W. LANGE.
Known methods of measuring Q in high Q resonant cavities, together with
their accuracies and sources of error, are discussed.   For relatively low
values of Q and of frequency, it is shown that band width methods are more
accurate than decrement methods.   For values of Q above 30,000 at fre-
quencies above 3,000 megacycles the reverse is true.   The significant feature
of the present method, the wide range heterodyne decrement method, is that
the accuracy is improved by observing the decay over a relatively long
interval of time.   An absolute accuracy of plus or minus three per cent and
a relative accuracy of plus or minus two per cent are achieved.   Design
features and performance are discussed and constructional details are
presented.

Absorbing Media for Underwater Sound Measuring Tanks and Baffles.[8]
W. P. MASON and F. H. HIBBARD.   By using absorbing walls surrounding
a small body of water, measuring tanks have been produced which will de-
termine the directional properties of underwater sound instruments down
to a level of 25 db below the direct beam.   These absorbing media are con-
structed by inserting fine mesh screen or packed copper wadding in a viscous
liquid such as castor oil.   These obstructions result in an enhanced viscous
action which is nearly independent of the frequency above 10 kilocycles.   A
six-inch wall can reduce the reflections by 20 db.   Tanks using such ab-
sorbing media were used for testing transducers at the manufacturing plant
and were used for determining the approximate characteristics of small sized
instruments.   Absorbing media were also used in the sound transparent
dome housing the transducer and in the back of the QJB transducers.

Calculation of the Directivity Index for Various Types of Radiators.[9]   C.
T. MOLLOY.   This paper gives the derivations of the "directivity index"
formulas for several types of sound radiators.   The "directivity index" is
defined as "the ratio of the total acoustic power output of the radiator to
the acoustic power output of a point source producing the same pressure at
the same point on the axis."   The utility of the directivity index concept is
that it permits power calculations to be made for all radiators in the same
manner as for point sources.   Directivity index formulas, together with
graphs covering practical cases, are given for the following types of radiators:

   1. General plane piston in infinite baffle,
   2. Circular plane piston in infinite baffle,
   3. Rectangular plane piston in infinite baffle,
   4. Sectoral horn,

[7] *Trans. A. I. E. E.*, vol. 66, 1947 (pp. 161–166).
[8] *Jour. Acous. Soc. America*, July 1948 (pp.476–483).
[9] *Jour. Acous. Soc. America*, July 1948 (pp. 387–405).

5. Multicellular horn,

6. Piston set in sphere.

A Magnetic Field Strength Meter Employing the Hall Effect in Germanium.[10] G. L. PEARSON. The instrument to be described measures magnetic field strengths as determined from the Hall effect in germanium. The essential parts of this instrument include a small germanium probe, and a panel type microammeter calibrated directly in gauss. Its accuracy is ± 2 percent at fields between 100 and 8000 gauss. At higher fields the readings are too low, the error amounting to 9 percent at 20,000 gauss. The chief advantages of this instrument are: (a) small size and portability, (b) continuous reading rather than ballistic as in ordinary field strength meters, and (c) a small nonmagnetic probe with which one can search in very narrow gaps.

The Representation of Vowels and their Movements.[11] RALPH K. POTTER and GORDON E. PETERSON. It is shown that movement of the major resonances in the voiced sounds of speech may be represented by traces in a three-dimensional graph. Apparently a great deal can be learned about speech through investigation of such traces, and they suggest a new method for vowel designation that is particularly adaptable to quantitative analysis.

General Mobile Telephone System.[12] H. I. ROMNES and R. R. O'CONNOR. The tremendous need for communication with ships, airplanes, trucks, tanks, and other mobile units used in such large quantities during the war accelerated the development of practical mobile radiotelephone equipment for use in the 30 to 200 megacycle range and emphasized the practicability and usefulness of mobile telephone service. By the end of the war the art had advanced sufficiently in the applications of these higher frequencies so that it seemed practicable to provide telephone service to mobile units on a general basis rather than limit it to safety and emergency services as had been the case before the war. The Federal Communications Commission therefore made available a few frequencies for experiments in this field. In the two years which have elapsed, the Bell System has made this service available on an experimental basis in more than 60 cities and about 100 more systems are under construction. This paper describes the arrangements used and outlines the experience obtained to date with this service. Improvements are being made constantly so that this must be regarded as an interim report on a rapidly changing and expanding service.

Interference between Very-High-Frequency Radio Communication Circuits.[13] W. RAE YOUNG, JR. Interference between different radio circuits is an old problem, one which in the past generally has been solved by trial and error

[10] *Rev. Sci. Instruments*, April 1948 (pp. 263–265)
[11] *Jour. Acous. Soc. America*, July 1948 (pp. 528–535).
[12] *Trans. A. I. E. E.*, vol. 66, 1947 (1658–1666).
[13] *Proc. I. R. E., Waves and Electrons Section*, July 1948 (pp. 923–930).

and by hand tailoring (special filters, etc.). With the general increase in the usage of radio communication, however, the amount of potential interference is greatly increased. This paper will be concerned principally with the v.h.f. problem.

There is generally a large difference between transmitting and receiving power levels. As a result, spurious radiations, spurious responses, and lack of sufficient receiver selectivity may in many instances cause interference. Situations are described in which such interferences are likely.

In mobile systems interference can occur if the interfering station is close enough to "capture" it from the desired signal. This, in turn, depends upon the selectivity and spurious response of the receiver and the amount of spurious radiation from the transmitter. The problem can be approached in a statistical manner.

The types of spurious radio behavior which are common causes of interference are discussed. Sample measurements are given to illustrate the relative magnitude of the various modes of behavior. Formulas are given which permit computation of the frequency of the disturbances. A method is described for making charts suitable for a given type of equipment from which the spurious frequencies can be read directly as a function of the operating frequency.

Contributors to this Issue

J. T. Muller, Technical College, Amsterdam, Holland, 1923; M.S., Stevens Institute of Technology, 1943. Mr. Muller came originally to the United States to continue his studies in 1923, became interested in the design and development of high-speed automatic equipment for a number of companies and joined Western Electric in 1941 and the Bell Telephone Laboratories in 1943. He has been primarily concerned with the protection of radar equipment against shock and vibration and the development of new types of shock mounts. His interest is in the field of experimental and mathematical dynamics.

William W. Mumford, B.A., Willamette University, 1930. Bell Telephone Laboratories, 1930–. Mr. Mumford has been engaged in work that is chiefly concerned with ultra-short-wave and microwave radio communication.

Liss C. Peterson, Chalmers Technical University, Gothenburg, 1921; Technical Universities of Charlottenburg and Dresden, 1921–23. American Telephone and Telegraph Company, 1925–30; Bell Telephone Laboratories, 1930–. Mr. Peterson has recently been concerned with the theory of hearing.

J. R. Pierce, B.S. in Electrical Engineering, California Institute of Technology, 1933; Ph.D., 1936. Bell Telephone Laboratories, 1936–. Engaged in study of vacuum tubes.

Claude E. Shannon, B.S. in Electrical Engineering, University of Michigan, 1936; S.M. in Electrical Engineering and Ph.D. in Mathematics, M. I. T., 1940. National Research Fellow, 1940. Bell Telephone Laboratories, 1941–. Dr. Shannon has been engaged in mathematical research principally in the use of Boolean Algebra in switching, the theory of communication, and cryptography.

M. K. Zinn, B.S. in Electrical Engineering, Purdue University, 1918; U. S. Army Signal Corps and Air Service, 1918–19. American Telephone and Telegraph Company, Department of Development and Research, 1919–34; Bell Telephone Laboratories, 1934–. Mr. Zinn's work has been concerned mainly with transmission engineering problems.